



1991

Dynamic and Spectroscopic Studies of Triplet State Nitrogen

Scott M. Hurst
Loyola University Chicago

Follow this and additional works at: https://ecommons.luc.edu/luc_diss

 Part of the [Chemistry Commons](#)

Recommended Citation

Hurst, Scott M., "Dynamic and Spectroscopic Studies of Triplet State Nitrogen" (1991). *Dissertations*. 3203.

https://ecommons.luc.edu/luc_diss/3203

This Dissertation is brought to you for free and open access by the Theses and Dissertations at Loyola eCommons. It has been accepted for inclusion in Dissertations by an authorized administrator of Loyola eCommons. For more information, please contact ecommons@luc.edu.



This work is licensed under a [Creative Commons Attribution-NonCommercial-No Derivative Works 3.0 License](#).
Copyright © 1991 Scott M. Hurst

Dynamic and Spectroscopic Studies of Triplet State Nitrogen

by

Scott M. Hurst

A Dissertation Submitted to the Faculty of the Graduate School
of Loyola University of Chicago in Partial Fulfillment
of the Requirements for the Degree of

Doctor of Philosophy

March

1991

This Dissertation is dedicated to my wife, Pamela, whose support, confidence, and understanding coupled with patient love has enriched my life abundantly.

ACKNOWLEDGMENTS

I wish to thank:

Professor Daniel Graham for his patience, optimism, and sincere concern throughout this work.

Dwayne LaBrake and Jing-Chen Luo, my lab partners, for their support, insight, and encouragement, throughout my tenure at Loyola.

Cynthia LaBrake, Glenn Noronha, and David Rockcliffe for their generous assistance in the preparation of this manuscript.

The Department of Chemistry and Graduate School of Loyola University of Chicago for support throughout my tenure at Loyola.

Special thanks to my mother, Frances Hurst, and father, Frank Hurst, whose encouragement, love, and support have motivated me throughout my life.

TABLE OF CONTENTS

	Page
ABSTRACT	ii
ACKNOWLEDGEMENTS	iii
LIST OF FIGURES	vi
CONTENT OF APPENDICES	viii
Chapter	
I. INTRODUCTION	1
A. Approaching Gas Phase Triplet State Spectroscopy	
B. On Triplet State Molecular Nitrogen	
C. Triplet State Molecular Complexes	
II. THEORETICAL FOUNDATIONS	9
A. Optical Selection Rules Versus Collisional Excitation Rules	
B. Physics of a Point Corona Electric Discharge	
C. The Chemical Physics of Supersonic Jets	
III. EXPERIMENTAL APPARATUS AND PROCEDURE	21
A. Apparatus	
1. Gas Handling System	
2. Supersonic Discharge Nozzle	
3. Vacuum System	
4. Optical System	
5. Data Acquisition	
B. Procedure	

	1. Gas Flow Adjustment	
	2. Discharge Initiation	
	3. Spectral Data Collection	
	4. Intensity Dependence on Pressure Measurements	
IV.	RESULTS	45
V.	DISCUSSION	68
	APPENDICES	90
	REFERENCES	120
	VITA	124

LIST OF FIGURES

Figure

1.	Hyperboloid versus plane electrode equipotentials	14
2.	Plot of force field as a function of distance	16
3.	Shock structure surrounding the expanding gas of a free jet	18
4.	Gas handling system	22
5.	Cathode assembly	26
6.	Anode assembly	28
7.	Body of the supersonic jet	29
8.	Assembled discharge nozzle	31
9.	Diagram of the electronics to the discharge	32
10.	Schematic representation of vacuum system	34
11.	Optical system	36
12.	Schematic for data acquisition	38
13.	Second positive system	47
14.	First positive system	48
15.	First negative system	49
16.	Illustration of the increase of the first negative emission intensity with increasing voltage, relative to the first and second positive group intensity. (a) 1.75 KV and (b) 2.5 KV are representative figures.	51
17.	Representative data correlating the visible length of the jet with the nozzle	

pressure as a log - log plot.	52
18. Log - log plot of spectral intensity versus nozzle reservoir pressure	54
19. Log - log plot of spectral intensity versus nozzle reservoir pressure	55
20. Log -log plot of spectral intensity versus pressure showing three selected bands .	56
21. Second positive 0 - 0 band at different pressures	58
22. Natural log - linear plot presenting the vibrational distribution of the C - state of nitrogen at ca. 900 K and 3300 K.	60
23. Natural log - linear plot presenting the electronic - vibrational emission of the first negative group. This corresponds to a vibrational temperature near 1800 K.	61
24. Natural log - linear plot presenting the electronic - vibrational emission of the first positive group. This corresponds to a vibrational temperature near 1900 K	62
25. B - state populations	64
26. Second positive 0 - 0 band rotational envelope	65
27. (a) Calculated 2nd positive 0 - 0 band rotational lines (b) 2nd positive 0 - 0 band rotational envelope.	67
28. Potential energy diagram of molecular nitrogen and ion	78

CONTENT OF APPENDICES

Appendix

A.1	Program 1 -- Collect Data	91
A.2	Program 2 -- Plot Data	99
B.1	Formulae for Calculating Rotational Lines	108
B.2	Program 3 -- Rotational Lines	111
B.3	Program 4 -- Rotational Envelope	115
C.1	Nitrogen Purity and Supplier	119

CHAPTER I

INTRODUCTION

A. *Approaching Gas Phase Triplet State Spectroscopy*

The triplet state is the lowest electronic excited state of closed shell organic molecules [1]. Understanding the structure and dynamics associated with molecular triplet states is central to understanding triplet state chemistry and physics. For these reasons, a large number of spectroscopic works which focus on molecular triplet states has evolved from the pioneer days of Lewis and Kasha [2].

The vast majority of triplet state molecular spectroscopic studies to date has been confined to the condensed phase at low temperatures. This is due, in part, to the radiatively-forbidden nature of singlet-triplet transitions and the conveniently available, non-radiative ways of preparing triplet states in the condensed phase at low temperatures.

Spectroscopic studies of molecular triplet states in the gas phase are sparse by comparison. This is unfortunate as all rotational data is lost in the condensed phase and, in turn, all structural information inherent to it. Further, in

condensed phase experiments, the data is contaminated by fields induced by nearest neighbor molecules.

The importance of understanding the physical properties intrinsic to triplet state molecules has motivated three approaches of gas phase spectroscopy.

The first has made use of low energy electron beams and the fact that singlet-triplet transitions are allowed during molecule-electron collisions [3-5]. Experiments feature a monoenergetic electron beam which is scattered from a target vapor in a collision cell. The scattered electrons are collected and energy-analyzed at selected angles with respect to the incoming beam.

Electron-energy-loss spectra result from this experiment. These are an indirect measure of the population of excited states during electron-molecule collisions. The resultant spectral bands have an important distinguishing feature. On the one hand, electron-spin-forbidden bands exhibit a relatively constant intensity as a function of scattering angle in that electrons are deflected equally in all directions. Spin-allowed bands, on the other hand, are heavily forward-peaked in that electrons are only sparsely deflected.

The most attractive feature of this first approach to triplet state spectroscopy of the gas phase is that the angular dependence of scattered electrons allows for recording spectra in ways which discriminate between singlet-singlet and

singlet-triplet transitions. Experiments using this approach, however, are not without limitations. In particular, the spectra which result from electron-molecule scattering experiments are limited to a resolution of ca. 200 cm^{-1} . While this admits information regarding the electronic and vibrational nature of triplet state molecules, the lack of resolution omits information regarding triplet state fine structure.

The second approach makes use of laser and supersonic jet techniques [6-8]. In these studies, organic molecules are prepared under the appreciably dense, cold conditions of a supersonic jet. Gas phase molecules under such conditions can be examined using high resolution lasers. In this way researchers have recorded high resolution, fine structure spectra of large ($N > 10$) polyatomics through laser induced phosphorescence excitation spectroscopy.

This second approach has considerably enhanced knowledge of the physical properties intrinsic to the triplet states of selected molecules. Yet this optical technique also has limitations, as it is governed by radiative selection rules. In particular, this approach is limited to molecular triplet states which are significantly contaminated by the singlet manifold through spin-orbit coupling. Thus, it excludes from investigation those molecular triplet states with little or no singlet character.

A third approach makes use of photochemical sensitization techniques [9,10]. The triplet state of one molecule with mixed singlet-triplet character is populated via electric-dipole radiation. This molecule is then allowed to collide with a second. Energy and spin are conserved during the collision. This leads to population of the triplet state of the second molecule.

Energy and angular momentum conservation direct molecular collisions in such a way that the above constitutes a general, efficient recipe by which molecular triplet states can be prepared in the gas phase. On the negative side, however, as this approach entails a chemical reaction wherein energy and angular momentum are exchanged between colliding species, many details exist which are case-specific.

We have worked to establish yet another approach to triplet state spectroscopy by adopting and combining key features of the above three. It utilizes the electron-molecule collisional excitation of the first approach as well as spin conserving collisions involving triplet state molecules of the third. In addition, high resolution optical techniques are applied to the cold, dense conditions of supersonic jets native to the second approach.

A large number of physical processes operate in this approach to triplet state spectroscopy of the gas phase. Unraveling the results of the experiments thereby demands an understanding of how triplet state molecules can be prepared

and cooled in a supersonic jet, and how they undergo electronic collisional relaxation with neighboring molecules.

First steps to this approach involved designing and constructing new apparatus to make possible the above collisional processes. These steps included directing the apparatus toward new experiments with small molecule systems about which much is known from the work of previous researchers.

Toward these ends, the engineering physics which makes possible the efficient, selective population of molecular triplet states in a supersonic jet are identified. The necessary apparatus was designed and constructed. The apparatus was applied to a study of the triplet state excitation and collisional relaxation properties of molecular nitrogen.

B. On Triplet State Molecular Nitrogen

Molecular nitrogen is an important, paradigmatic system for our approach to triplet state spectroscopy of the gas phase for at least two reasons. First, the vast majority of spectroscopic studies involving triplet state nitrogen has been performed using electric discharge techniques [11]. A unique characteristic of these discharges has been the segregation of different nitrogen excited species into different regions between the electrodes [12]. Positively

charged cations predominate in the region near the cathode known as the negative glow. Neutral molecules and negatively charged anions predominate in the region near the anode known as the positive column. Since nitrogen anions are very unstable, the majority of the species in the positive column are neutral. Of the excited neutral species formed in the positive column, the majority of the long lived species involve precisely the triplet states of nitrogen. By allowing the positive column of the discharge to undergo a free jet expansion into a vacuum chamber, it should be possible to separate the triplet state species along with ground state nitrogen as a carrier gas from the discharge environment.

Second, much is already known about the triplet states of nitrogen along with their collisional dynamics by way of a multitude of high resolution spectroscopy experiments applied to discharge/bulb systems [13-15]. Indeed, molecular nitrogen has commanded a formidable literature over the past century and is arguably the most-studied diatomic molecule.

Yet very few jet spectroscopy experiments have been reported. To our knowledge, no studies which employ the excitation conditions described in this work have been reported.

Thus this thesis intends to enhance knowledge of triplet state nitrogen by way of its excitation and collisional relaxation properties in a supersonic jet. This thesis, in turn, is directed toward understanding the general chemical

physics surrounding the electron-molecule collisional excitation and collisional sensitization of triplet state molecules in supersonic jets.

c. Triplet State Molecular Complexes

Supersonic jet techniques make possible gas phase, high resolution studies of molecules at extraordinarily low translational and rotational temperatures [16]. These techniques, over the years, have also provided ways to prepare and study relatively high concentrations of exotic clusters and aggregates under translationally- and rotationally-cold conditions [17-20].

Jet work directed toward understanding the cluster energetics and dynamics, however, has been limited largely to species of a closed-shell nature with singlet spin multiplicity. A relatively small number of open-shell species has been studied by way of free-radicals with doublet spin multiplicity [21,22]. To our knowledge, there have been no reports of electronically-excited, metastable clusters and aggregates with triplet spin multiplicity.

The supersonic jet technique outlined in the previous section provides a way to prepare triplet state species under translationally- and rotationally-cold conditions. It follows that this technique offers a possible way to prepare a new class of molecular clusters, namely ones involving molecular

triplet states.

It further becomes the purpose of this thesis to seek evidence for the existence of triplet state clusters prepared in a supersonic jet. In particular, the conditions under which triplet state nitrogen clusters can be prepared and interrogated using optical spectroscopy in a supersonic jet are explored.

CHAPTER II

THEORETICAL FOUNDATIONS

This thesis focuses upon the preparation of triplet state species by electron-molecule collision processes and collisional relaxation of these species in a supersonic jet. The essential physics thereby entails three areas:

(A) The selection rules which govern radiative versus electron collision excitation.

It is emphasized why molecular triplet states, in the absence of contamination with the singlet manifold, cannot be accessed radiatively. It is pointed out why triplet states must be accessed via collision processes.

(B) The electrodynamics of point corona discharges.

How molecular triplet states can be populated in a selective way is emphasized. Further, the basis on which the apparatus has been designed and constructed is presented.

(c) The collisional processes inherent to supersonic jets.

The collisional processes operative in a supersonic jet are qualitatively discussed. A more quantitative discussion applied to our data is presented in Chapter V.

These three areas will be addressed in the order presented above.

A. Optical Selection Rules Versus Collisional Excitation Rules

All selection rules governing the excitation of a molecule are realized by considering how a stationary state, e.g. with wavefunction Ψ_k composed of both electron spatial and spin components, is affected by a perturbation to the molecular Hamiltonian. In particular one must consider how the perturbation couples Ψ_k to a second stationary state with wavefunction Ψ_m .

In the case of a molecule exposed to light of wavelength much larger than the molecular dimensions, the electric dipole operator directs the coupling of stationary states according to the integral

$$\langle \Psi_k | \sum_i q_i r_i | \Psi_m \rangle$$

where the sum of the $q_i r_i$ includes all components of the molecular transition dipole.

The electric dipole operator concerns and thereby affects only spatial components of the molecular electrons. The operator has no effect on the electron spin parts of the molecular wavefunctions. The electric dipole operator is thereby responsible for coupling only those Ψ_k and Ψ_m with equivalent spin multiplicity. In the case where Ψ_k represents the ground state wavefunction with singlet spin multiplicity, electric-dipole radiation only accesses excited states with singlet spin multiplicity.

We note that electric-dipole transitions are a specific case of radiative excitations. However, the same ideas of spin conservation hold true in the general case of perturbing multipolar radiation fields.

The whole point is that the very pure, excited triplet states of molecules cannot be accessed by radiative excitation.

In the case of electron collisional excitation, the perturbation is the coulomb operator. Coupling of Ψ_k and Ψ_m is directed by the integral

$$\langle \Psi_k X \mid \sum_{ij} q_i q_j / r_{ij} \mid \Psi_m X' \rangle$$

Here $\Psi_k X$ and $\Psi_m X'$ are the zero-order wavefunctions of the

colliding species, i.e. concerning the electron and molecule. The operator is summed over all charges of the colliders.

The coulomb operator affects only spatial components of the electrons of the colliders. This stipulates that the total spin associated with Ψ_k and Ψ_m be equal. Yet the above integral can be factored into both coulomb and exchange components. Proper antisymmetrization of the $\Psi_k X$ and $\Psi_m X'$ ensures that the total spin of each be described by a superposition of spin states. It is this antisymmetrization property along with the exchange integral component which provide for the possibility of Ψ_k having different spin from Ψ_m upon separation of the colliders.

In the case where Ψ_k represents the ground state wavefunction with singlet spin multiplicity, collisional processes access Ψ_m which can have either singlet or triplet spin multiplicity.

In summary, processes have the capability of accessing excited states which are forbidden by radiative excitation. Radiative excitation events dominate the spectroscopic literature surrounding closed shell molecules. However, excitation processes involving electron-molecule and molecule-molecule collisions are central to this thesis.

B. *Physics of a Point Corona Electric Discharge*

What we want to convey here is the strategy behind the

design and construction of our supersonic discharge nozzle.

Consider the geometry of the metallic electrodes in Figure one. The illustration features one electrode in the shape of a hyperboloid of revolution. The other electrode consists of a plane located some distance from the hyperboloid [23,24].

The essential physics of our supersonic discharge nozzle can be realized by considering Laplace's equation applied to this geometry. Solution of this differential equation yields the equipotential surfaces of this geometry. Gradients of the solution yield the electric force fields associated with these surfaces.

Laplace's equation applied to this geometry is a standard problem of electromagnetic theory. We ignore mathematical details here as they may be found in References 23 and 24. Instead we call attention to the equipotential surfaces illustrated in Figure one. Like the upper electrode, these surfaces are hyperbolic in nature. Further we illustrate the lines of force by computing the gradients of the potentials. These lines of force compose half ellipses orthogonal to the equipotential surfaces.

We observe that the force fields are markedly compressed close to the hyperbolic electrode. We further observe that force fields are relatively expanded near the metallic plane.

A plot of the force field intensity as a function of distance from the hyperbolic electrode is presented in Figure

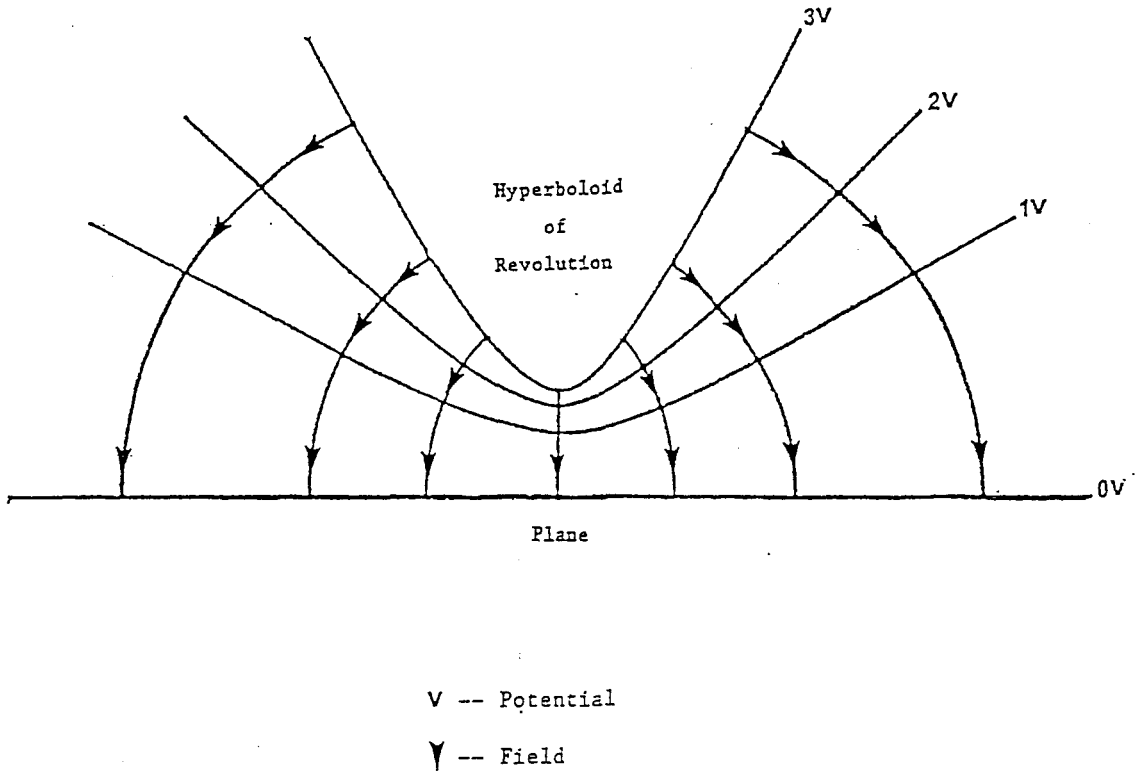


FIGURE 1.
HYPERBOLOID VERSUS PLANE ELECTRODE

two. The force field is observed to fall as $(1+x^2)^{-1}$, where x is the distance from the hyperbolic electrode along the line normal to the plane and through the foci of the hyperboloid.

Now our supersonic discharge nozzle has been designed and constructed to mimic the geometry of Figure one, save for having a 100 micron hole in the center of the metallic plane. This apparatus works in a manner directed by electromagnetic theory.

Using the polarity illustrated in Figure one, intense force fields pull electrons from the hyperbolic electrode. These electrons, in turn, experience the most intense electric force fields in the region of this electrode and are accelerated toward the metallic plane. It is in this region where electron-molecule collisions are most energetic. It is in this region where ionization processes are most prevalent.

The electrons lose energy to molecules as they travel toward the metallic plane. In the region of the metallic plane, the electric force fields are of low intensity. Here electron-molecule collisions are of relatively low energy.

If a supersonic expansion is allowed to take place via the hole in the metallic plane, this expansion will be biased toward products resulting from low energy electron-molecule collisions. The higher energy products undergo collisional relaxation and are confined to the vicinity of the hyperbolic electrode.

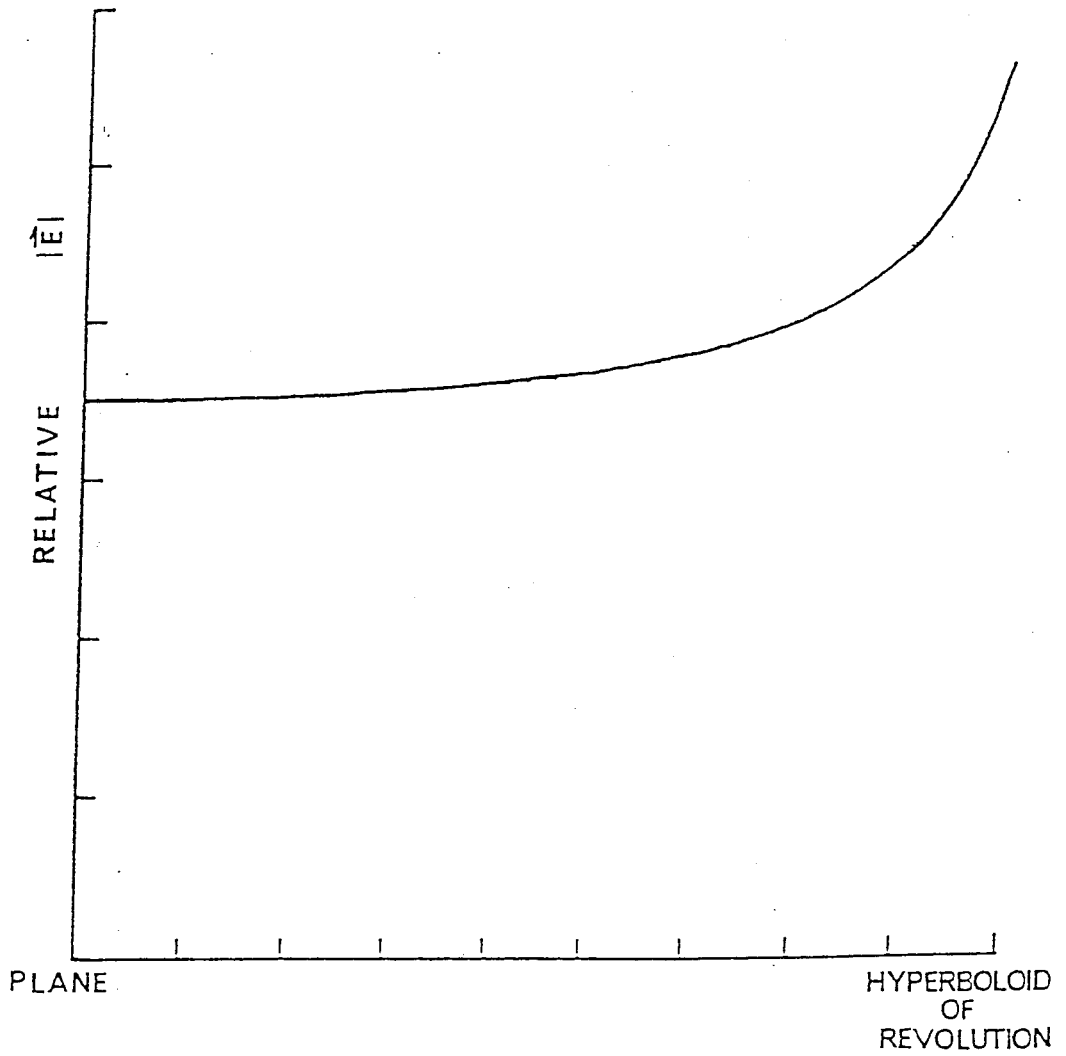


FIGURE 2.
 RELATIVE $|\vec{E}|$ ALONG LINE NORMAL TO PLANE AND THROUGH FOCI
 OF HYPERBOLOID.

We note that the geometry of Figure one is in marked contrast to other electrode configurations, e.g. those consisting of two parallel plates. Here the force fields fall linearly with distance. Such configurations combined with a supersonic discharge would offer little chance of sequestering neutral products of electron-molecule collisions.

C. The Chemical Physics of Supersonic Jets

Expansion of a high pressure gas through a nozzle leads to a highly directional mass flow. Elevated nozzle pressures indeed encourage the situation where the expanding gas in the region upstream from a shock structure is virtually unaffected by the background gas. The core structure (c.f. Figure three) in this case largely approximates a free jet expanding into an infinite vacuum. A supersonic jet is the result with translational energy stemming from energy stored in both internal and external degrees of freedom of the molecules in the nozzle reservoir [25-30].

During the expansion, the most probable velocity exceeds that operative inside the nozzle reservoir. Further, the velocity distribution is markedly narrower than that operative inside the nozzle reservoir. This narrow velocity distribution of the expanding molecules reflects a translational temperature much lower than that of the nozzle source. All the molecular degrees of freedom are in thermal

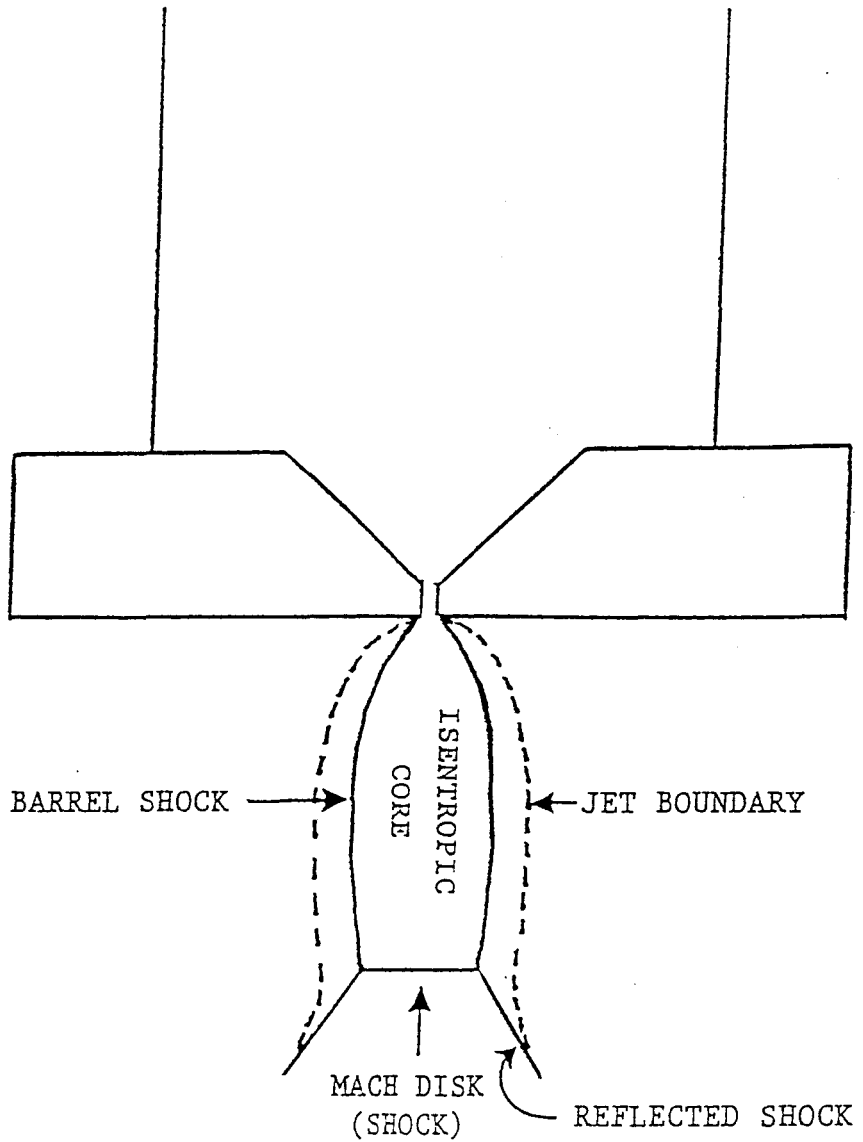


FIGURE 3.
SHOCK STRUCTURE SURROUNDING THE EXPANDING GAS OF A
FREE JET.

contact to some extent during the expansion via collisions. Collisions bring about energy exchange among the degrees of freedom. Such internal degrees are cooled with the external degrees serving as a heat bath.

Collisional processes in an expanding jet are complicated for two interdependent reasons: (1) Different degrees of freedom relax at different rates, and (2) The collision frequency decreases as the expansion proceeds.

Concerning the first reason, while vibrational, rotational, and translational degrees of freedom leave the nozzle in thermal equilibrium with each other, these degrees of freedom do not stay in equilibrium as the expansion proceeds. In particular, the vibrational and rotational degrees of freedom relax more slowly than translational. Departure from an equilibrium state generally occurs first with respect to vibrational-translational degrees and second with respect to rotational-translational.

Concerning the second reason, as the supersonic expansion proceeds, the rates of energy transfer within the beam decrease to near-zero. At some point during the expansion, vibrational and rotational distributions essentially "freeze". At these points the temperatures characteristic of the vibrational and rotational degrees of freedom may greatly exceed the characteristic translational temperature. These points usually occur a few nozzle diameters from the nozzle source where the expansion can be

characterized as a molecular flow, rather than hydrodynamic flow.

How do the above ideas relate to our experimental work? The above offer the essential physics underlying the behavior of the vibrational and rotational degrees of freedom in a supersonic jet. Such behavior appears to be well understood in both theory and experiment [31,32].

However, the essential physics underlying chemical relaxations in a supersonic jet is more difficult to pinpoint, generalize, and predict. Further, there appears to be very little by way of theory and experiment concerning chemical relaxation events in supersonic discharges.

This thesis focuses on chemical events surrounding triplet state molecules in a supersonic jet. The task will be to deduce from optical spectroscopy of the supersonic jet, information, about the chemical relaxation processes of triplet state molecules in the supersonic jet.

CHAPTER III

EXPERIMENTAL APPARATUS AND PROCEDURE

A. *Apparatus*

The apparatus is discussed in terms of five sections: gas handling system, supersonic discharge nozzle, vacuum system, optical system, and data acquisition system. These sections are illustrated separately. Dimensions and other details are noted in the figures.

The electronic equipment necessary for the interface of each section with the computer is discussed in conjunction with that section. The software written to orchestrate the experiments is described.

(1) Gas Handling System

The gas handling system is illustrated in Figure four. The system is designed to introduce single component or binary mixtures of gas to the discharge nozzle. Two-stage regulators are used to discharge the contents of the two compressed gas cylinders. These regulators maintain a

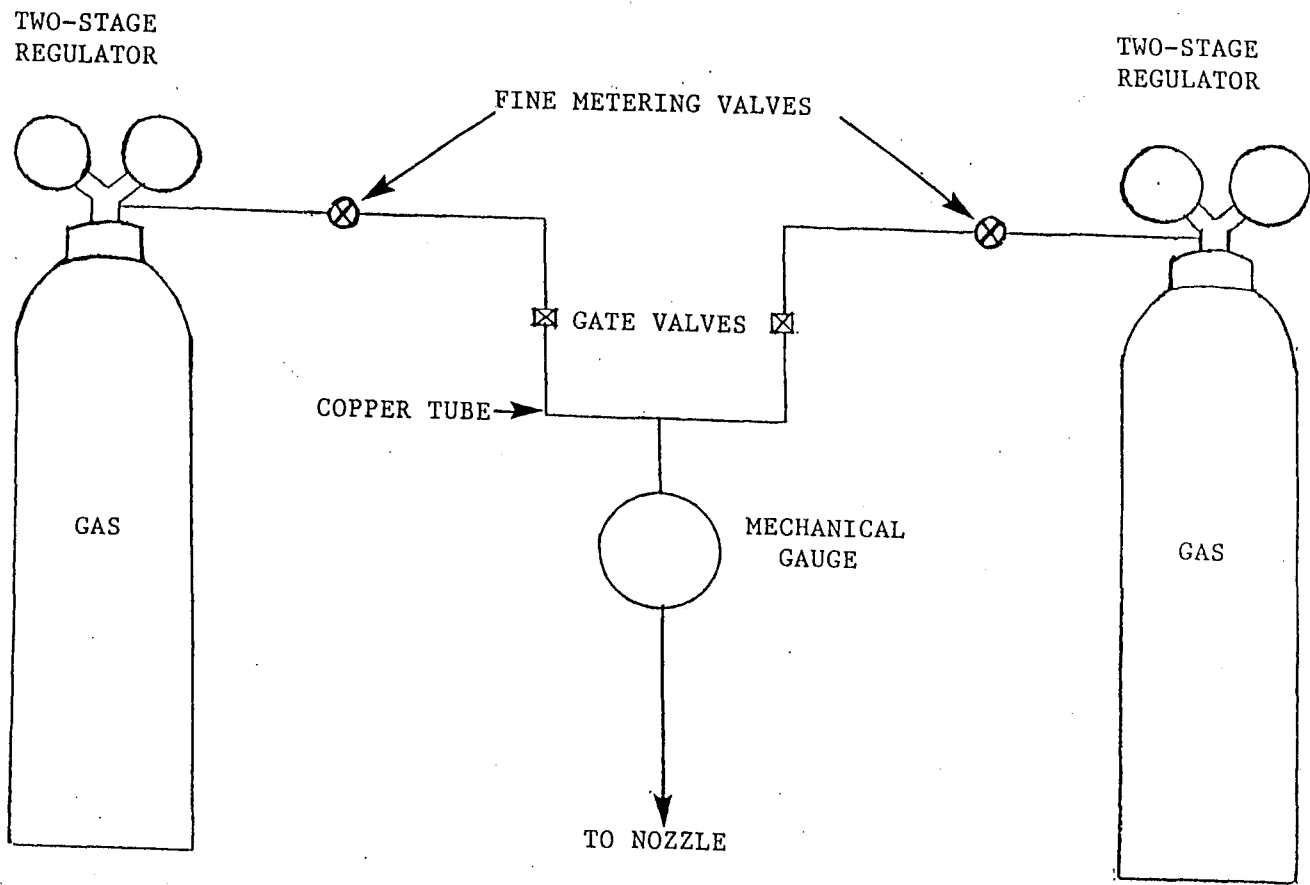


FIGURE 4.
GAS HANDING SYSTEM

constant pressure at their outlets throughout the discharge of the entire contents of the compressed gas. A fine metering valve and a gate valve are connected in series to the discharge outlets of each regulator. The connections are made using two one-inch lengths of quarter inch diameter, hard copper tubing and the compression fittings on the regulator, metering valve, and gate valve. The outlets of both gate valves are connected to a 1/4 " compression tee using two 18" lengths of soft copper tubing. The third tee junction is connected to a second tee using a 36" length of soft copper tubing. The second tee is connected to a 0 - 1000 torr mechanical pressure gauge which has a 1/2 " NPT male connector. The connection is made using the following in series between the tee and gauge:

- (a) a 1" length of hard copper tubing
- (b) a 1/4 " compression "L"
- (c) a second 1" length of 1/4 " hard copper tubing,
and
- (d) a 1/4" compression to 1/2" NPT female connector.

The second tee is also connected to the discharge nozzle which has a 1/4" NPT female connector. The connection is made using the following in series between the tee and discharge

valve:

- (a) a 3 " length of 1/4 " hard copper tubing
- (b) a 1/4 " compression to 1/2 " NPT male connector
- (c) a 16 " long, 1/2" diameter, teflon lined, braided stainless steel hose with 1/2 " NPT female connectors,

and

- (d) a 1/2 " NPT male to 1/4 " NPT male connector.

Two ancillary devices have for some experiments been integrated into the gas handling system. The first device is an oxygen trap. The oxygen trap is a 6' long, 1/4" diameter plated copper tube bent into a 4" diameter coil. This coil contains an activated copper complex which will remove oxygen and sulphur compounds from inert gases. The trap has a 1/4 " compression fitting which allows for installation at any point within the gas handling system.

The second device is a sublimation chamber. This device is a modified, in-line gas purifier. The molecular sieve in the gas purifier was removed. A solid sample dispersed throughout glass wool is placed in the empty chamber of the purifier. The glass wool is used to provide channels for the carrier gas to flow through. The wool also reduces the

possibility of the sample clogging the steel frits at both the inlet and outlet of the chamber. The chamber has 1/4 " compression fittings which allow installation at any point within the gas handling system. This provides a means of saturating the gas going to the discharge nozzle with a sublimable sample.

(2) Supersonic Discharge Nozzle

Our supersonic discharge nozzle resembles that employed in the low stagnation pressure experiments with argon atoms of Kessler and Koglin [33]. Our supersonic discharge nozzle differs, however, with respect to key dimensions and operation.

The cathode assembly is illustrated in figure five. The cathode is formed from a 1/4 " diameter, 8 1/4 " long, stainless steel rod with a thirty degree point. This rod is machine-tapped to mount on the threaded high voltage feedthrough. The tap depth of the rod and thread length of the feedthrough are sufficient to allow for adjusting overall length of the cathode assembly, i.e. the rod mounted on the feedthrough. The cathode assembly is adjustable from 8 3/4" to 9 1/4 " relative to the 2 3/4 " diameter, 1/2 " thick ConFlat flange of the high voltage feedthrough. A lock nut is placed on the threaded portion of the feedthrough. In the course of preparing the nozzle for experiments, this nut is

HV FEEDTHROUGH
ON $2\frac{3}{4}$ " CONFLAT
FLANGE

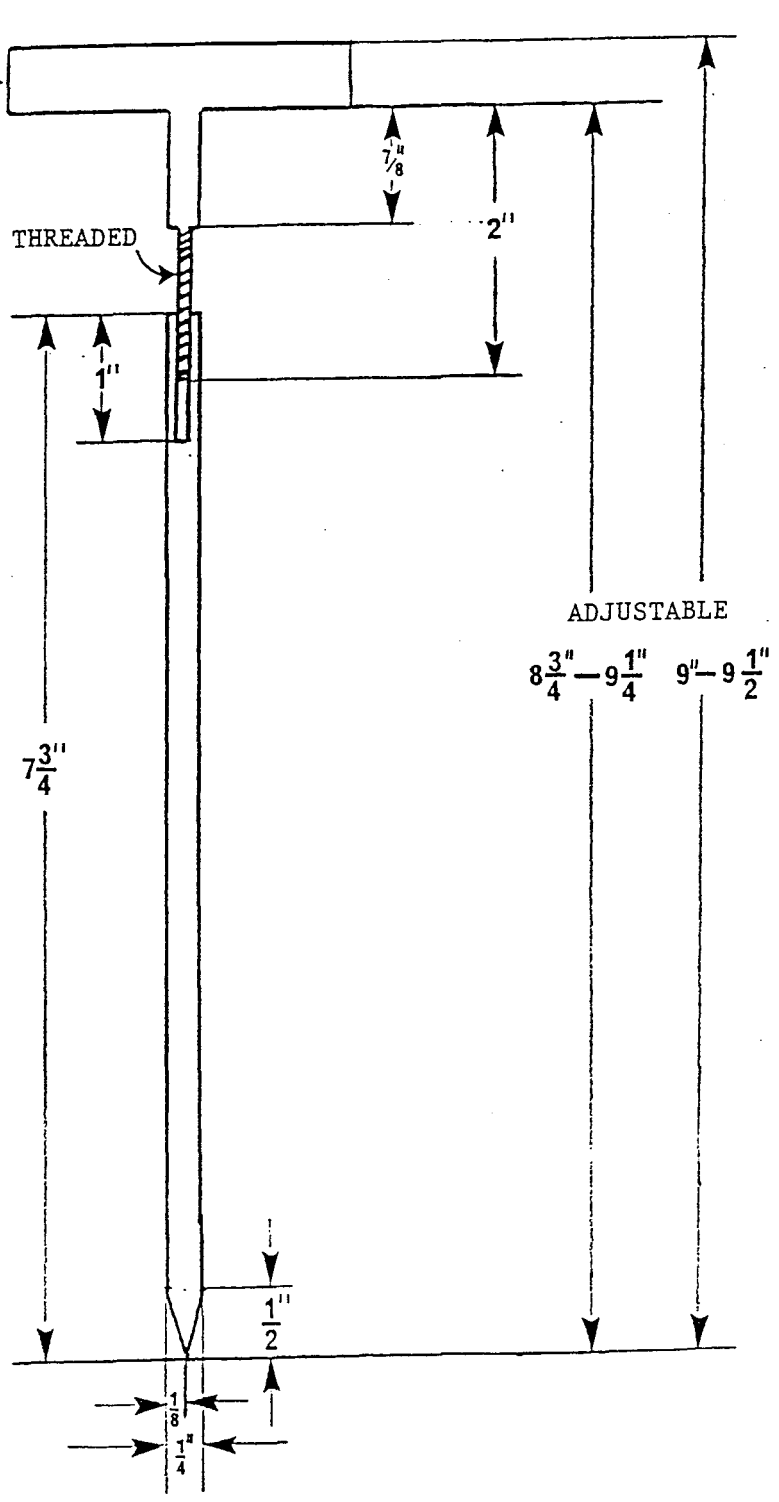


FIGURE 5.
CATHODE ASSEMBLY.

tightened against the rod once the cathode assembly is adjusted to the proper length. The lock nut keeps the rod in place once it is positioned.

The anode of the supersonic discharge nozzle is illustrated in Figure six. The anode is formed by a 1 1/3 " diameter, 1/4 " thick ConFlat flange. The flange is modified in a particular way: a forty-five degree, conical cavity with axis perpendicular and through the center of the plate is machined into the flange. The apex of this cavity is approximately 1/16" from the smooth surface of the flange. A 0.004 inch hole passes from the apex of the cavity through the smooth side of the plate. This forms the 0.004 inch diameter, 1/16 " long cylindrical aperture through which a gas discharge can be expanded.

The body of the supersonic nozzle is illustrated in Figure seven. The body is nine inches in length. A 3/4 " half-nipple is welded to a 3/4 " stainless steel tube. The tube is welded to a spacer to fill the space between the outer diameter of the tube and the inner diameter of the 65/40 spherical joint. The outer edge of the spacer is welded to the inner surface of the vacuum side of the 65/40 spherical joint. A 1 1/2 " half-nipple is welded to the inner surface of the external side of the spherical joint. A double-sided, 3 3/4 " ConFlat flange with two 1/8 " normal pipe threaded holes is mounted on the 3 3/4 " flange of the 1 1/2 " nipple using a copper gasket. One hole is plugged. The second hole

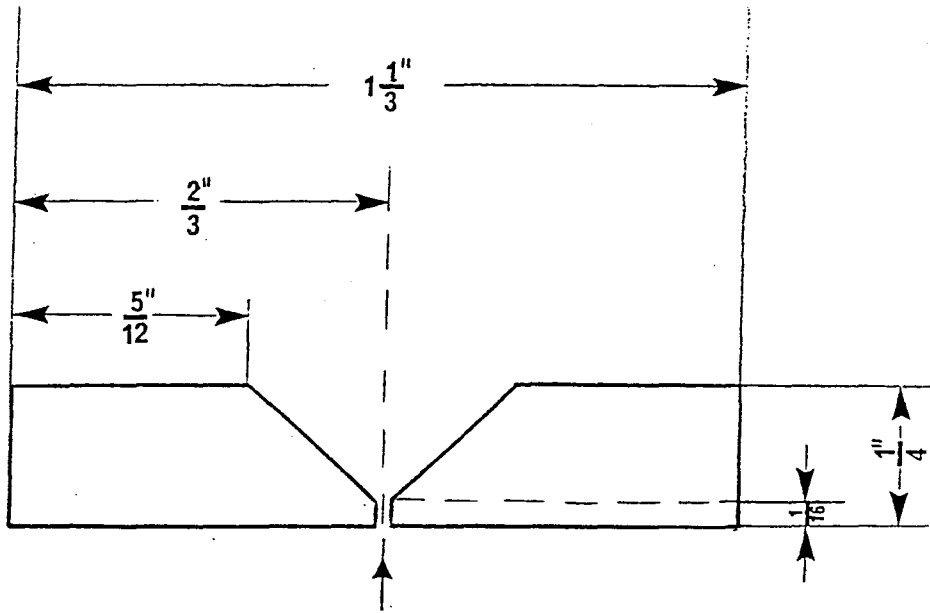


FIGURE 6.
ANODE ASSEMBLY

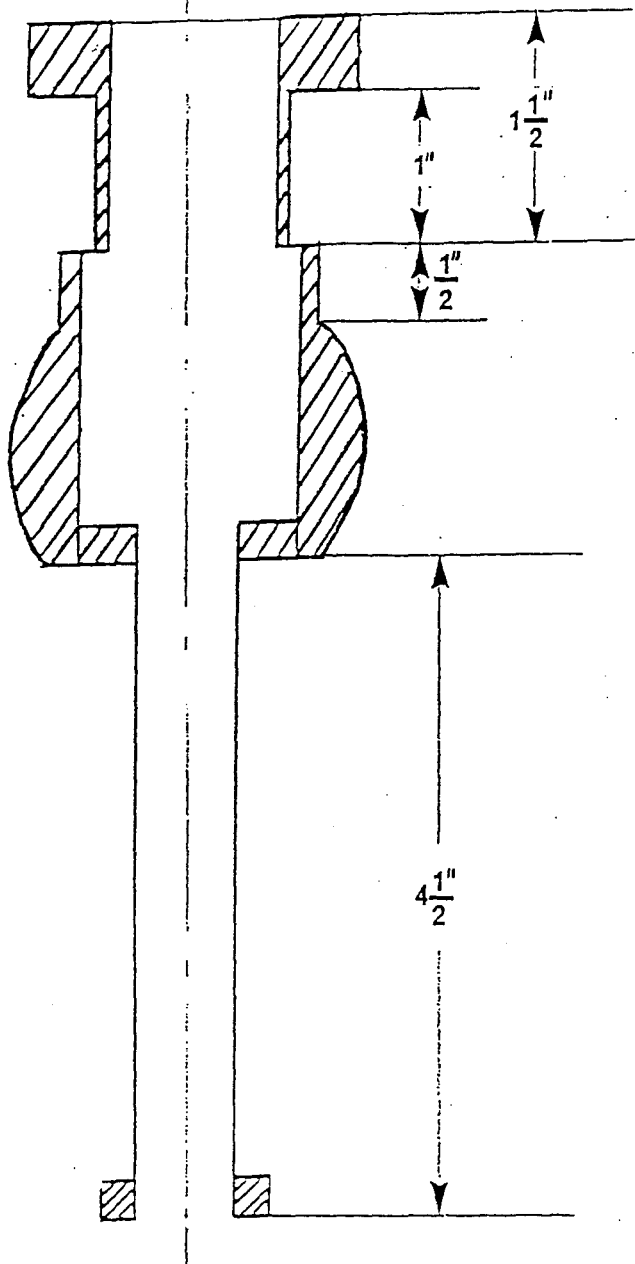


FIGURE 7.
BODY OF THE SUPERSONIC JET.

is used for connecting the discharge nozzle to the gas handling system.

The assembled discharge nozzle consisting of cathode assembly, anode, and body is illustrated in Figure eight. The cathode assembly is mounted on the 3 3/4" flange of the body. Special attention is paid to the length adjustment of the cathode assembly to ensure proper electrode gap. The anode is mounted on the 1 1/3 " Conflat flange using a copper gasket.

The electronics which interface to the supersonic discharge nozzle are illustrated in Figure nine. An adjustable 1800 W, 12 KV power supply is used to initiate and maintain the discharge. A 1 KW, 50 kilo-ohm, current limiting resistor bank is placed in line between the high voltage output of the power supply and the cathode of the supersonic discharge nozzle. The voltage-drop across a ten kilo-ohm resistance of the resistor bank serves to measure the current through the circuit containing the discharge nozzle. A voltage divider is placed between the high voltage output of the power supply and ground. The divider provides a 60 mV response per applied kilovolt and draws less than twenty microamps at 12 KV, i.e. less than 0.3 W power consumption at 12 KV. The body of the discharge valve is held at a common ground potential with respect to the power supply and other components of the apparatus.

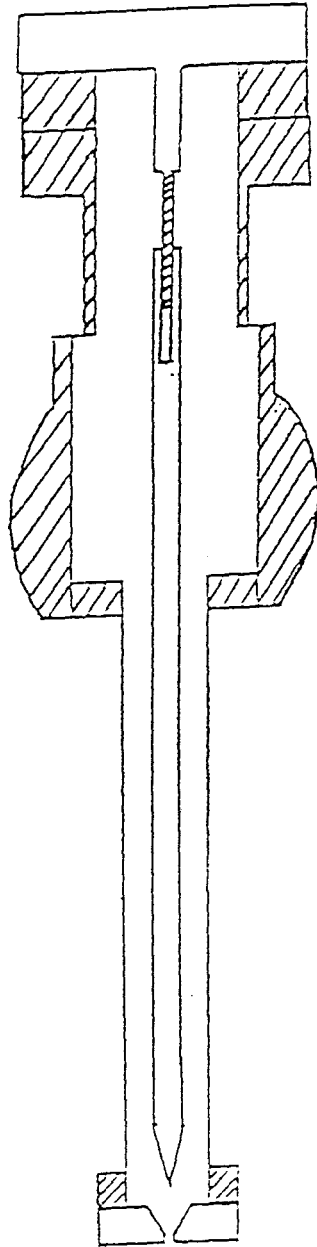


FIGURE 8.
ASSEMBLED DISCHARGE NOZZLE.

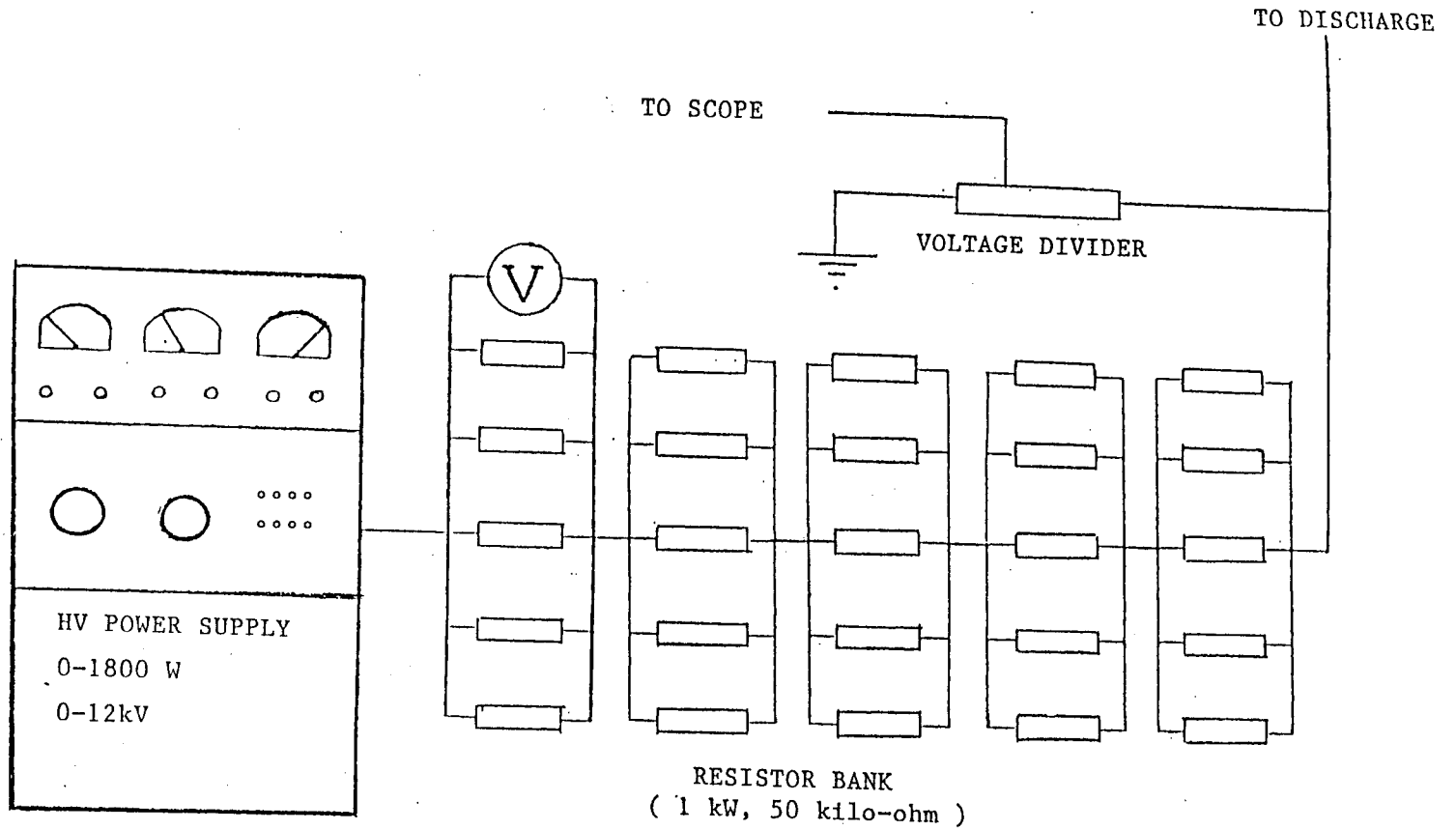


FIGURE 9,
DIAGRAM OF THE ELECTRONICS TO DISCHARGE

(3) Vacuum System

The vacuum system is illustrated in Figure ten. The main chamber is 20 1/2 " long and constructed of borosilicate glass. The discharge nozzle inlet is composed of a ground glass 65/40 spherical socket. The 3 3/4 " long, 1 3/4 " diameter shank of the spherical socket is connected to the 1 3/4 " diameter opening of a sixty degree cone. The 4 " diameter opening of the cone is connected to a 16 " long, 4" diameter cylinder. Two ground glass, 35/25 spherical sockets are connected to opposite sides of the 4 " cylinder. The 35/25 socket axes are perpendicular to the axis of the cylinder. These sockets are placed 8 1/2 " and 15 " from the top of the chamber. The glass chamber is mounted on the outside of the 3 5/8 " diameter shank of a 9 " stainless steel flange. The vacuum integrity is maintained by a greased rubber gasket which fills the small gap between the inner surface of the glass chamber and the outer surface of the stainless steel shank.

The 9 " stainless steel flange is mounted on a liquid nitrogen cryotrap with a nominal air conductance of 1100 liters/second. The cryotrap is mounted on a water cooled baffle with a nominal air conductance of 900 liters/second. The baffle is mounted on an oil diffusion pump with a maximum air pumping speed of 800 liters/second. The diffusion pump is water-cooled using the in-house closed cycle cooling

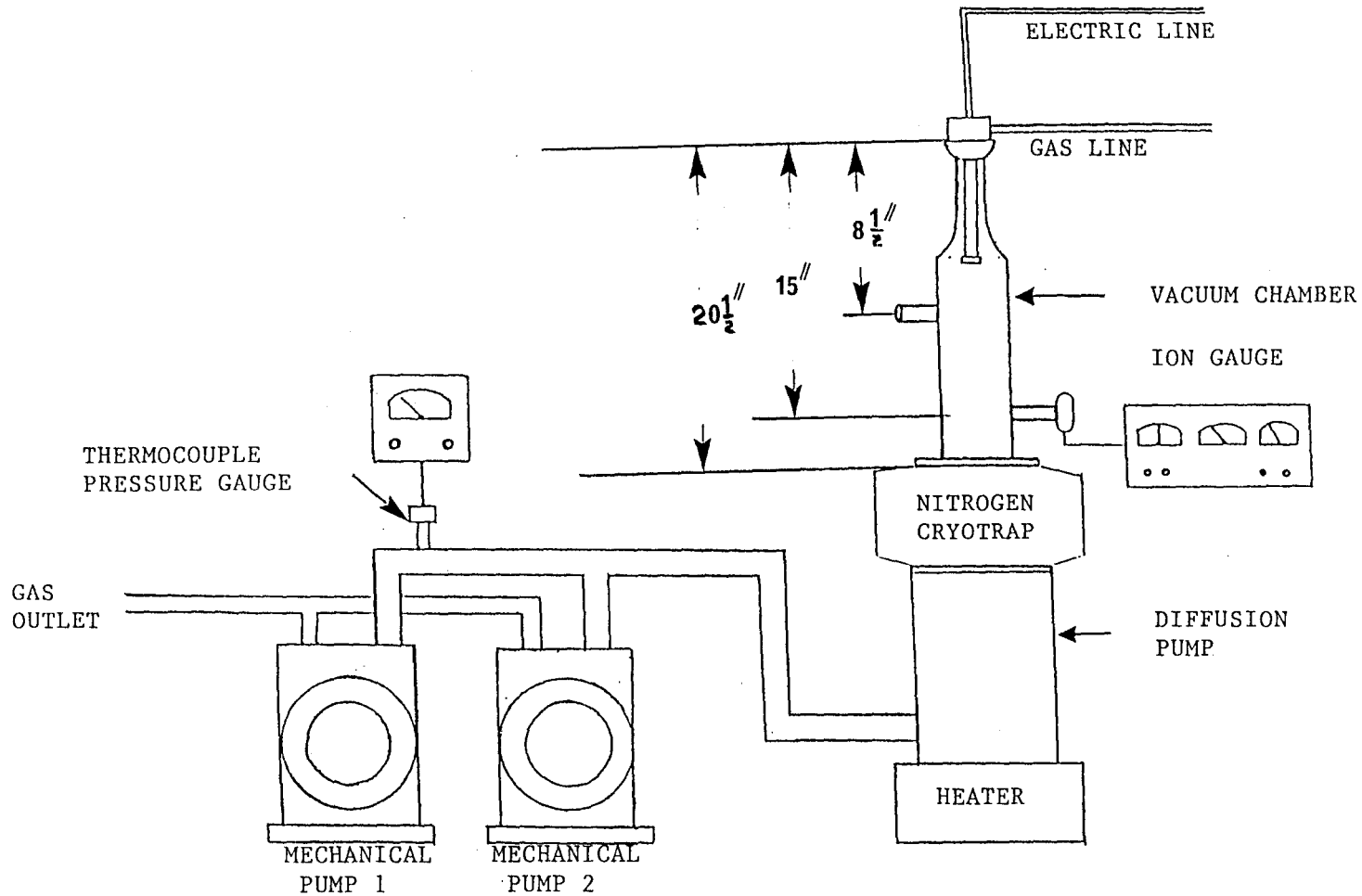


FIGURE 10.
SCHEMATIC REPRESENTATION OF VACUUM SYSTEM.

system. A thermal switch set at 225° F is mounted on the body of the diffusion pump. The switch is used in line with the 1190 W, 120 V diffusion pump heater as an interlock to prevent overheating. Two direct-drive mechanical pumps with nominal air pumping speed of 3.25 liters/second back the diffusion pump. These pumps are configured in parallel and maintain a nominal air pumping speed of 6.5 liters/second at the outlet of the diffusion pump. A thermocouple gauge is used to monitor the forepressure of the diffusion pump. A Bayard-Alpert ionization gauge is used to monitor the pressure in the main chamber. An additional port on the vacuum chamber allows for leak detection trouble-shooting.

(4) Optical System

The dispersed emission system is illustrated in Figure eleven. The main component of this system is a Czerny-Turner Monochromator with a focal length of 480 mm. The reciprocal linear dispersion of the monochromator is 1.6 nm/mm with a 1200 g/mm grating. An end-on photomultiplier tube with a spectral response range of 300 to 850 nm is used as a detector. The photomultiplier tube is chilled by a water-cooled Peltier refrigerator. A 1/2" diameter aluminum rod is connected to a five pound weight on top of the monochromator. The rod extends an adjustable 6 " to 12 " from the side of the monochromator. The rod is parallel to the

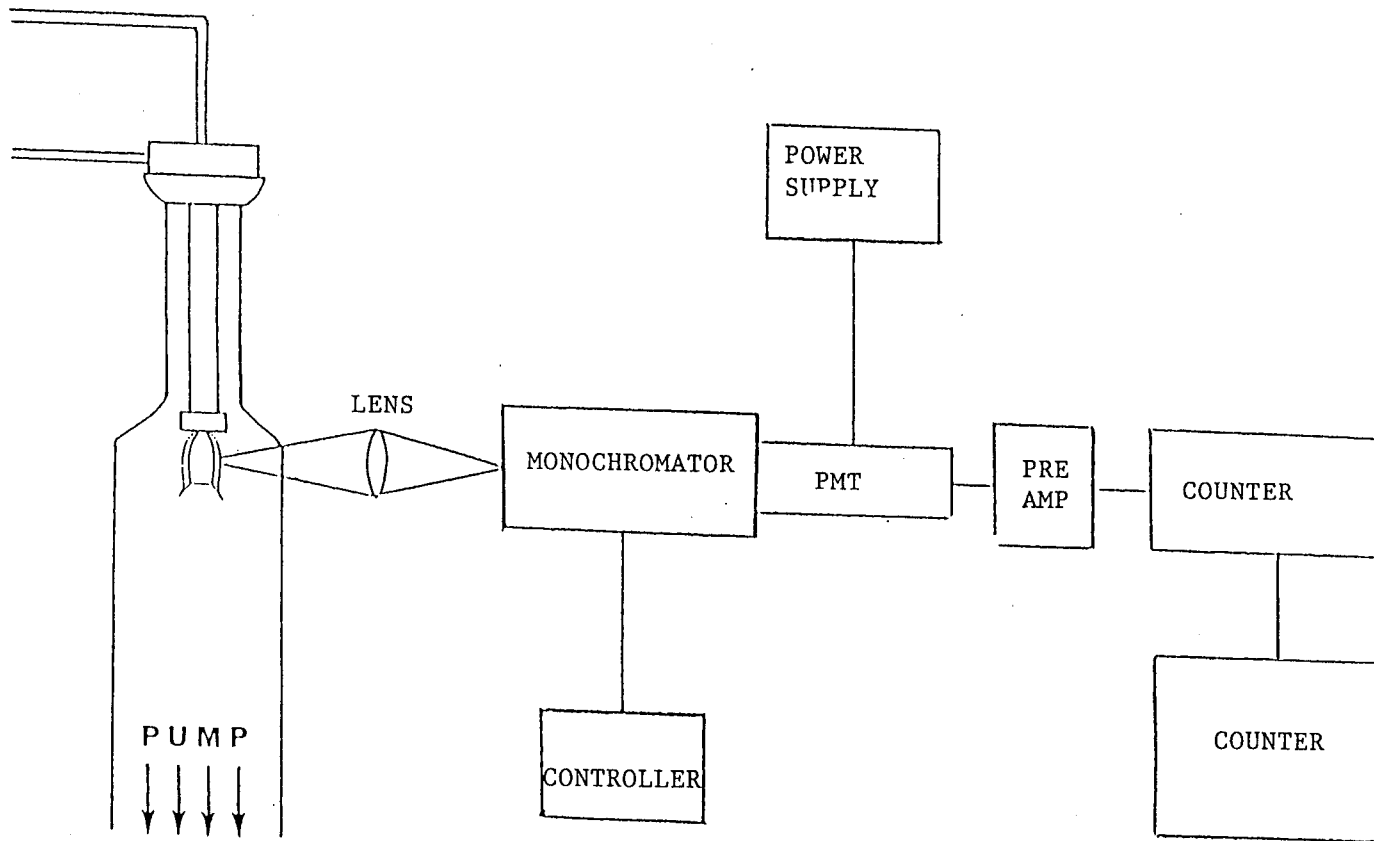


FIGURE 11.
OPTICAL SYSTEM

optical axis of the slits. The collection optics are mounted in standard cylindrical lens holders. The 1/2 " posts of these holders are connected to the aluminum rod using right angle clamp holders. The monochromator, high voltage power supply for the phototube, and power supply for the refrigerator are all mounted on a wooden platform which rests upon three lab jacks. This arrangement allows for positioning the optical axis of the detection system at different distances from the nozzle by moving the entire detection system up or down on the platform while maintaining the relative positions of the monochromator and collection optics. The axes of the optical components are maintained perpendicular to the vacuum chamber axis and thus the jet axis.

The monochromator has a key pad module for manual control. A standard RS-232 C cable connects the serial communications port of a microcomputer to the 25 pin connector on the keypad module. This connection allows for remote control of the monochromator using a computer.

(5) Data Acquisition

The data acquisition electronics are illustrated in Figure 12. The signal from the anode of the photomultiplier tube passes through a Modern Instrument Technology Combo-100 preamplifier. The Combo-100 is a dual unit consisting of F-

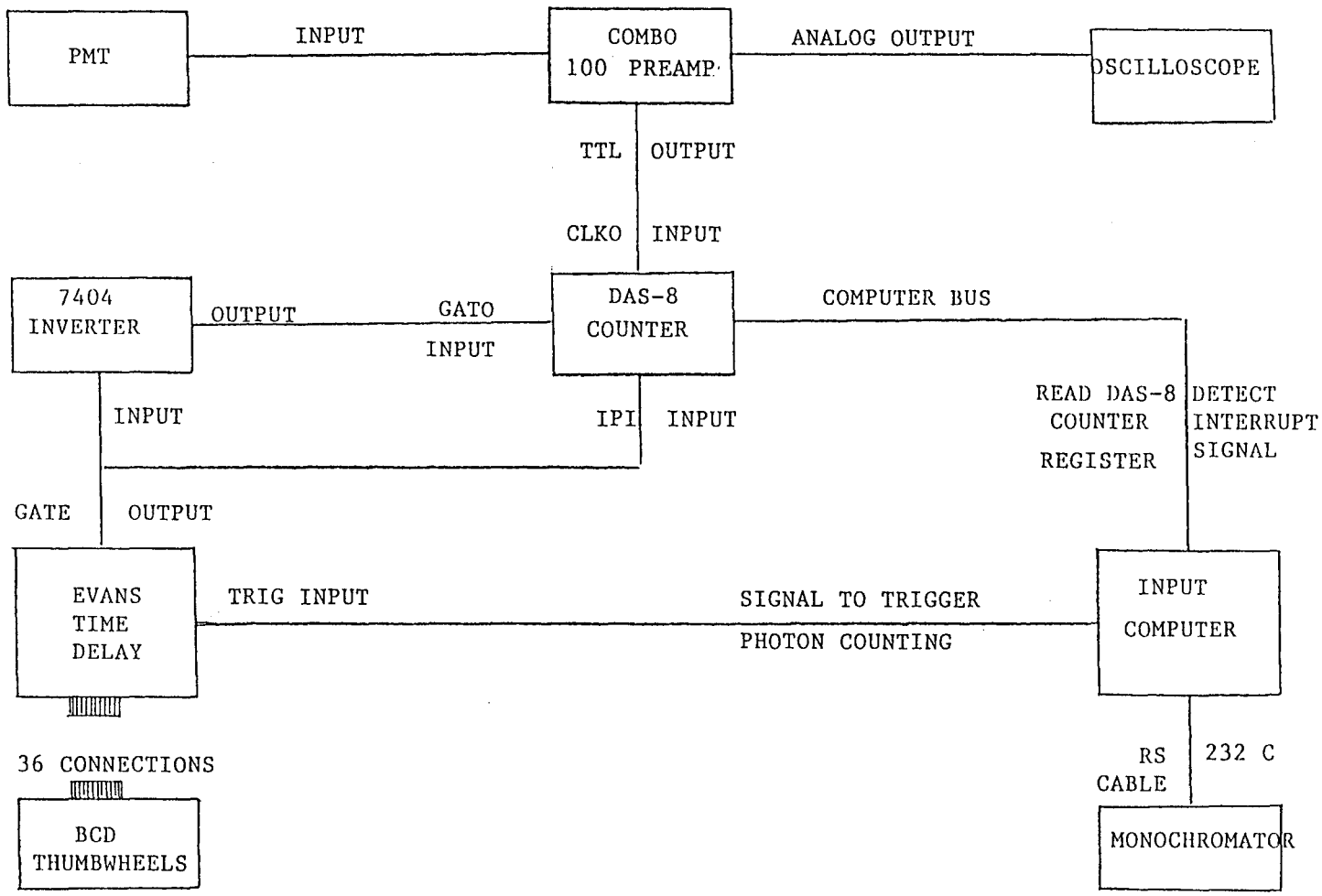


FIGURE 12.
SCHEMATIC FOR DATA ACQUISITION.

100T pulse preamplifier and current-to-voltage converter operating in parallel. The analog output of the Combo-100 is monitored using a Tektronix 100 MHz digital storage oscilloscope. This allows for real time observation of the photomultiplier signal. The TTL pulse output of the Combo-100 is connected through a coaxial cable to the pin 2 (CLK0) of the MetraByte DAS-8 main I/O connector. The TTL transitions are counted and the total number stored in a register on the DAS-8 board. The register is subsequently read and reset to zero by the computer. Counting is inhibited by a low level input (e.g. shunt to ground) at pin 21 (GATE0) of the MetraByte DAS-8 main I/O connector. The counting period is controlled in this way by providing a variable length low level input at pin 21 using the inverted output of pin 13 (GATE) of the Evans 4145/4146 programmable time delay module.

The Evans 4145/4146 time delay module has three outputs, each of which produces a time-delayed pulse following a low level transition applied to a single input. The output at pin 13 (GATE) of the Evans 4145/4146 module is the only one used. It generates a pulse which is coincident in time with the programmed delay interval, i.e. the pulse width is equal to the delay interval. The time delay interval is set by inputs at 36 pins of the module. Inputs are negative, or ground, true only. The A8 (pin 17), A4 (pin U), A2 (pin V), and A1 (pin 18) inputs comprise the least significant BCD digit. The

B inputs comprise the next most significant BCD digit, and so on. These logic inputs are provided by BCD thumbwheel switches. The time delay is adjustable to 9.99999999 seconds in increments of 10 nanoseconds. The output at pin 13 (GATE) is connected to the input of a 7404 inverter. The output of the inverter is connected to MetraByte DAS-8 pin 21 (GAT0). This provides gating of the count period.

A hardware interrupt of the computer must be provided to prevent execution of software program lines before the count period is complete. For example, the count register should not be read during the count period. Pin 13 (GATE) of the time delay module is connected at pin 25 (IP1) of the MetraByte DAS-8 main I/O connector. The software is written to halt program execution when the output at pin 13 is negative logic ground. Pin 13 is negative logic ground during the count period.

The counting process is initiated by a negative logic pulse applied to pin 11 (TRIG) of the time delay module. Pin 11 (TRIG) is connected to pin 6 (OUT2) of the DAS-8 main I/O connector. The counting process is initiated by a software triggered strobe, i.e. a negative logic pulse is software initiated.

The use of the latter mentioned components in obtaining a spectrum is summarized as follows. The count register is software zeroed. The monochromator's angular grating position and slit widths are set by software controlled serial

communication through the RS-232 C ports. The photon counting process is initiated by the software triggered strobe. Program line execution is halted until the hardware interrupt indicates positive logic, true, i.e. until the counting process is completed. The count register is read. The wavelength calculated from the grating position and the count are stored in random access files on a floppy disk drive. The last process is repeated using another grating position. The resulting wavelength, grating position, and count arrays constitute a spectrum.

B. Procedure

(1) Gas Flow Adjustment

The essential apparatus is illustrated in Figure four. Low-oxygen nitrogen is used in all experiments. Prior to opening the cylinder valve, the fine metering valve and the gate valve are closed completely. The cylinder valve is opened completely. The pressure at the outlet of the nitrogen cylinder's two-stage regulator is adjusted to 30 psig (approx. 3 atm absolute). This pressure is maintained for all experiments. The pressure in the discharge nozzle is adjusted by opening the fine metering valve till the desired pressure is indicated on the mechanical gauge. This pressure is typically not more than 1 atm. The mass flow through the

fine metering valve remains essentially constant irrespective of whether another source of gas increases the pressure in the discharge nozzle. The mass flow remains essentially constant due to the large pressure gradient between the inlet (>3 atm) and outlet (>1 atm) of the fine metering valve. This feature is not used in these experiments but would be useful for creating binary mixtures using the second gas source of the apparatus.

(2) Discharge Initiation

The essential apparatus is illustrated in Figure nine. The discharge is initiated by manually adjusting the rheostat of the high voltage power supply until a voltage drop is read across the resistor bank. This indicates current flow. The potential for the onset of the discharge is typically 2 kV. A continuous discharge can subsequently be maintained at potentials as low as 1.5 kV. The intensity of the emission fluctuates initially. This fluctuation subsides markedly within a 15 minute warm-up period. Long-term fluctuations persist even after the warm-up. These fluctuations have a period of approximately five minutes. They are attributed to the unavoidable changes in the electrode surfaces and hence the discharge conditions of a flowing system. Subsequent procedures were developed with consideration directed toward this observation.

(3) Spectral Data Collection

The essential apparatus is illustrated in Figure eleven. The collection optic used in these experiments is a 40 mm diameter, 75 mm focal length lens. The lens is placed approximately 300 mm from the axis of the vacuum chamber and hence the fluorescing nitrogen jet. The entrance slits of the monochromator are placed approximately 100 mm from the lens. The large distance between the jet axis and the lens is used to minimize the aberrations induced by trying to image a source of emission which is large (the jet is 1 cm in diameter) in comparison to the focal length of the lens. Collection of the spectra is computer controlled. Spectra are saved on floppy disks. The software written to control the collection and display of the spectra is in Appendix A.

(4) Intensity Dependence on Pressure Measurements

The essential apparatus is illustrated in Figure four. A stop flow technique is used to determine the dependence of a bands emission intensity on pressure. The pressure in the discharge nozzle is adjusted to exceed the highest pressure for which the intensity is to be measured, typically 1000 torr. The gate valve is closed. The pressure in the discharge nozzle begins to drop immediately after the valve is closed. The time it takes the pressure to drop from 1000

torr to 950 torr, 1000 torr to 900 torr, and so on is recorded. The functional relationship between the pressure change and time is exponential. The latter data can be used to calculate the pre-exponential and exponential factors. Subsequent to obtaining this information the monochromator is adjusted to the frequency of interest. The pressure is readjusted to exceed 1000 torr. The gate valve is closed. When the pressure drops to 1000 torr a program is initiated which repeatedly integrates for one second intervals the intensity signal. The number of times the program performs the integration depends on the lower pressure limit desired. This gives a record of the change in intensity as a function of time. This information coupled with the functional dependence of pressure on time gives the intensity dependence on pressure.

CHAPTER IV

RESULTS

Using the polarity illustrated in Figure one, we are able to strike the discharge using voltages in excess of 1.5 KV and nozzle reservoir pressures in excess of 400 torr. The current flow is found to depend on voltage. Applied voltages of 1.75 KV result in a current of 20 milliamps using a nozzle pressure of approximately 1000 torr. Applied voltages of 2.5 KV result in a current of approximately 30 milliamps at the same nozzle pressure. The current is found to depend only mildly on nozzle pressure. Holding the voltage constant, the current is found to vary less than three percent over a pressure range of 500 - 1000 torr.

We observe the discharge to be maintainable at voltages as low as 1.3 KV and nozzle pressures as high as about two atmospheres. Much beyond these limits, we observe the discharge to be unstable in both electric and optical respects.

We note that by using a polarity opposite to that illustrated in Figure one, we are able to strike the discharge only with voltages in excess of 4.0 KV. The resulting

discharge is dark.

Using the polarity illustrated in Figure one within limits cited above, we observe the expanding supersonic jet discharge to be visibly yellow. The jet extends as much as 30 cm beyond the discharge nozzle at stagnation pressures exceeding one atmosphere. The jet is visibly of width less than a centimeter.

Emission spectra recorded in the range of 3000 - 6000 Angstroms are observed to be composed of three systems:

(1) The second positive group emission. This stems from radiative transitions involving the C- and B-electronic states of molecular nitrogen.

(2) The first positive group emission. This stems from radiative transitions involving the B- and A-electronic states of molecular nitrogen.

(3) The first negative group emission. This stems from radiative transitions involving the B- and the X-electronic states of molecular nitrogen ion.

Of the above three spectroscopic systems of molecular nitrogen, we observe the second positive group emission to be the dominant one. Representative spectra for the above three systems are presented in Figures thirteen - fifteen.

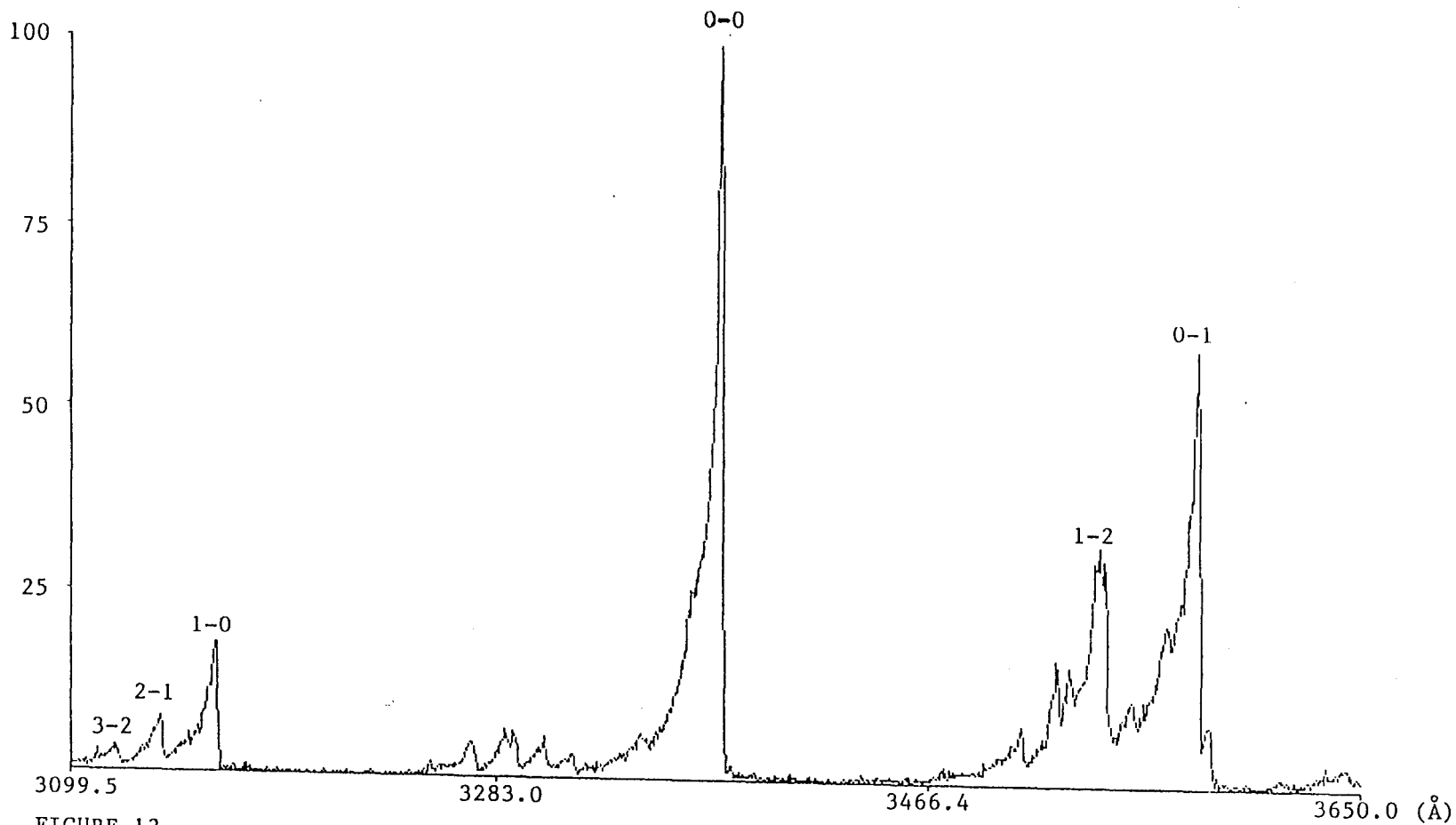


FIGURE 13.
SPECTRUM OF THE C³Π_u - B³Π_g SECOND POSITIVE SYSTEM

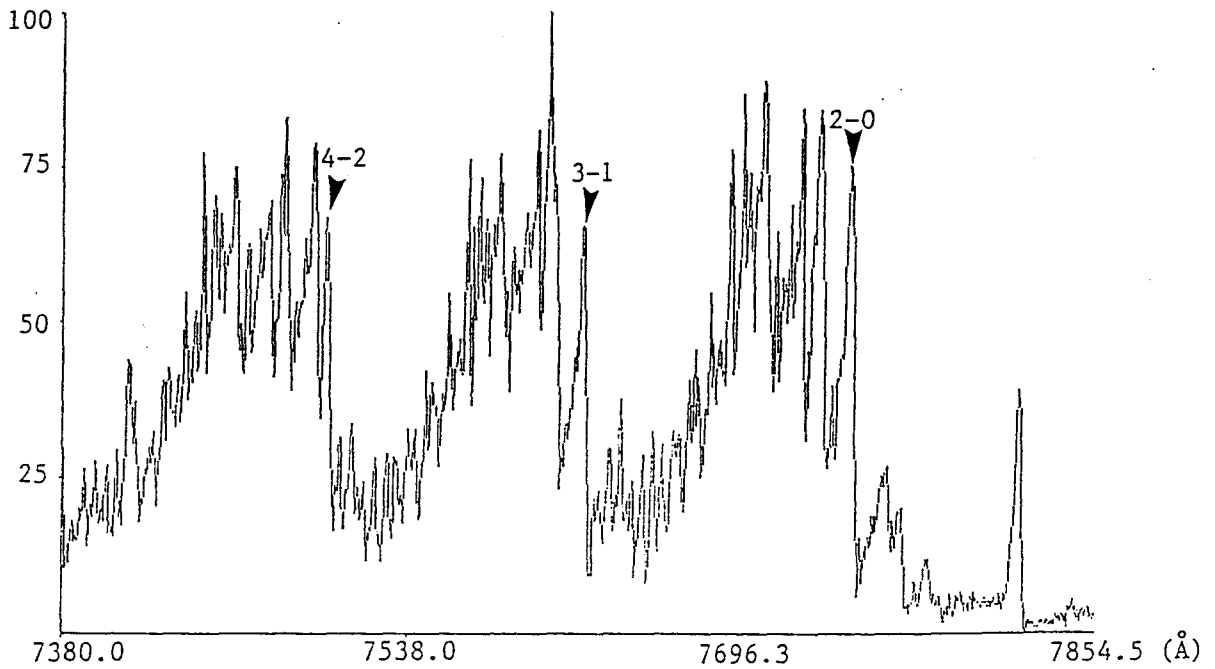
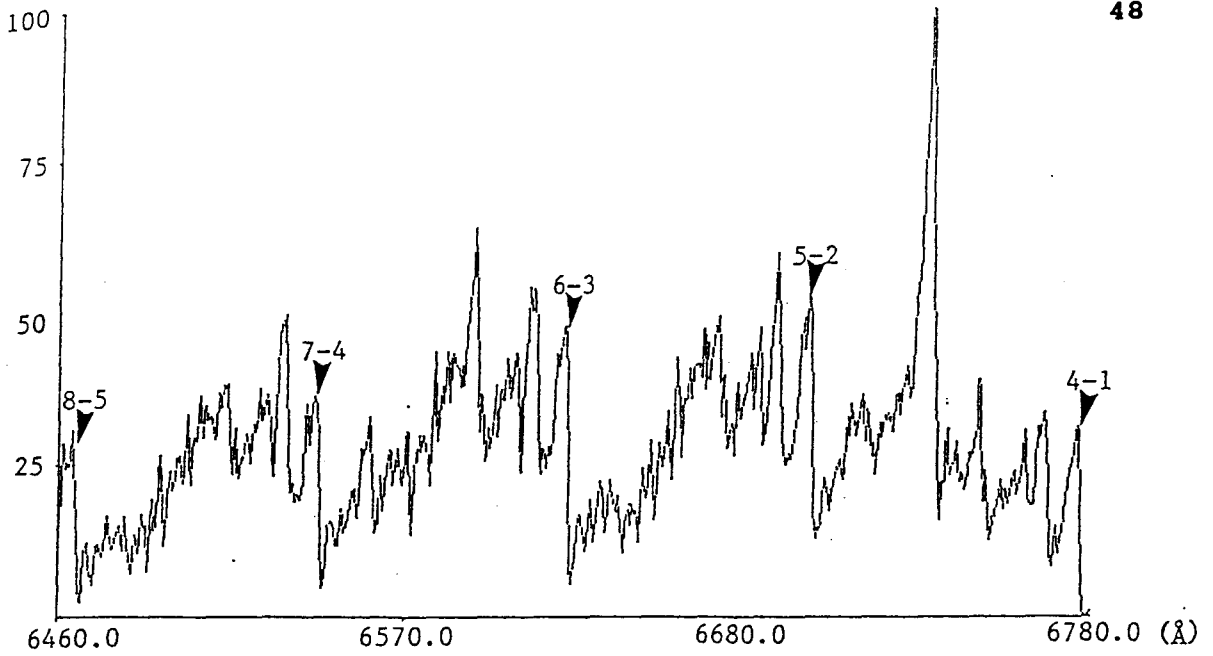


FIGURE 14.
SPECTRA OF THE $B^3\Pi_g - A^3\Sigma_u^+$ FIRST POSITIVE SYSTEM

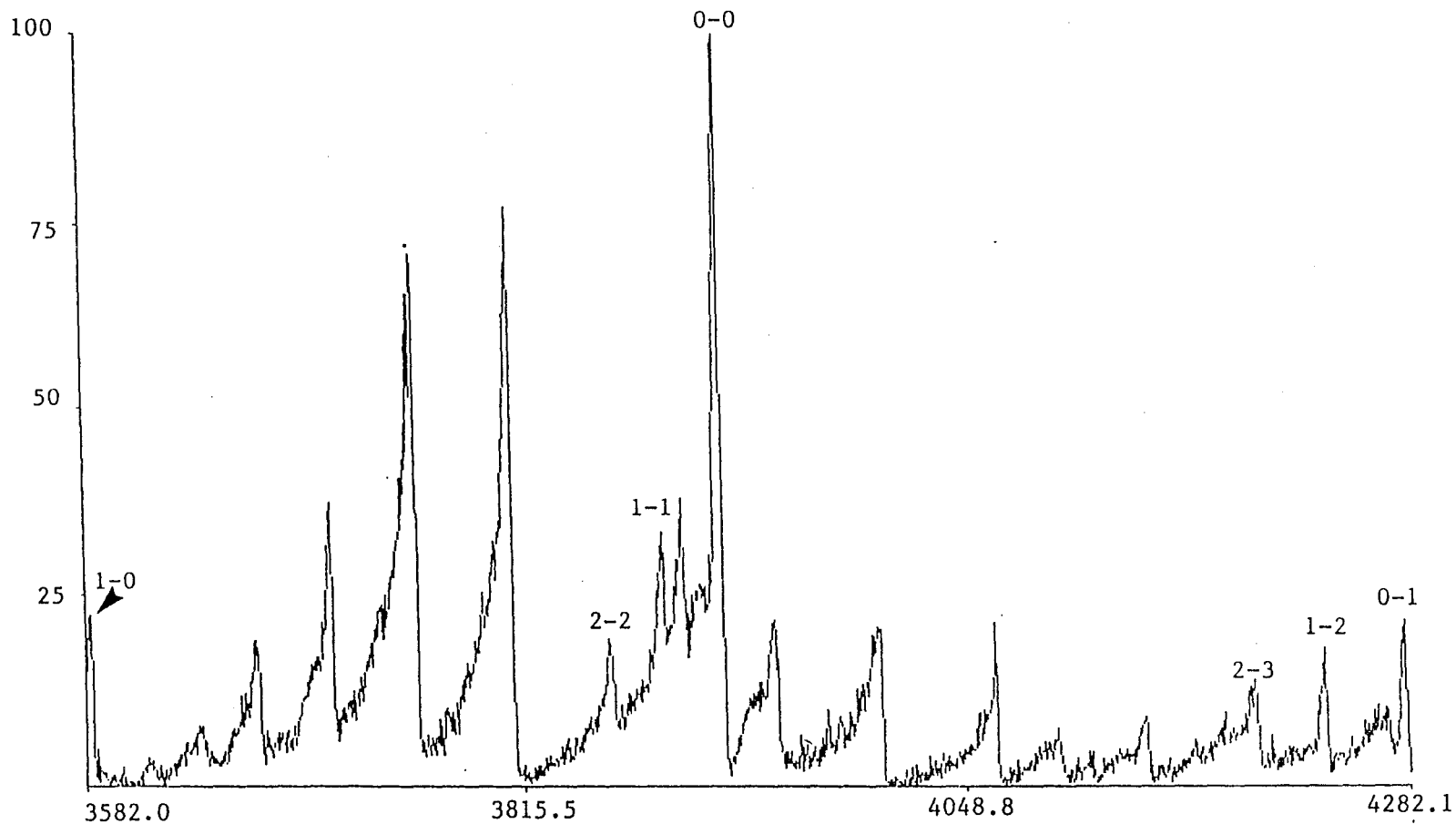


FIGURE 15
 SPECTRUM OF THE $B^2\Sigma_u^+ - X^2\Sigma_g^-$ FIRST NEGATIVE SYSTEM

We observe no emission associated with other systems of nitrogen molecule and nitrogen ion. We observe no impurity emission by way of metal atoms and ions sputtered from the discharge nozzle. We observe no emission from nitrogen atoms or ions. We observe no emission from possible gas cylinder contaminants, e.g. molecular oxygen.

We observe that the contribution of nitrogen ion signals (i.e. the first negative emission) relative to those of nitrogen molecule (i.e. the first and second positive group emissions) to the spectra is determined by applied voltage. In particular, we observe the first negative emission intensity to increase with increasing voltage, relative to the first and second positive group intensity. Representative data are presented in Figure sixteen by way of spectra recorded at 1.75 and 2.5 KV applied to the nozzle.

We observe the visible length of the expanding supersonic jet to be dependent on the nozzle reservoir pressure. We have measured the visible length as a function of nozzle pressure. In particular, we observe the length to scale as the square of the reservoir pressure. Representative data correlating the visible length of the jet with nozzle pressure are presented in the log-log plot of Figure seventeen.

We observe the spectral intensity derived from the core of the expanding supersonic jet to depend on the nozzle pressure. Representative data correlating intensity derived from the core of the jet five centimeters downstream from the

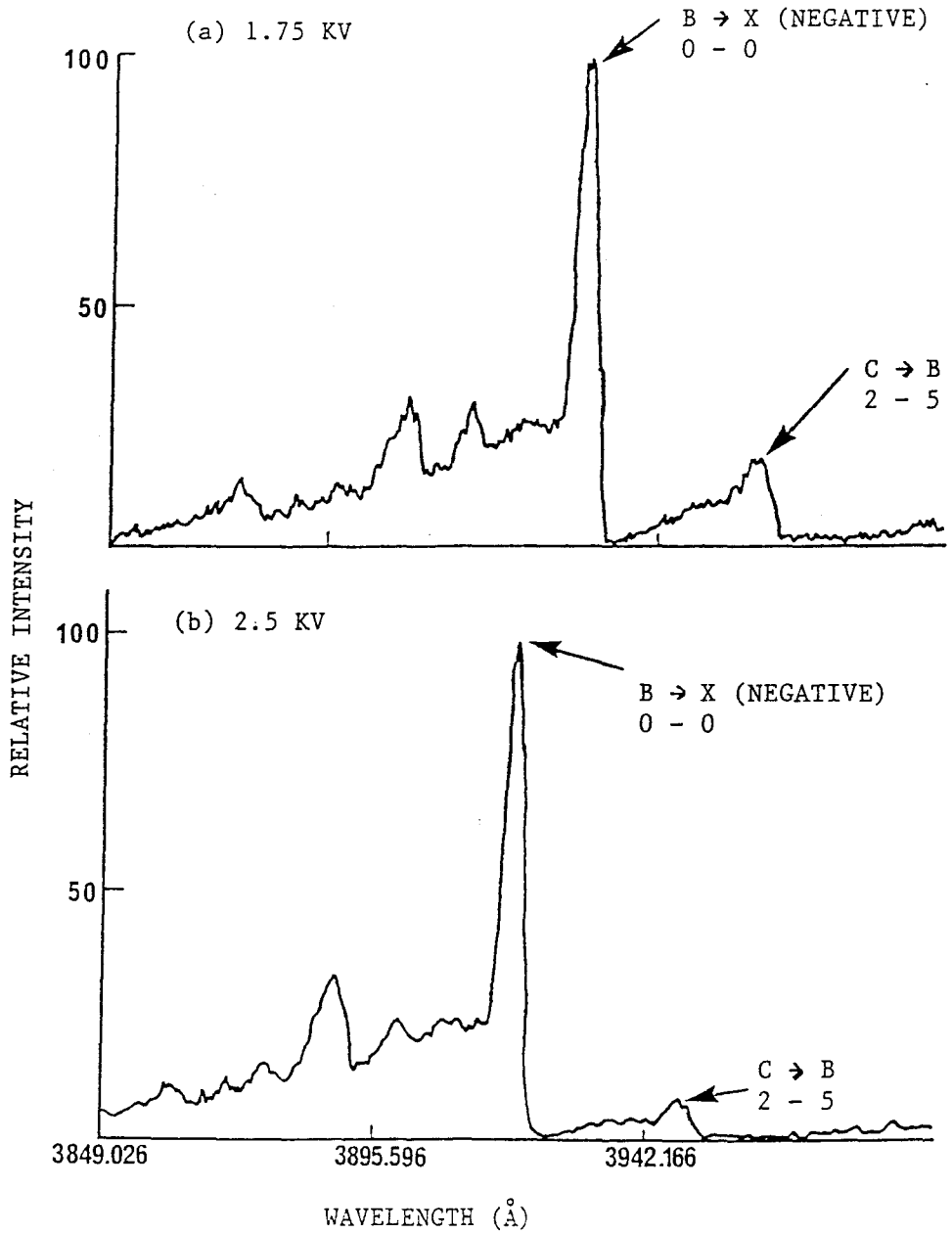


FIGURE 16.
ILLUSTRATION OF THE INCREASE OF THE FIRST NEGATIVE
EMISSION INTENSITY WITH INCREASING VOLTAGE, RELATIVE
TO THE FIRST AND SECOND POSITIVE GROUP INTENSITY.
(a) 1.75 KV AND (b) 2.5 KV ARE REPRESENTATIVE FIGURES.

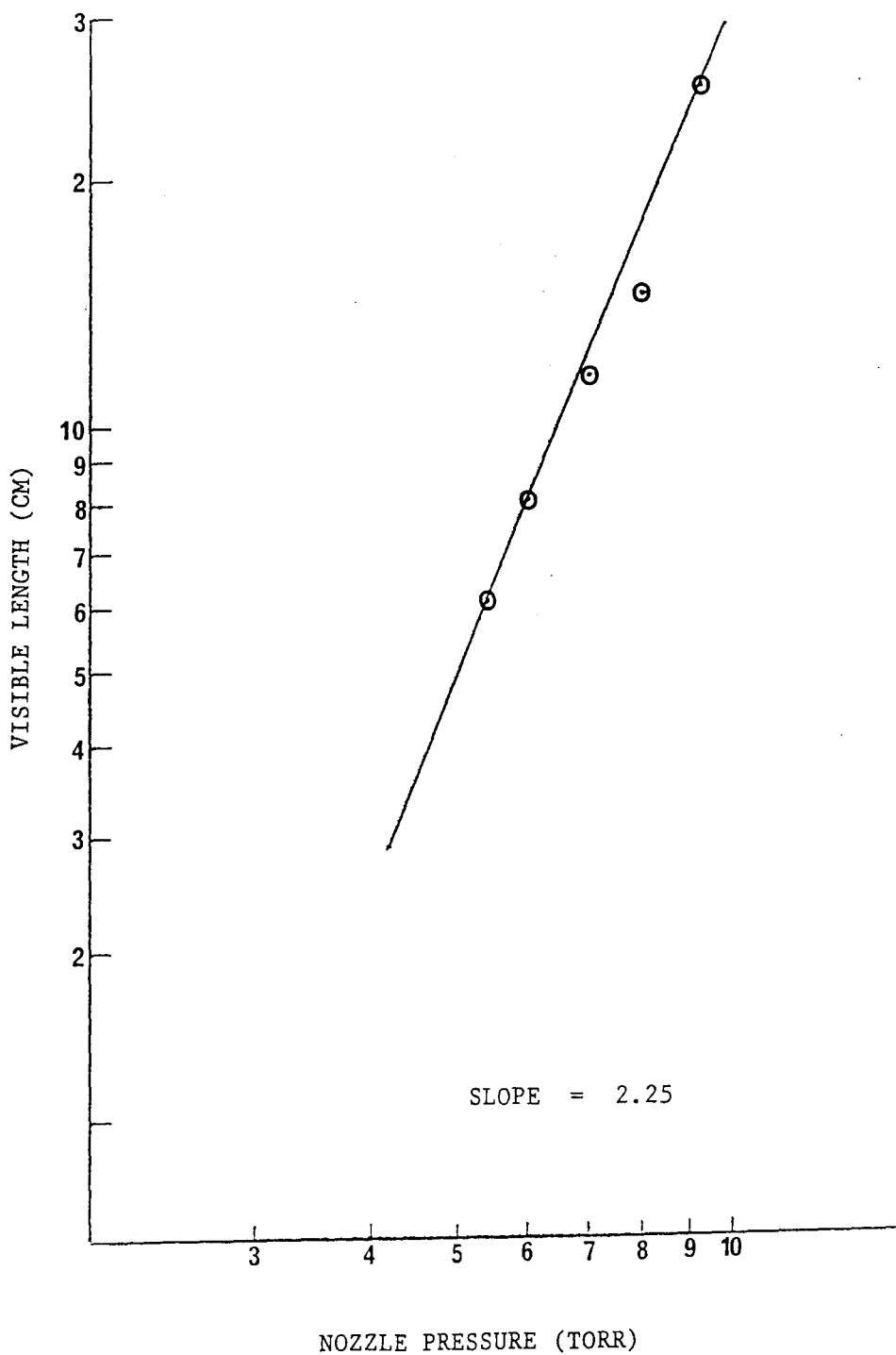


FIGURE 17.
REPRESENTATIVE DATA CORRELATING THE VISIBLE LENGTH OF
THE JET WITH THE NOZZLE PRESSURE.

nozzle as a function of nozzle pressure are presented in Figure eighteen and nineteen. The data concern transitions of the second positive group. Spectral intensities are found to scale as p^n where n ranges from 1.65 - 1.85 (+/- 0.2).

Under most conditions, e.g. those concerning Figures eighteen and nineteen, the spectral intensity is found to scale approximately as the square of the nozzle reservoir pressure. The word "most" is used as we find the intensity-versus-pressure dependence to be sensitive to the conditions under which the nitrogen is excited inside the nozzle. By "excitation conditions", we refer to a number of factors including the electrode gap and applied field within the nozzle. For example, under other excitation conditions, we have found the spectral intensity to scale as p^n where n has run as high as 4. Representative data are presented in Figure twenty.

While we observe the intensity-versus-pressure dependence to be sensitive to the excitation conditions, we find the opposite situation concerning the pressure dependence of the structure and intensity distribution within the individual spectroscopic systems. In particular, the spectral intensity distribution derived from the core of the expanding supersonic jet is found to be nearly independent of nozzle pressure. Spectra recorded using nozzle pressures in the range of 0.5 to 2 atm are virtually identical. Further, the spectral intensity distribution derived from the core of the jet is

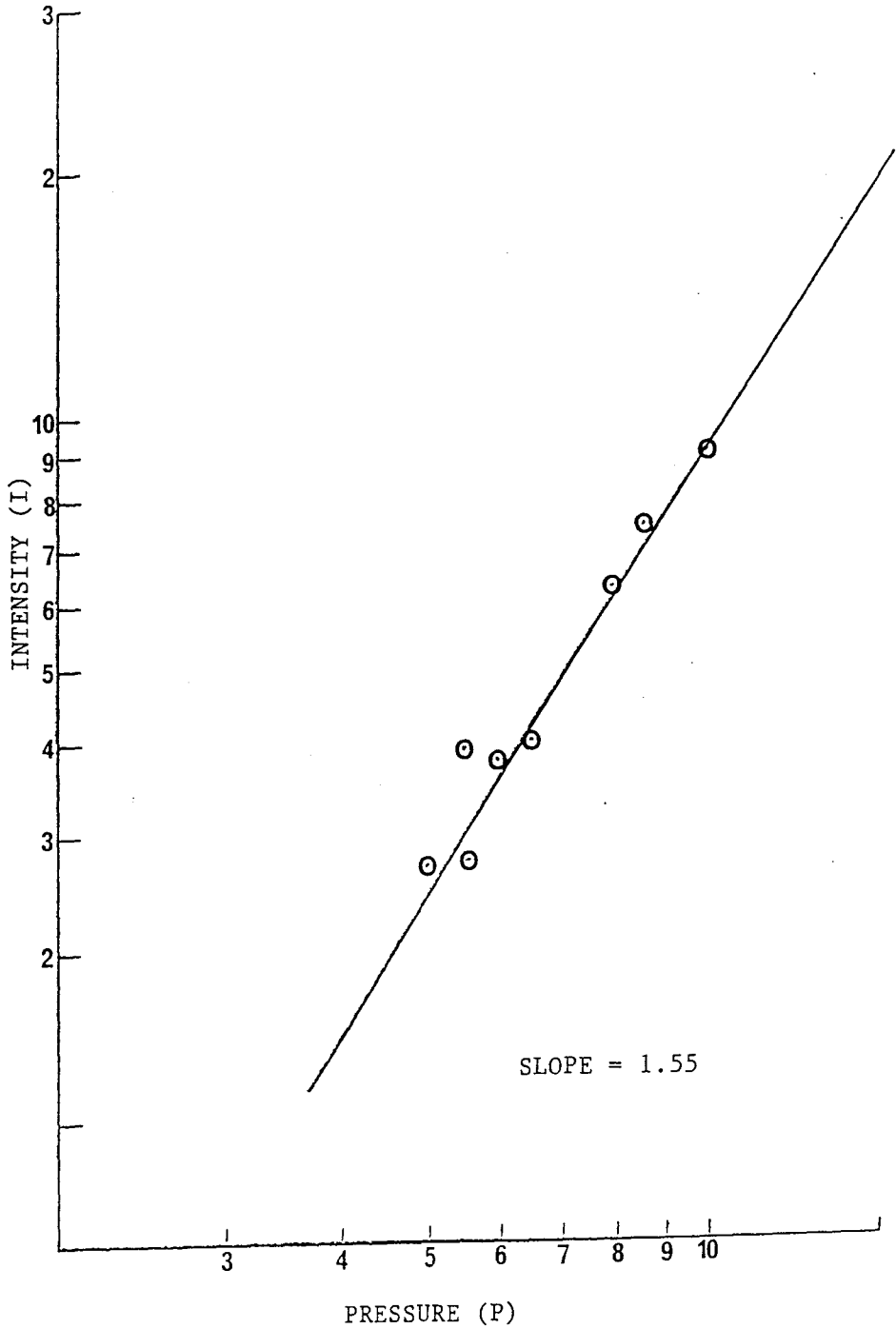


FIGURE 18.
SPECTRAL INTENSITY VERSUS NOZZLE RESERVOIR PRESSURE FOR
THE SECOND POSITIVE 1 - 0 BAND.

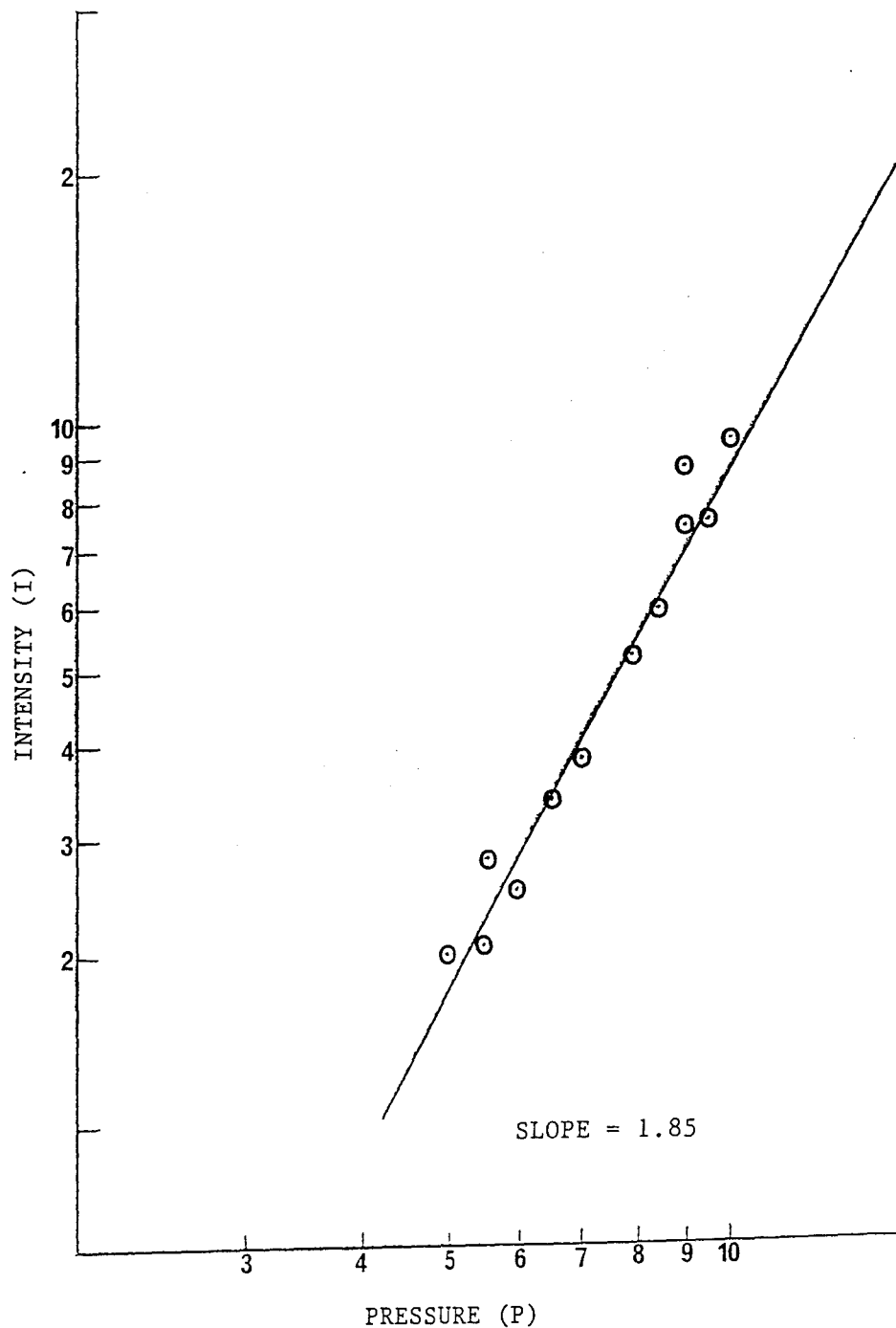


FIGURE 19.
SPECTRAL INTENSITY VERSUS NOZZLE RESERVOIR PRESSURE FOR
THE SECOND POSITIVE 2 - 1 BAND.

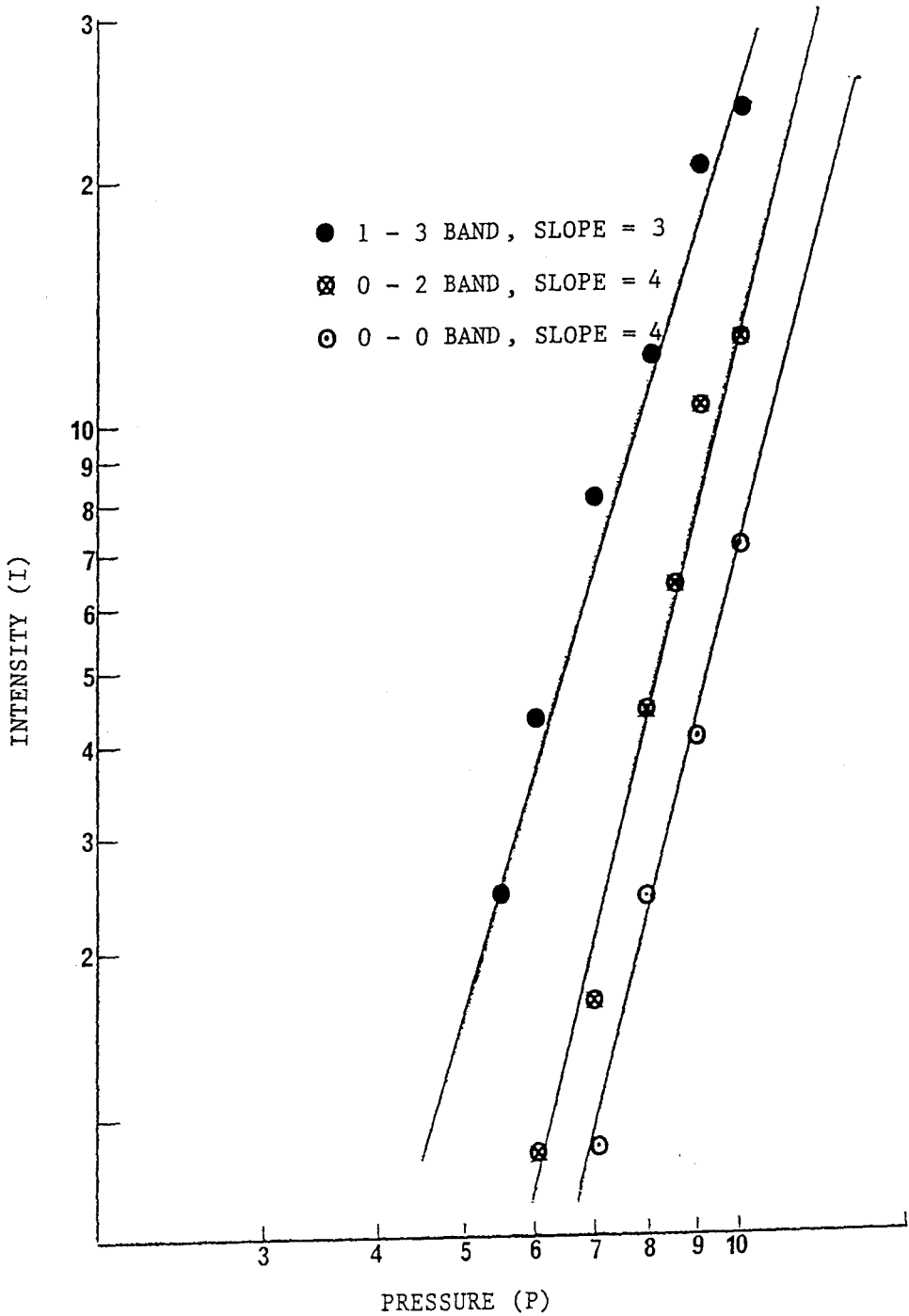


FIGURE 20.
 SPECTRAL INTENSITY VERSUS NOZZLE RESERVOIR PRESSURE
 SHOWING THREE SELECTED BANDS.

found to be independent of observation distance from the nozzle along the axis of the jet. Representative data are presented in Figure twenty-one regarding the second positive group emission recorded at different reservoir pressures, all other conditions remaining the same. We have observed only slight differences concerning the spectral distribution when using nozzle pressures of two atmospheres, i.e. near the limit of stable operation of the nozzle. Toward these limits, we observe the distributions to be altered slightly insofar as a greater proportion of intensity is found in transitions involving higher vibrational levels of the C-electronic state.

Electronic-vibrational transition intensities scale as

$$I_{\nu'} \propto R^2 q_{\nu'} \nu^4 N_{\nu'}$$

where ν is the characteristic frequency, R is the transition moment, $q_{\nu'}$ is the Franck-Condon factor, and $N_{\nu'}$ is the population of the emitting state.

Under equilibrium conditions, the population term is proportional to the Boltzmann factor, viz.

$$N_{\nu'} \propto \exp (- \beta E_{\nu'})$$

where $\beta = (k_B T)^{-1}$ and $E_{\nu'}$ is the vibrational energy relative to that of the $\nu' = 0$ level. It follows that under equilibrium circumstances, plotting the natural log of

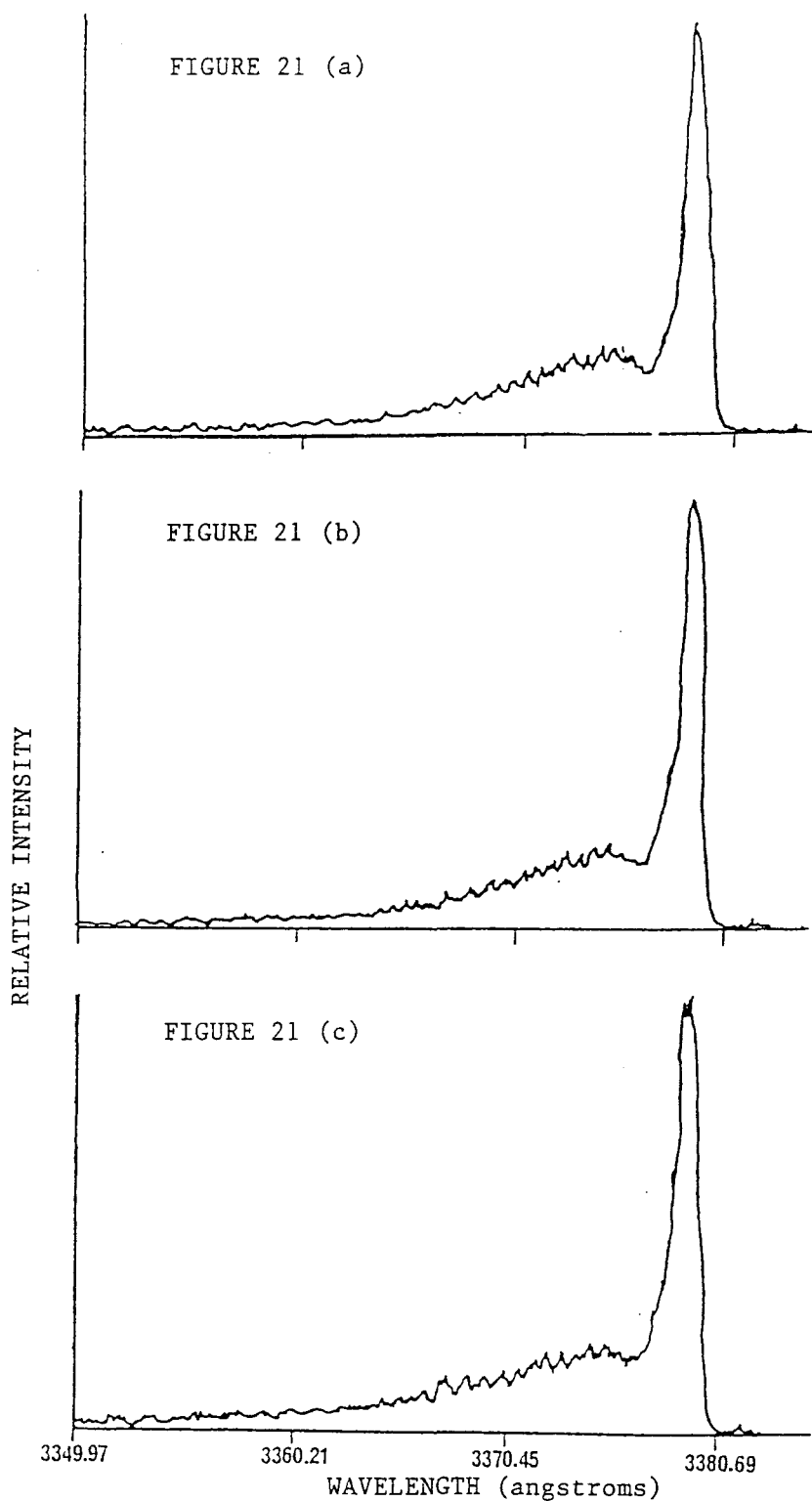


FIGURE 21.
SECOND POSITIVE 0 - 0 BAND AT DIFFERENT PRESSURES:
(a) 8, (b) 14, AND (c) 16 psig RESPECTIVELY.

$I_{v'}/R^2v^4q_{v'}$ versus $E_{v'}$, one obtains a straight line with slope $-\beta$. In this way one can associate a vibrational distribution and, in turn, a temperature with the emission spectrum.

We direct the above ideas to our own data for the second positive group emission of molecular nitrogen in a supersonic jet. Illustrated in Figure twenty-two is a natural log-linear plot presenting the vibrational distribution of the C-state of nitrogen. We have made use of measured values for the Franck-Condon factors cited in Reference 13. We observe the vibrational distribution to be arguably non-Boltzmann in that two temperatures appear to be suggested by the data points. "Best" straight lines correspond to vibrational temperatures of ca. 900 and 3300 K. The "best" straight line taking into account all of the data points corresponds to a vibrational temperature near 2800 K for C-molecular nitrogen in the supersonic jet.

Electronic-vibrational emission of the first negative group is given analogous treatment by way of the natural log-linear plot presented in Figure twenty-three. We have used the Franck-Condon factors listed in Reference 13. The "best" straight line corresponds to a vibrational temperature near 1800 K for B-molecular nitrogen ion in the supersonic jet.

We extend analogous treatment to the electronic-vibrational emission of the first positive group by way of the natural log-linear plot of Figure twenty-four. We have

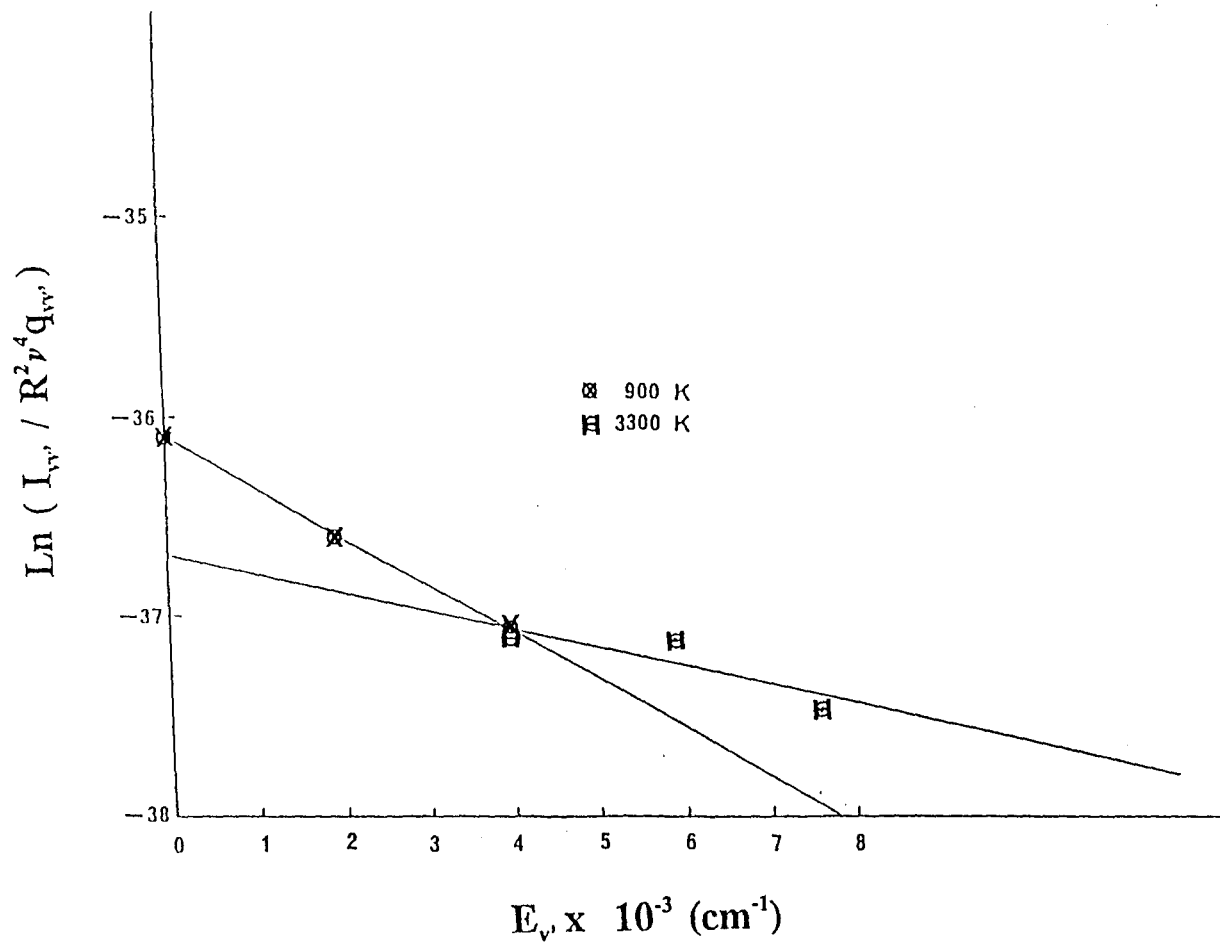


FIGURE 22.
 THE VIBRATIONAL DISTRIBUTION OF THE C - STATE OF NITROGEN AT
 CA. 900 K AND 3300 K.

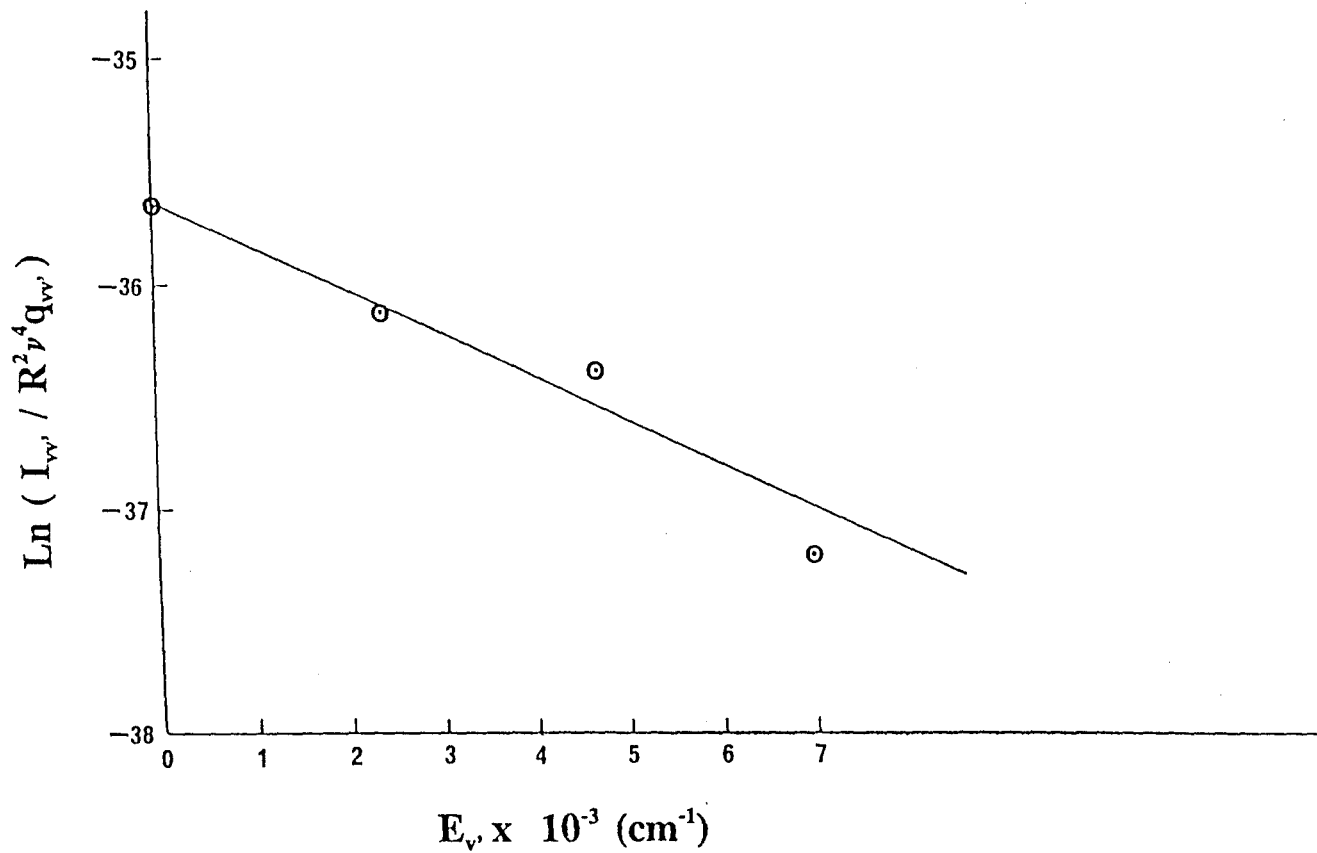


FIGURE 23.
 THE ELECTRONIC - VIBRATIONAL EMISSION OF THE FIRST NEGATIVE GROUP.
 THIS CORRESPONDS TO A VIBRATIONAL TEMPERATURE NEAR 1800 K.

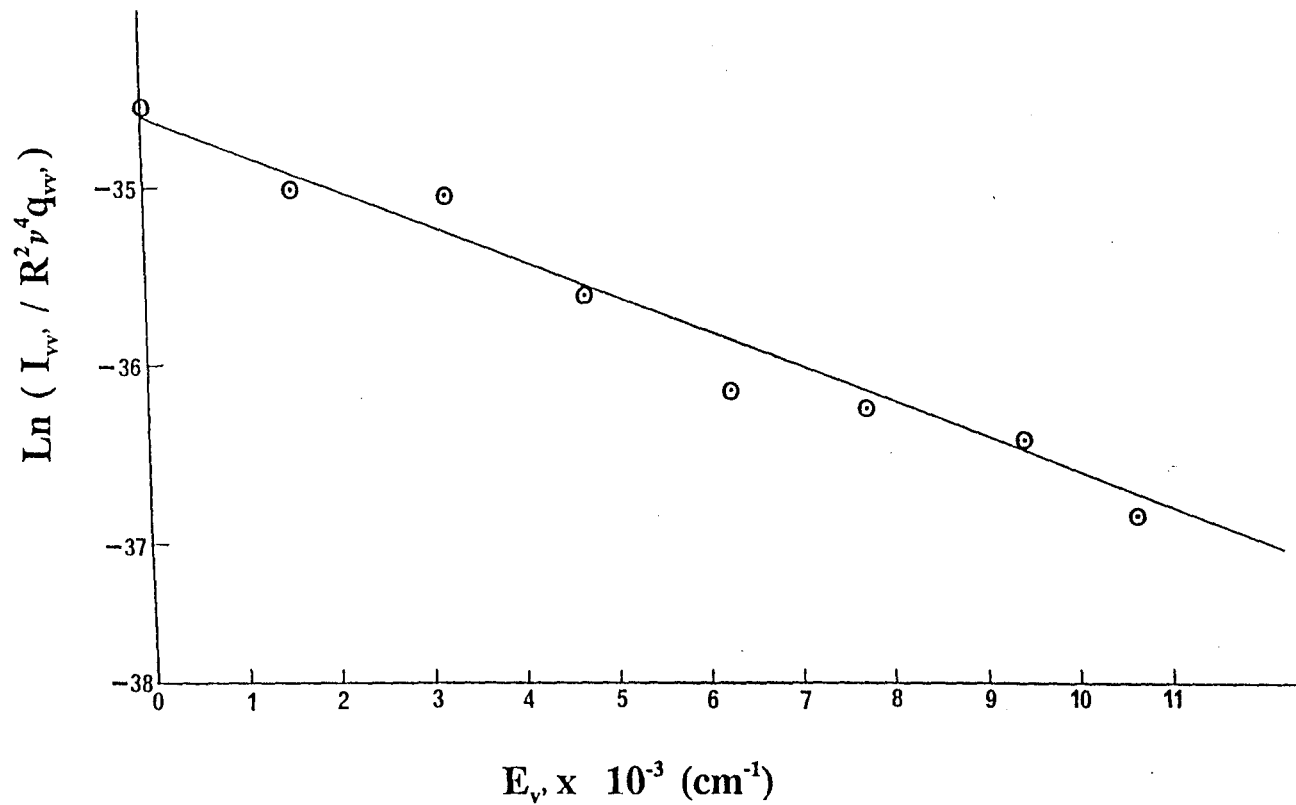


FIGURE 24.
 THE ELECTRONIC - VIBRATIONAL EMISSION OF THE FIRST POSITIVE GROUP.
 THIS CORRESPONDS TO A VIBRATIONAL TEMPERATURE NEAR 1900 K.

used the Franck-Condon factors listed in Reference 13. The "best" straight line corresponds to a vibrational temperature near 1900 K.

Our spectra of the second positive group emission intensity are diagnostic of the relative populations of vibrational levels of the C-electronic state of molecular nitrogen. These relative populations derived from the spectra can be used in turn to calculate the populations of the B-state of nitrogen which result from the $N_2(C) \rightarrow N_2(B)$ radiative transitions.

Our spectra of the first positive group emission intensity are diagnostic of the relative population of vibrational levels of the B-electronic state of molecular nitrogen. We illustrate in Figure twenty-five the B-state relative populations computed from the first positive emission intensity along with the relative populations which derive from the $N_2(C) \rightarrow N_2(B)$ radiative transitions. We find both relative population sets to be nearly equivalent with respect to the vibrational levels of the B-electronic state of nitrogen.

The spectra can be observed at higher resolution in order to gain information about the rotational distribution. Representative data are presented in Figure twenty-six by way of the 0 - 0 band of the second positive group. The profile of the 0 - 0 band is found to be nearly independent of the reservoir pressure.

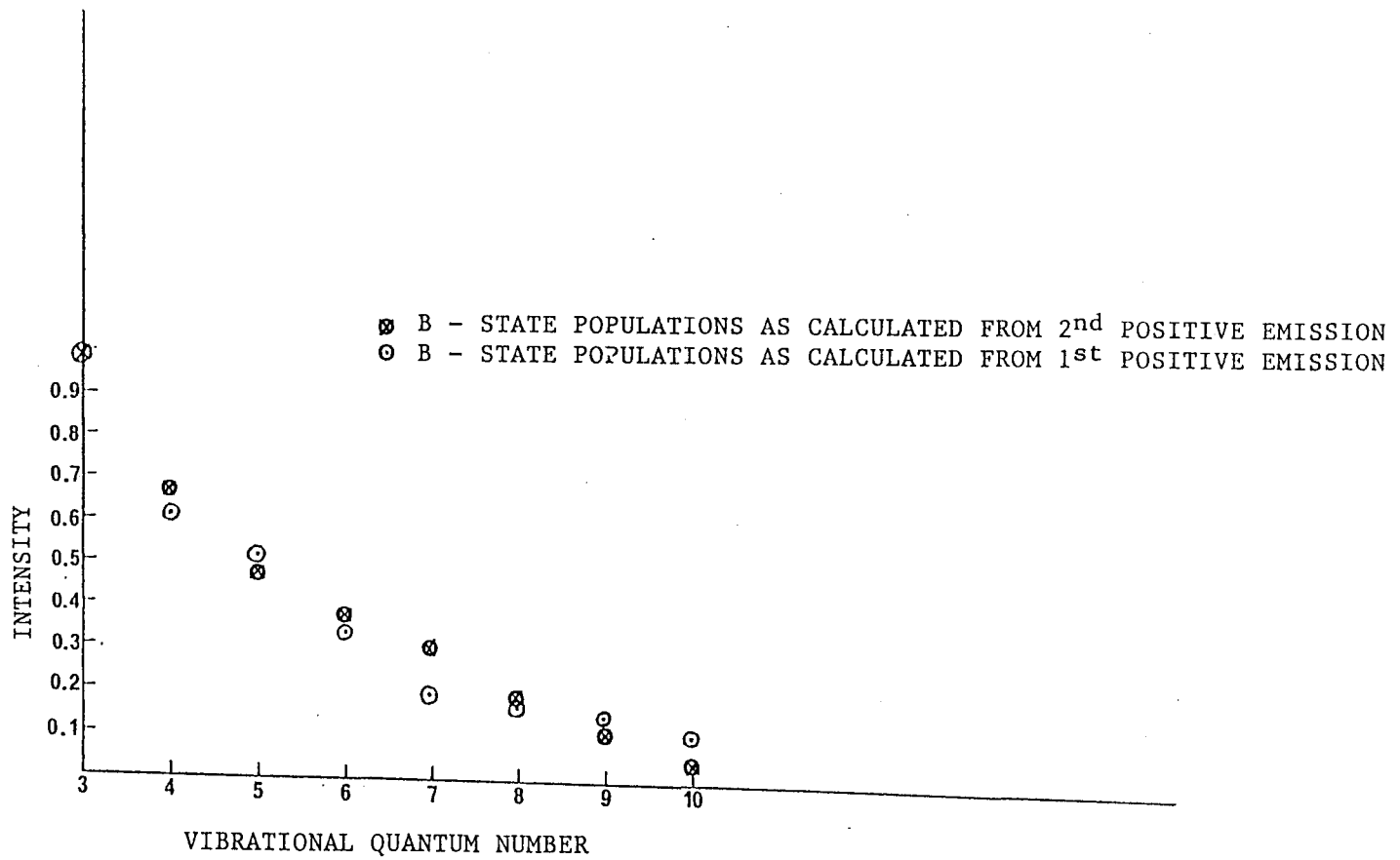


FIGURE 25.
 B - STATE POPULATIONS.

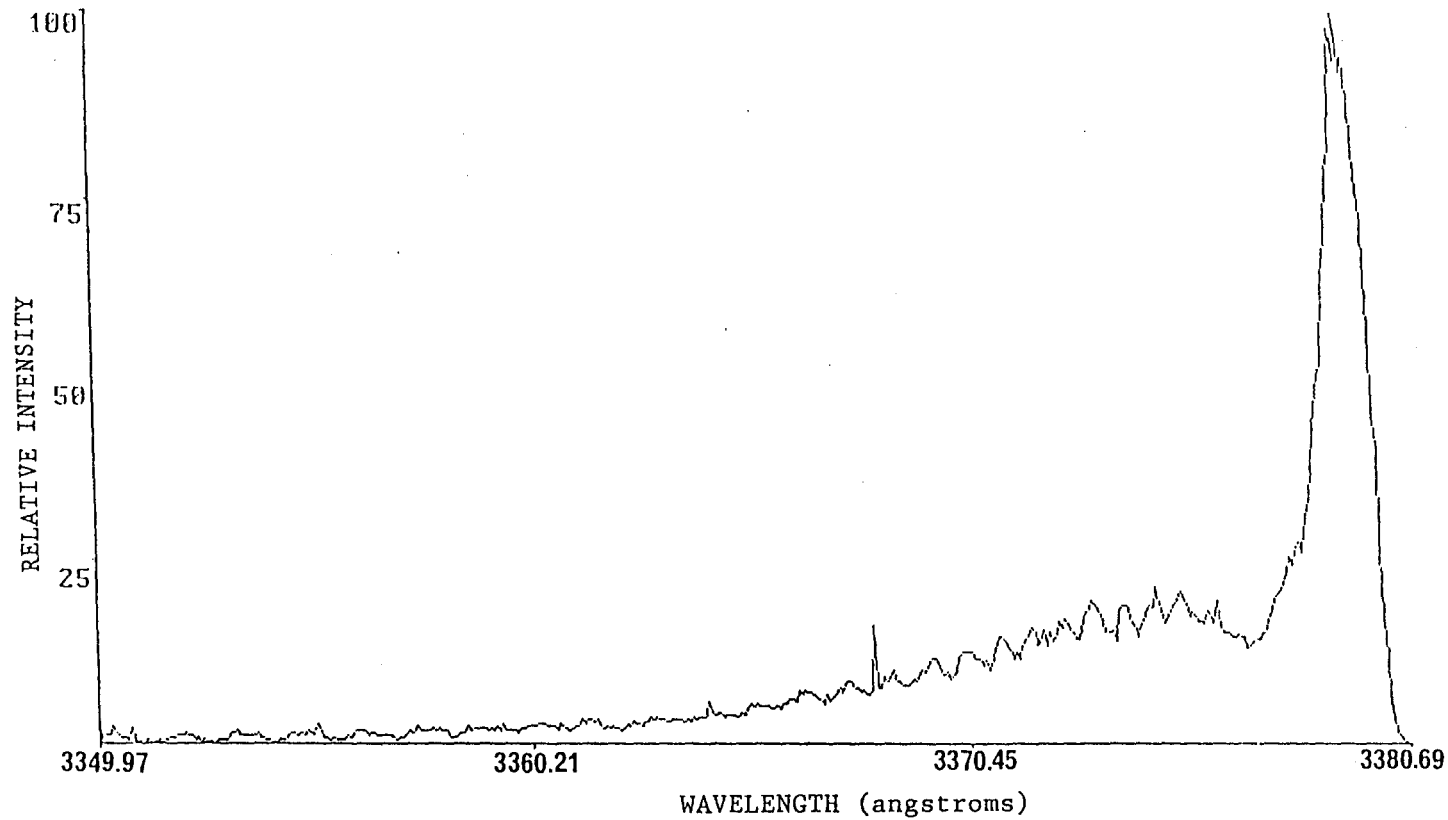


FIGURE 26.

SECOND POSITIVE 0 - 0 BAND ROTATIONAL ENVELOPE.

The rotational temperature for the 0 - 0 band of the second positive group is 250 (+/- 25)K. This calculation is based on the rotational profile (i.e. the envelope formed by the unresolved rotational transitions) of the band. Simulations of the rotational structure of this band are presented in Figure twenty-seven. The simulated line spectrum is based on vibrational and rotational constants given in Reference 12. The second spectrum in Figure twenty-seven represents more closely that which is experimentally obtained. It is calculated by averaging the intensities of lines contained within a one angstrom bandpass (i.e. the resolution of the experimentally obtained spectrum). An intensity measurement is calculated for a certain wavelength by averaging the intensities of lines contained within plus or minus one half the bandpass.

Bands in the first positive and first negative groups overlap. This precludes the simulation of their rotational profiles using this technique.

CHAPTER V

DISCUSSION

Understanding the emission spectroscopy of molecular nitrogen and nitrogen ion in a supersonic jet is not a straightforward task for at least two reasons:

(A) A comprehensive theory describing the excitation and relaxation kinetics in a supersonic discharge jet appears, to our knowledge, not to have been developed. This is in contrast to the kinetic theory literature surrounding conventional supersonic jets.

(B) The large number (> 80) of electronic states inherent to molecular nitrogen and nitrogen ion go hand-in-hand with a large number of potential curve crossings leading to emitting states.

The above complexities notwithstanding, we believe that good starting points lie in (1) formulating a first model for the gas physics of a supersonic nitrogen discharge jet and, (2) using this model along with the nitrogen spectroscopic

literature as vehicles for interpreting our experimental results.

Concerning the first step, an elementary physical model of a supersonic nitrogen discharge can be constructed by viewing the system as being very similar to a ground state nitrogen jet. In particular, we take the major difference between our supersonic discharge jet and a conventional ground state jet to involve the starting temperature. In particular, an extremely high temperature operates in the nozzle reservoir of a supersonic discharge. Conventional nitrogen jets ordinarily operate with the gas in the nozzle reservoir at room temperature prior to expansion. This way of viewing the situation, while oversimplified, links our apparatus and experiments to the work of previous gas phase researchers concerning nitrogen [34-37]. It further directs the following calculations:

- (1) The maximum starting temperature of the nitrogen molecules prior to the supersonic expansion.
- (2) The maximum number of excited state species present in the supersonic jet prior to expansion.
- (3) The maximum terminal translational temperature in the jet far downstream from the supersonic discharge nozzle at the point where our spectroscopic observations have been made.

(4) The maximum collision rate in the jet far downstream from the supersonic discharge nozzle at the point where our spectroscopic observations have been made.

(5) An estimate for the total number of collisions experienced by each molecule within regions of free molecular flow along the axis of the jet where our spectroscopic observations have been made.

Toward obtaining the first of the above calculations, we consider that typical input powers of our apparatus are approximately fifty watts. Typical densities in the nozzle reservoir are 5×10^{19} molecules/cm³, measured by comparing the pressure in the nozzle reservoir with the discharge off (and therefore with the nitrogen gas at room temperature) and with the discharge on. Typical flow rates are computed to be approximately 1.5×10^{20} molecules/sec given the nozzle dimensions and operating limits.

We further consider the extreme case whereby the nitrogen molecules absorb all of the input power prior to expansion. Under this assumption, each molecule receives on the average of 3.33×10^{-12} ergs. We then take this amount of energy to be equipartitioned among translational, rotational, vibrational, and electronic degrees of freedom. Then each of these degrees of freedom receives approximately 8.33×10^{-13} ergs for each molecule.

Taking nitrogen to be an ideal gas, the translational energy for each molecule equals $(5/2)k_bT$. Then

$$T = 2 \times 8.33 \times 10^{-13} \text{ ergs}/5k_b$$

$$T = 2415 \text{ K.}$$

So we take 2400 K to approximate the maximum possible temperature of the nitrogen prior to expansion. The significance of this calculation is that it illustrates one essential difference (i.e. concerning the temperature) between our supersonic discharge nozzle and conventional apparatus. However, we emphasize that this calculation corresponds to a situation whereby only nitrogen is treated as the energy sink. All others, e.g. the apparatus and the radiation field, have been ignored.

Toward obtaining the second of the above calculations, we consider the maximum number of excited nitrogen molecules prepared in the discharge nozzle using the same assumptions. We further assume that energy is directed into the nitrogen via the electronic degrees of freedom.

Excitation energies of molecular nitrogen are of order $100,000 \text{ cm}^{-1}$ (i.e. 2×10^{-11} ergs). If on the average 8.33×10^{-13} ergs are supplied to the electronic degrees of freedom, then on the average about one in twenty-five molecules is excited. We thereby take the maximum concentration of excited state species prior to expansion to be a few percent.

The significance of this calculation is that it illustrates that the density of excited state species can be rather high in the expanding jet.

Toward obtaining the third calculation, we confine attention to the region far from the nozzle (e.g. five centimeters) under conditions of free molecular flow and terminal Mach number. We further make use of the ground state nitrogen collisional relaxation studies of previous researchers.

The theory of conventional supersonic jets holds that the terminal Mach number follows the form

$$M_t = F(\gamma) (K/\epsilon)^{-(\gamma-1)/\gamma}$$

where K is the Knudsen number given by the ratio of the mean free path to nozzle diameter at the nozzle throat. ϵ is the collisional effectiveness parameter concerning the exchange of energy between degrees of freedom. $F(\gamma)$ is a parameter dependent on the ratio $\gamma = C_p/C_v$.

ϵ has been determined to be approximately 0.4 for molecular nitrogen in a supersonic jet by previous researchers [38]. $F(\gamma)$ has been determined to be 2.48 for diatomic molecules [39].

We approximate the mean free path λ in the nozzle throat by

$$\lambda = 2^{-1/2} \sigma / \text{gas density.}$$

Using the hard sphere kinetic cross section for molecular nitrogen, i.e. 43 Angstroms², we calculate a value of 5.5×10^{-6} cm for the mean free path.

We find the Knudsen number to be approximately 5×10^{-4} using our nozzle diameter of 0.01 cm. We finally calculate a value of 16.93 for the terminal Mach number.

Taking the terminal Mach number to be approximately 17, we are then able to compute the maximum value of the terminal translational temperature T_t far from the expansion point using the value of 2400 K = T_0 for the source temperature, viz.

$$T_t = T_0 [1 + (0.5) (\gamma - 1) M_t^2]^{-1}$$

Again taking the nitrogen to be an ideal gas with $\gamma = 7/5$, we find the maximum terminal translational temperature to be 41 K far from the expansion nozzle.

The significance of this calculation is that it illustrates how the translational degrees of freedom of the nitrogen molecules are cooled significantly in the supersonic expansion. This cooling occurs in spite of the very high source temperature.

Energy transfer between translational and rotational degrees of freedom is ordinarily very efficient. We can then

take the calculated terminal translational temperature to serve as a first estimate of the rotational temperature of the expanding nitrogen. Such an estimate appears to be reasonable. Other researchers working with supersonic discharges of various configurations report similarly low rotational temperatures [40-42].

Toward obtaining the fourth calculation, we consider the collision rate z at a distance x from the nozzle to be given by the expression

$$z = \sigma \left(8k_B T / \pi \mu \right)^{1/2} n(x)$$

Here $n(x)$ is the density of the jet along the axis at distance x away from the nozzle. In the region of free molecular flow, $n(x)$ has the form

$$n(x) = n(0) \left(x_r / x \right)^2$$

where $n(0)$ is the gas density in the nozzle reservoir. x_r is given by the expression

$$x_r = D \left[1/2 (\gamma - 1) A^2 \right]^{-1/[2(\gamma - 1)]}$$

where D is the nozzle diameter and A depends on γ . Given the nozzle diameter of our apparatus along with the value of A determined by previous researchers [39], we compute a value

of 0.00294 cm for x_r . Taking the collision cross section of nitrogen to equal that of the gas kinetic, we compute a value of order 10^3 sec^{-1} for the bimolecular collision rate five centimeters from the expansion nozzle. Here we have used the terminal translational temperature of 41 K computed from above along with the nozzle density of $5.5 \times 10^{19} \text{ molecules/cm}^3$ computed above.

We see that the collision frequency calculated far from the nozzle is orders of magnitude less than that operative inside the throat of the nozzle. This collision frequency in the core of the jet axis scales as the square root of the temperature and the inverse square of the distance from the nozzle source. This calculation is significant in that it illustrates important guidelines for comparing collision rates and radiative decay rates of molecules in the supersonic discharge.

Toward obtaining the fifth of the above calculations, we confine attention to the case where the expanding molecules have reached their terminal Mach number and terminal velocity. The terminal velocity (v_t) at infinite Mach number is given by the expression

$$v_t = [\gamma / (\gamma - 1)]^{1/2} (2k_B T_0 / m)^{1/2}$$

where T_0 is the temperature prior to the expansion. Using the value of 2400 K for T_0 we calculate a v_t value of $2.2 \times$

10^5 cm/sec.

The total number of collisions (dZ) experienced by a molecule moving within the core along an element of the length dx along the axis is

$$dZ \sim \sigma (8k_B T / \pi \mu)^{1/2} n(x) / v_t dx$$

Then the total number of collisions (Z) experienced by a molecule moving within the core along the axis between the points x_1 and x_2 far from the nozzle is given by

$$\begin{aligned} Z &= \int_{x_1}^{x_2} \sigma (8k_B T / \pi \mu)^{1/2} n(0) / v_t (xv/x)^2 dx \\ &= \sigma (8k_B T / \pi \mu)^{1/2} (n(0) / v_t) x_r^2 [1/x_1 - 1/x_2] \end{aligned}$$

A sample calculation takes x_1 and x_2 to be one and five centimeters and $n(0)$ from above. We obtain a value of 0.116 collisions.

The importance of this calculation is that it illustrates how few are the total number of collisions experienced by a molecule in the region of free molecular flow (assuming gas-kinetic cross sections). Such is the case in spite of the high source temperature native to the discharge nozzle.

We are now ready to examine our experimental results. A potential energy diagram illustrating some of the electronic states of molecular nitrogen and nitrogen ion is presented in

Figure twenty-eight. Conventional electric discharges of nitrogen gas typically populate many of these states in an unselective way. In turn, many spectroscopic systems characteristic of excited molecular nitrogen and nitrogen ion can be observed, the relative contributions being very dependent on the discharge, observation, and high pressure conditions [11].

The results of the relatively few nozzle studies (e.g. using high power radiofrequency discharges) of electronically excited nitrogen parallel those obtained from conventional discharge apparatus. Multiple spectroscopic systems of nitrogen are excited in such nozzles, the relative contributions of which are sensitive to excitation conditions [43].

The above-cited results concerning electronically excited nitrogen appear very different from our experimental results with supersonic nitrogen discharges in two important respects. First, we observe only three spectroscopic systems of excited nitrogen by way of the first positive, second positive, and first negative emission groups. Second, the nature of these spectroscopic systems by way of their vibrational and rotational distributions appears to be relatively insensitive to excitation conditions or observation point in the supersonic jet.

It becomes important to ascertain the mechanism by which the spectra of excited nitrogen molecule and nitrogen ion

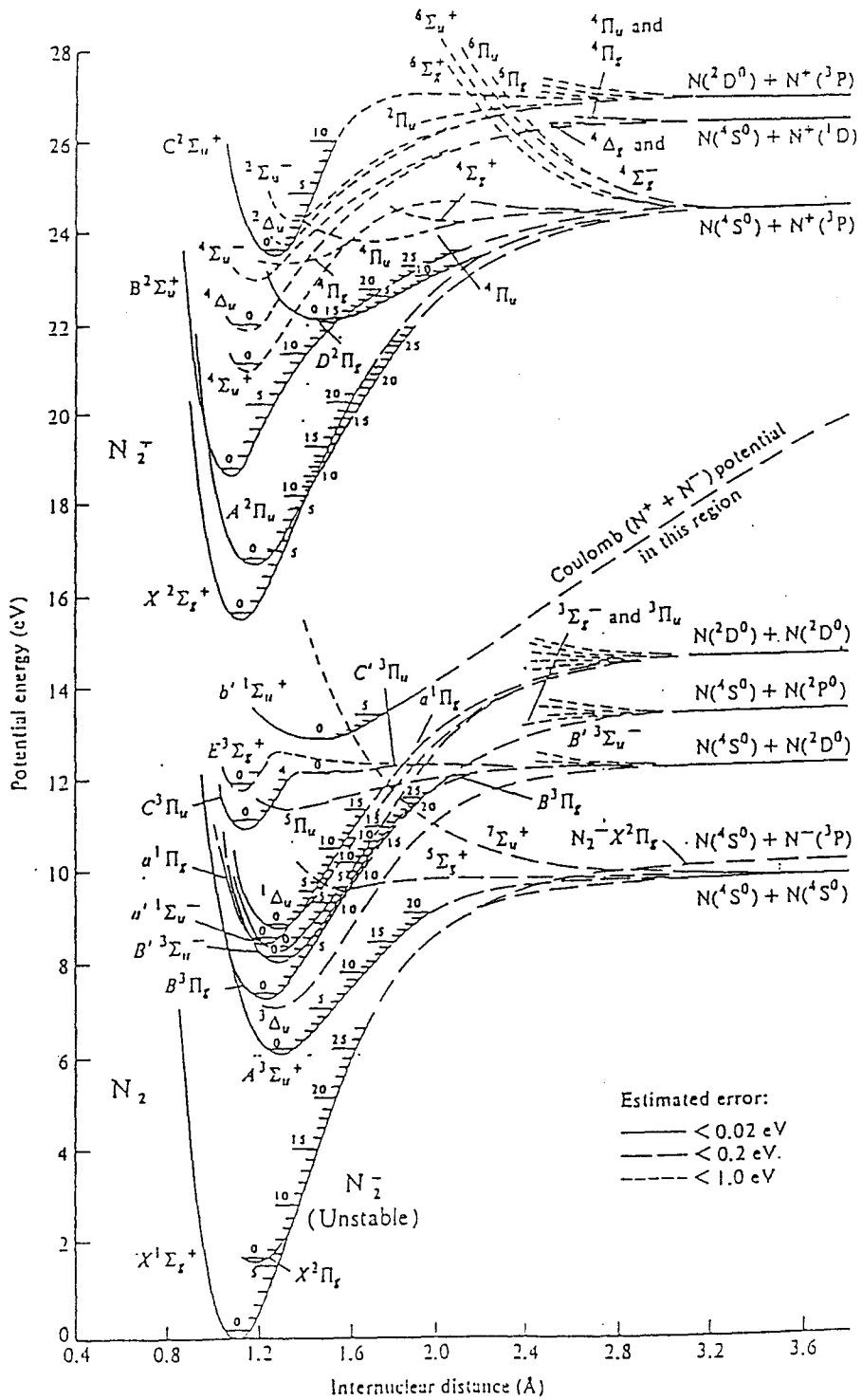


FIGURE 28.
 POTENTIAL ENERGY DIAGRAM OF MOLECULAR NITROGEN AND ION.
 (Source: F. R. Gilmore, "Potential Energy Curves for N_2 ,
 NO and O_2 and corresponding Ions," RAND Corporation
 Memorandum R-4034-PR (June 1964).)

originate. First considerations are the radiative lifetimes of the C- and B-electronic states of molecular nitrogen, and the B-electronic state of nitrogen ion along with the fact that the spectra reported in Section IV have been recorded by collecting light from the core of the jet far downstream (e.g. five centimeters) from the nozzle.

The radiative lifetimes associated with the $N_2(C)$ state, $N_2(B)$ state, and $N_2^+(B)$ state are respectively 50 nsec, 10 microseconds, and 100 nsec [13,44,45]. Ignoring the possibility of collisions occurring outside the nozzle, and taking the nitrogen gas velocity to be of the same order as the terminal velocity, i.e. 10^5 cm/sec, the $N_2(C)$ and $N_2^+(B)$ populations prepared inside the nozzle decay exponentially to 3% of initial intensity at distances (i.e. $5\tau \ln(2)$ where τ is the radiative lifetime) 0.0173 and 0.035 cm, respectively. The corresponding calculation applied to the $N_2(B)$ population prepared inside the nozzle yields a length of 3.5 cm.

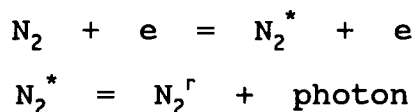
These calculations are important as they lead us to our first important conclusion: that the second positive and first negative group spectra that we observe in the expanding supersonic jet stem from events which occur far outside the nozzle.

Lifetime considerations point to the fact that any $N_2(B)$ population prepared inside the nozzle would be observable far downstream in the expanding jet. The spectra, however, argue otherwise by way of the vibrational populations of $N_2(C)$ and

$N_2(B)$, cf Figure twenty-five. Therefore, we do not believe that radiation we observe from $N_2(B)$ stems directly from population formed inside the nozzle. Our experiments instead evidence that population of the B-electronic state is derived from the C-electronic state by a radiative relaxation processes.

The above considerations, along with the essential physics of the discharge nozzle, lead us to our second important conclusion: that all radiation observed from the supersonic jet discharge stem from processes which populate the C-electronic state of molecular nitrogen and the B-electronic state of nitrogen ion outside the nozzle. These processes necessarily involve long-lived states of molecular nitrogen and/or nitrogen ion in the supersonic expansion.

It becomes important to ascertain whether $N_2(C)$ and $N_2^+(B)$ are formed by radiative or non-radiative relaxation of metastable species prepared inside the discharge nozzle and expand in the free jet. In the former case, we consider the mechanism



where N_2^* represents molecular nitrogen in a metastable state with radiative rate constant k prepared via an electron-molecule collision inside the nozzle. N_2^r represents

molecular nitrogen in a radiative state (e.g. the C-electronic state) with radiative rate constant k' .

We take the initial N_2^* density to be proportional to the local gas density in the expanding jet. This in turn is proportional to the gas density inside the nozzle. Then the radiative intensity I_k , derived from N_2^* a distance x from the nozzle would be proportional to

$$I_k \propto k' n(x) e^{-kx/v}$$

$$\propto k' n(0) (x_r/x)^2 e^{-kx/v}$$

where $n(0)$, v , and x_r have been defined previously.

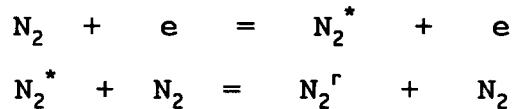
The above expressions follow from elementary considerations of an ideal gas undergoing supersonic expansion. They are applicable under conditions far from nozzle source in region of free molecular flow. This is the region we have interrogated in our spectroscopic experiments with supersonic nitrogen discharges.

Considerations of this first mechanism suggest that the intensity of an emitting species at distance x from nozzle should scale linearly with gas density of the nozzle reservoir.

Our experiments do not support this mechanism for the formation of $N_2(C)$ and $N_2^+(B)$ in the supersonic jet. Our experiments instead found both visible length of the beam and light intensity measured in the core of the jet to scale at

least as the square of the nozzle pressure, c. f. Figures seventeen - twenty.

We consider then a collisional mechanism by which a radiative species with rate constant k' could be formed in the supersonic jet, viz.



We then take the radiative signal of N_2^r at distance x away from the nozzle source to be proportional to the local N_2^* density times the local collision rate, viz.

$$I_{k'} \propto k'n(0) e^{-kx/v} z(x)$$

Here we are using the collision rate defined in equations applicable to the core of the expanding jet along the axis.

Then

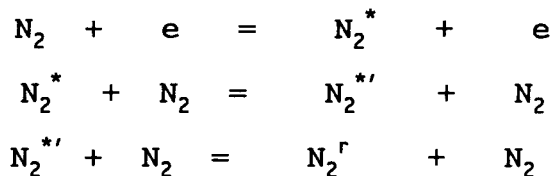
$$I_{k'} \propto k'n(0) e^{-kx/v} \sigma (8k_B T / \pi \mu)^{1/2} n(0) (x_r/x)^2$$

The above suggests that the radiative intensity of N_2^r should scale as the square of nozzle gas density. We find most of our experiments to support such a mechanism in two respects. First the visible length of the supersonic jet is observed to scale as the square of the nozzle pressure, c.f.

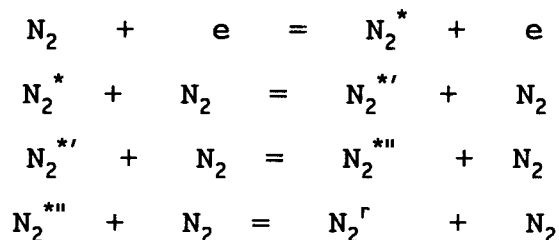
Figure seventeen. Further, the intensity integrated from the core of the jet is found to scale almost as the square of the nozzle pressure, c.f. Figures eighteen and nineteen.

The above point toward a second important conclusion: that the population of $N_2(C)$ and $N_2^+(B)$ in the supersonic jet occur by non-radiative, collisional processes outside the nozzle.

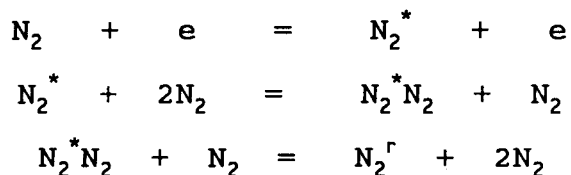
We recognize the fact that some of our experimental results do not offer such straight forward conclusions. Namely we have observed spectral intensities to scale as third and fourth power of the nozzle pressure, dependent on excitation voltage and electrode gap. However, such variance in the data is not surprising given that higher-order excitation and collisional relaxation mechanisms are certainly possible. Foremost examples include two-body collisional mechanisms, e.g.



and



Three-body processes can also be envisioned, e.g.



Such would account for spectral intensities scaling as p^n , $n = 3, 4, 5 \dots$. The fact that reactive cross sections are functions of the local temperature and, in turn, the nozzle pressure, is yet another added complexity.

But we point out that regardless of the order by which the collisional relaxation takes place in our apparatus, our resultant spectra are fundamentally constant with respect to rotational and vibrational distributions. We then take the variance concerning the excitation and collisional relaxation with pressure as evidence of several possible reaction mechanisms which ultimately lead to the metastable precursors of $N_2(C)$ and $N_2^+(B)$. We further take these different mechanisms to involve events occurring inside the nozzle.

We then take all our spectra to derive from collision processes involving fundamentally the same precursors. We also take the cross section of this precursor to be not too sensitive to the pressure conditions within the nozzle.

Well-known long-lived states of molecular nitrogen are listed in below along with their energies and radiative lifetimes [48].

<u>State</u>	<u>Energy (cm⁻¹)</u>	<u>Lifetime (s)</u>
X ¹ Σ _g ⁺	0	∞
A ³ Σ _u ⁺	49755	1.3
W ³ Δ _u	59380	>10 ⁻³
a ¹ Σ _u ⁻	67739	40 x 10 ⁻³
ω ¹ Δ _u	71698	300 x 10 ⁻⁶
E ³ Σ _g ⁺	95771	300 x 10 ⁻⁶
a ¹ Σ _g ¹	98840	?

Concerning the states in the above list, all meet the lifetime criteria for surviving many centimeters downstream in the expanding jet after being populated in the discharge nozzle.

The C-electronic state of molecular nitrogen lies near 89,000 cm⁻¹. Concerning the states of the above list, energy considerations then point only to two, namely the E- and a"-electronic states, as being able to populate the C-state by a collisional process. Here we are assuming that interactions between excited nitrogen and ground state nitrogen do not drastically perturb molecular potentials illustrated in Figure twenty-eight.

Concerning the E- and a"-states, considerations of spin conservation operative during molecular collisions, would argue against the likelihood of the a"-state playing a vital role in the population of the C-state.

We are directed toward the hypothesis that the E-state

of molecular nitrogen is involved in the population of the C-electronic state in the expanding supersonic jet. Such population likely occurs by a binary collision involving $N_2(E)$ and $N_2(X)$.

A number of data appear to support this hypothesis. First, the vibrational distributions we record are not much different from those recorded by previous researchers working with $N_2(E)$ in molecular beams. In particular, Freund recorded the radiation correlated with $N_2(E)$ populated in effusive molecular beams using electron beams [46]. The spectra recorded resemble ours with respect to vibrational distribution.

Second, other researchers studying supersonic discharges of nitrogen, found $N_2(E)$ to be populated in rather large numbers [48]. To be sure, many of the details depend on experimental conditions. But we gather that formation of $N_2(E)$ appears to be a general property of supersonic nitrogen discharges.

The calculations presented above demonstrate the collision rates are orders of magnitude less than the radiative decay rates of the emitting species. So the emission spectra are diagnostic of the nascent vibrational and rotational distributions. Essentially the products of the collisions emit light long before they experience another collision.

Then proceeding further with our hypothesis, we suggest

that a large portion of the excess electronic energy between the E- and the C-states is stored as vibrational energy in the products of the collision. We note that the vibrational temperature evidenced by the data are in excess of the maximum source temperature of 2400 K based on our elementary model.

The rotational temperatures of 250 K are also significantly greater than predicted by our calculation of the terminal translational temperature. However, this is not surprising. The emitting species in our supersonic discharge are products of a chemical reaction involving colliding species. While the reactants are rotationally cold due to the supersonic expansion, the energy of reaction is distributed among the degrees of freedom of the products. Only if the collisions are collinear whereby no torque is exerted on the reaction products can the product rotational temperatures remain cold. This latter situation is unlikely on symmetry grounds. If $N_2(E)$ and $N_2(X)$ define the reactant states and $N_2(C)$ and $N_2(X)$ define the product states, such a reaction is symmetry forbidden as a linear transition state. Only collisions which involve a non-linear transition state are then allowed. These must create torque in the products and, in turn, rotational excitation of products.

The vibrational temperatures evidenced in the spectra far exceed the rotational temperatures. We take from this observation that the reaction energy is preferentially stored in the vibrational degrees of freedom of the reaction

products.

We note that alternative mechanisms for populating the C-state are possible employing molecular nitrogen states of the above list. For example, collision of two $N_2(A)$ molecules can lead to the products $N_2(C)$ and $N_2(X)$ if the transition state is not collinear.

However, there are several reasons to rule out such processes as likely mechanisms for populating the C-state in our experiments. First, such processes involve great excesses of electronic energy in the collision. Second, such processes appear rather improbable given the low collision environment of the expanding jet. Third, data of other researchers tends to rule out the above processes. For example, vibrational distributions are markedly different from what we observe, having roughly equal population in the 0 and 1 vibrational levels [47].

That we do not observe direct spectroscopic evidence of E-state by way of electronic emission is not surprising given our optical integration times (ca. one second/channel) and slow radiative decay rate of E-state. In the supersonic discharge work of previous researchers which featured high concentrations of $N_2(E)$, direct evidence in the emission spectra was also lacking [48].

Of the metastable states of nitrogen on the list, all except the A-state are capable of populating the B-state of nitrogen ion upon collisions with $N_2^+(X)$. It is thereby more

difficult to hypothesize a mechanism behind the spectra of $N_2^+(B)$. We can only say that some nitrogen ions formed in the discharge undergo collisions with nitrogen metastables far downstream in the supersonic jet.

APPENDIX A

A.1 Program 1 -- Collect Data

This program is used to take spectra and to conduct the stop flow experiments. REM statements within the program outline the electronic setup for proper use of the program. A screen display of commands is given while the program is running.

```

10 DIM A$(20),Y(2000):KEY OFF:CLS:LOCATE 1,1
20 PRINT"THIS PROGRAM IS FOR USE WITH THE DIGIKROM
MONOCHROMATOR, THE 4145 2/4146"
30 PRINT"TIME DELAY MODULE, THE 7404 INVERTER, AND THE
COMBO-100 PREAMP. THE "
40 PRINT"CONNECTIONS WHICH SHOULD BE MADE FOR USE OF THIS
PROGRAM ARE AS FOLLOW:":PRINT
60 PRINT"(1) CONNECT THE COMPUTER'S RS-232C SERIAL
COMMUNICATIONS PORT TO THE"
70 PRINT" DIGIKROM 240'S CONTROL MODULE WITH A 25 PIN
D-SUBMINATURE CABLE.":PRINT
80 PRINT"(2) JUMPER THE 4145 GATE TO THE 7404 INVERTER INPUT
AND THE DAS-8 IP.":PRINT
90 PRINT"(3) JUMPER THE 4145 TRIG TO THE DAS-8 OUT2.":PRINT
100 PRINT"(4) JUMPER THE DAS-8 GATE0 TO THE 7404 INVTER
OUTPUT.":PRINT
120 PRINT"(5) JUMPER THE DAS-8 CLK0 TO THE COMBO-100
PREAMP.":PRINT 130 PRINT"(6) JUMPER PREAMP TO THE
PMT.":PRINT:PRINT
135 PRINT"PRESS F5 TO CONTINUE.": STOP
136 CLS: LOCATE 12,23: PRINT"ATTEMPTING TO INITIATE"
137 LOCATE 13,23: PRINT"COMMUNICATION WITH MONOCHROMATOR."
140 AST=13839: GOSUB 2820: SLW(1)=50: SLW(2)=50
145 OPEN"COM1:9600,N,8,1,CS0,DS0" AS #1
146 PRINT#1,CHR$(11);CHR$(36);
147 IF INPUT$(1,#1)=CHR$(11) THEN 270 ELSE 147
270 LOCATE 1,1: CLS: KEY OFF
280 PRINT" ONE TEN
HUNDRED"
290 PRINT" STEP STEPS
STEPS"
300 PRINT" | |
|":PRINT
310 PRINT"STEP SHORT TO LONG -- 7 8
9":PRINT
320 PRINT"NO EFFECT ----- 4 5

```

```

6":PRINT
330 PRINT"STEP LONG TO SHORT --          1          2
      3":PRINT
340 PRINT"PRESS [INS] TO GO DIRECTLY TO AN INDICATED
WAVELENGTH."
350 PRINT"PRESS [PRT SC] TO CHANGE THE SLIT WIDTHS."
360 PRINT"PRESS [BACK SPACE] TO TAKE A SPECTRA."
370 PRINT"PRESS [ESC] TO TRANSFER TO INTENSITY VS. TIME
SUBROUTINE."
380 LOCATE 16,25: PRINT"PRESENT WAVELENGTH:"
390 LOCATE 17,25: PRINT"ENT. SLIT WIDTH:  "
400 LOCATE 18,25: PRINT"EXIT SLIT WIDTH:  "
410 LOCATE 16,46: PRINT USING"####.##";AWL
420 LOCATE 17,46: PRINT USING"####  ";SLW(1)
430 LOCATE 18,46: PRINT USING"####  ";SLW(2)
440 A$=INKEY$: IF LEN(A$)=0 THEN 440
460 IF ASC(A$)=55 THEN DIR=7: INC=1: PPS=1: GOTO 660
470 IF ASC(A$)=56 THEN DIR=7: INC=1: PPS=10: GOTO 660
480 IF ASC(A$)=57 THEN DIR=7: INC=1: PPS=100: GOTO 660
490 IF ASC(A$)=49 THEN DIR=1: INC=-1: PPS=1: GOTO 660
500 IF ASC(A$)=50 THEN DIR=1: INC=-1: PPS=10: GOTO 660
510 IF ASC(A$)=51 THEN DIR=1: INC=-1: PPS=100: GOTO 660
520 IF ASC(A$)=27 THEN GOSUB 3000:GOTO 270
530 IF ASC(A$)=8 THEN GOTO 940
540 IF ASC(A$)=42 THEN GOTO 730
550 IF ASC(A$)=48 THEN 560 ELSE 440
560 LOCATE 20,25: INPUT"ENTER WAVELENGTH: ",AWL
570 IF AWL>=0 AND AWL<=16000 THEN GOTO 610
580 LOCATE 20,25: PRINT"!!!!OUT OF RANGE!!!!          "
590 FOR PAUSE=1 TO 999: NEXT: LOCATE 20,25: PRINT"
      "
600 GOTO 560
610 LOCATE 20,25: PRINT"
      "
620 OAST=AST: GOSUB 2790: PPS=AST-OAST: AST=OAST
630 IF PPS<0 THEN DIR=1: INC=-1
640 IF PPS>=0 THEN DIR=7: INC=1
650 PPS=ABS(PPS)
660 OAST=AST: AST=AST+(PPS*INC): GOSUB 2820: AST=OAST
670 IF AWL<0 OR AWL>16000 THEN GOTO 450
677 LOCATE 20,25: PRINT"!!!!POSITIONING GRATING!!!!"
680 FOR I=1 TO PPS: PRINT#1, CHR$(DIR);: AST=AST+INC
690 IF INPUT$(1,#1)=CHR$(24) THEN 700 ELSE 690
700 NEXT
701 LOCATE 20,25: PRINT"          "
710 LOCATE 16,46: PRINT USING"####.##";AWL
720 GOTO 440
730 LOCATE 20,25: INPUT"ENTER ENT. SLIT WIDTH:
",SLW(1):SLW(1)=INT(SLW(1))
740 IF SLW(1)>=0 AND SLW(1)<=2000 THEN GOTO 780
750 LOCATE 20,25: PRINT"!!!!OUT OF RANGE!!!!
      "

```

```

760 FOR PAUSE=1 TO 999: NEXT: LOCATE 20,25: PRINT"
      "
770 GOTO 730
780 LOCATE 20,25: PRINT"
      "
790   LOCATE 20,25:   INPUT"ENTER   EXIT   SLIT   WIDTH:
",SLW(2):SLW(2)=INT(SLW(2))
800 IF SLW(2)>=0 AND SLW(2)<=2000 THEN GOTO 840
810 LOCATE 20,25: PRINT"!!!!OUT OF RANGE!!!!"
      "
820 FOR PAUSE=1 TO 999: NEXT: LOCATE 20,25: PRINT"
      "
830 GOTO 790
840 LOCATE 20,25: PRINT"
      "
845 LOCATE 20,25: PRINT"!!!!ADJUSTING SLITS!!!!"
850 FOR K=1 TO 2
860 PRINT#1,CHR$(30+K);
870 IF INPUT$(1,#1)=CHR$(30+K) THEN 880 ELSE 870
880 PRINT#1,CHR$(INT(SLW(K)/256));CHR$(SLW(K) MOD 256);
890 IF INPUT$(1,#1)=CHR$(24) THEN 900 ELSE 890
900 NEXT
905 LOCATE 20,25: PRINT"                                     "
910 LOCATE 17,46: PRINT USING"####   ";SLW(1)
920 LOCATE 18,46: PRINT USING"####   ";SLW(2)
930 GOTO 440
940 REF=AST
950 CLS: LOCATE 1,1: PRINT"ENTER THE STARTING WAVELENGTH IN
ANGSTROMS (XXXXX). "
960   PRINT"THE   RANGE   IS   0   ANGSTROMS   TO   16000
ANGSTROMS. ":INPUT"START=",SWL: PRINT
970 IF SWL<0 OR SWL>16000 THEN PRINT"!!!!OUT OF RANGE!!!!":
GOTO 950
980 PRINT"ENTER THE FINAL WAVELENGTH IN ANGSTROMS (YYYYY). "
990   PRINT"THE   RANGE   IS   0   ANGSTROMS   TO   16000
ANGSTROMS. ":INPUT"FINAL=",FWL: PRINT
1000 IF FWL<0 OR FWL>16000 THEN PRINT"!!!!OUT OF RANGE!!!!":
GOTO 980
1010 PRINT"ENTER THE APPROXIMATE STEP SIZE IN ANGSTROMS
(XX.XX). "
1020 PRINT"THE RANGE IS 0.073 ANGSTROMS TO 32.00. ":INPUT"STEP
SIZE=",STP: PRINT
1030 IF STP<.073 OR STP>32 THEN PRINT"!!!!OUT OF RANGE!!!!":
GOTO 1010
1040 STP=INT(STP*1000)
1050 IF STP-INT(STP/73)*73=0 THEN 1060 ELSE STP=STP-1: GOTO
1050
1060 PPS=INT(STP/73)
1070 AST=PPS: GOSUB 2820
1080 STP=AWL
1090 MSLW=INT(STP*1000/16+1)
1100 STP=INT(STP*100)/100

```

```

1110 IF MSLW<10 THEN MSLW=10
1120 PRINT"ENTER THE ENTRANCE SLIT WIDTH IN MICRONS (YYYY).\"
1130 PRINT"THE RANGE IS 10 TO 2000 MICRONS.\"
1140 PRINT"THE MINIMUM SLIT WIDTH BASED ON THE STEP SIZE
INCREMENT IS ";MSLW;" MICRONS.\"
1150 INPUT"ENT. SLIT=",SLW(1):SLW(1)=INT(SLW(1)):PRINT
1160 IF SLW(1)<MSLW OR SLW(1)>2000 THEN PRINT"!!!!OUT OF
RANGE!!!!": GOTO 1120
1170 PRINT"ENTER THE EXIT SLIT WIDTH IN MICRONS (YYYY).\"
1180 PRINT"THE RANGE IS 10 TO 2000 MICRONS.\"
1190 PRINT"THE MINIMUM SLIT WIDTH BASED ON THE STEP SIZE
INCREMENT IS ";MSLW;" MICRONS.\"
1200 INPUT"EXIT SLIT=",SLW(2):SLW(2)=INT(SLW(2)):PRINT
1210 IF SLW(2)<MSLW OR SLW(2)>2000 THEN PRINT"!!!!OUT OF
RANGE!!!!": GOTO 1170
1220 PRINT"ENTER THE VOLTAGE APPLIED TO THE PMT IN VOLTS
(XXXX).\"
1230 INPUT"PMT=",PMT: PRINT
1240 PRINT"ENTER THE PMT TEMPERATURE IN DEGREES CELSIUS
(YYY).\"
1250 INPUT"TEMPERATURE=",CEL: PRINT
1260 PRINT"ENTER THE GATE TIME IN MICROSECONDS (XXXXXXX.XX).\"
1270 INPUT"GATE=",GAT: PRINT
1280 PRINT"ENTER THE TIME INTERVAL BETWEEN INTERRUPTS IN
MINUTES (YYY).\"
1290 INPUT"PAUSE=",PAU: PRINT
1300 AWL=SWL: GOSUB 2790
1310 IF AST=INT(AST/PPS)*PPS THEN 1320 ELSE AST=AST-1: GOTO
1310
1320 GOSUB 2820: SWL=AWL: SPL=AST
1330 AWL=FWL: GOSUB 2790: AST=AST+1
1340 IF AST=INT(AST/PPS)*PPS THEN 1350 ELSE AST=AST+1: GOTO
1340
1350 GOSUB 2820: FWL=AWL: FPL=AST
1360 NST=ABS(FPL-SPL)/PPS
1370 IF NST-INT(NST)=0 THEN 1390
1380 PRINT"!!!!INCREMENTATION ERROR!!!!": STOP
1390 DEL=FWL-SWL
1400 CLS:LOCATE 1,1
1410 OPEN"I",#2,"DFN": INPUT#2,DFN: CLOSE#2
1420 A$(1)="FILENUMBER:"+" "+"
A:D"+RIGHT$(STR$(DFN),LEN(STR$(DFN))-1)
1430 A$(2)="DATE:"+" "+DATE$
1440 A$(3)="START WAVE.:"+" "+STR$(SWL)+" ANGSTROMS\"
1450 A$(4)="FINAL WAVE.:"+" "+STR$(FWL)+" ANGSTROMS\"
1460 A$(5)="ENT. SLIT:"+" "+STR$(SLW(1))+" MICRONS\"
1470 A$(6)="EXIT SLIT:"+" "+STR$(SLW(2))+" MICRONS\"
1480 A$(7)="STEP SIZE:"+" "+STR$(STP)+" ANGSTROMS\"
1490 A$(8)="RESOLUTION:"+" "+STR$(SLW(1)*.016)+" ANGSTROMS\"
1500 A$(9)="PMT VOLT.:"+" "+STR$(PMT)+" VOLTS\"
1510 A$(10)="PMT TEMP.:"+" "+STR$(CEL)+" degC\"
1520 A$(11)="GATE TIME:"+" "+STR$(GAT)+" MICROSEC.\"

```

```

1530 CLS: LOCATE 1,1
1540 FOR I=1 TO 10 STEP 2
1550 PRINT A$(I) TAB(35) A$(I+1)
1560 NEXT I
1570 PRINT A$(11)
1575 PRINT (NST+1)*24+345;" BYTES ARE NECESSARY TO RECORD
SPECTRA."
1576 PRINT"PRESS F5 TO LIST FILES AND BYTES FREE ON DISK IN
DRIVE A.":STOP
1577 CLS:FILES"A:
1580 PRINT: PRINT"PRESS [ENTER] WHEN YOU WANT THE SCAN TO
BEGIN."
1590 PRINT"PRESS [DEL] IF PARAMETERS ABOVE ARE INCORRECT."
1600 A$=INKEY$: IF LEN(A$)=0 THEN 1600
1605 IF ASC(A$)=13 THEN 1610
1606 IF ASC(A$)=46 THEN 950
1607 GOTO 1600
1610 ST$=TIME$
1620 OT=VAL(MID$(TIME$,1,2))*60+VAL(MID$(TIME$,4,5))
1630 FOR K=1 TO 2
1650 PRINT#1,CHR$(30+K);
1660 IF INPUT$(1,#1)=CHR$(30+K) THEN 1670 ELSE 1660
1670 PRINT#1,CHR$(INT(SLW(K)/256));CHR$(SLW(K) MOD 256);
1680 IF INPUT$(1,#1)=CHR$(24) THEN 1690 ELSE 1680
1690 NEXT K
1700 PRINT#1,CHR$(30);
1710 IF INPUT$(1,#1)=CHR$(30) THEN 1720 ELSE 1710
1720 FOR K=1 TO 2
1730 SH$(K)=INPUT$(1,#1): SL$(K)=INPUT$(1,#1)
1740 NEXT K
1750 IF ASC(SH$(1))*256+ASC(SL$(1))=SLW(1) AND
ASC(SH$(2))*256+ASC(SL$(2))=SLW(2) THEN 1770 ELSE 1760
1760 PRINT"!!!!SLITWIDTH ERROR!!!!": STOP
1770 IF INPUT$(1,#1)=CHR$(24) THEN 1780 ELSE 1770
1780 CLS
1790 LOCATE 10,25: PRINT"STARTING WAVELENGTH:"
1800 LOCATE 11,25: PRINT"FINAL WAVELENGTH:"
1810 LOCATE 13,25: PRINT"PRESENT WAVELENGTH:"
1820 LOCATE 10,46: PRINT USING "#####.##";SWL
1830 LOCATE 11,46: PRINT USING "#####.##";FWL
1840 OPEN"R",#2,"A:D"+RIGHT$(STR$(DFN),LEN(STR$(DFN))-1),24
1850 FIELD#2,8 AS X$,8 AS AX$,8 AS Y$
1880 SPL=SPL-REF: AST=REF
1890 IF SPL<0 THEN DIR=1: INC=-1
1900 IF SPL>=0 THEN DIR=7: INC=1
1910 SPL=ABS(SPL)
1920 FOR K=1 TO SPL
1930 PRINT#1,CHR$(DIR);: AST=AST+INC
1940 IF INPUT$(1,#1)=CHR$(24) THEN 1950 ELSE 1940
1950 NEXT K
1960 GOSUB 2290:LSET X$=MKD$(AST):LSET AX$=MKD$(SWL):LSET
Y$=MKD$(D%):PUT#2,1

```

```

1970 LOCATE 13,46:PRINT USING"#####.##";SWL
1980 LOCATE 14,25:PRINT TIME$
1990 IF DEL<0 THEN DIR=1 ELSE DIR=7
2000 IF DEL<0 THEN INC=-1 ELSE INC=1
2010 FOR K=1 TO NST
2020 IF VAL(MID$(TIME$,1,2))*60+VAL(MID$(TIME$,4,5))-OT>PAU-1
THEN 2030 ELSE 2080
2030 LOCATE 15,25: PRINT"SCAN INTERRUPTED.": FOR W=1 TO 25:
BEEP: NEXT
2040 LOCATE 16,25: PRINT"PRESS F5 TO CONTINUE.": STOP
2050 OT=VAL(MID$(TIME$,1,2))*60+VAL(MID$(TIME$,4,5))
2060 LOCATE 15,25: PRINT"                ": LOCATE 16,25:
PRINT"                "
2070 PRINT"                ": PRINT"                ": PRINT"                "
2080 FOR I=1 TO PPS: PRINT#1,CHR$(DIR);:AST=AST+INC
2090 IF INPUT$(1,#1)=CHR$(24) THEN 2100 ELSE 2090
2100 NEXT I
2110     GOSUB     2290:GOSUB     2820:LSET     X$=MKD$(AST):LSET
AX$=MKD$(AWL):LSET Y$=MKD$(D%):PUT#2,K+1
2120 LOCATE 13,46: PRINT USING "#####.##";AWL
2130 LOCATE 14,25: PRINT TIME$
2140 NEXT K
2175 CLOSE#2
2180 FI$=TIME$
2190 A$(12)="SCAN TIME:"+" "+ST$+"-"+FI$
2200OPEN"O",#2,"A:D"+RIGHT$(STR$(DFN),LEN(STR$(DFN))-1)+"P":
PRINT#2,12
2210 FOR I=1 TO 12: PRINT#2,A$(I): NEXT I
2220 CLOSE#2
2230 CLS: LOCATE 1,1
2240 FOR I=1 TO 12 STEP 2: PRINT A$(I) TAB(35) A$(I+1): NEXT
I
2250 GOSUB 2390
2260 PRINT"THE DATA FILE NAME IS
"+"A:D"+RIGHT$(STR$(DFN),LEN(STR$(DFN))-1)+". "
2270 OPEN"O",#2,"DFN": PRINT#2,DFN+1: CLOSE#2
2280 PRINT"PRESS F5 TO CONTINUE.":STOP: GOTO 270
2290 B=784
2300 OUT B+7,&H30
2310 OUT B+4,&HFF: OUT B+4,&HFF
2320 OUT B+7,&HB8
2330 OUT B+6,&H0: OUT B+6,&H1
2340 IF (INP(B+2) AND &H10)<16 THEN GOTO 2340
2350 OUT B+7,&H0
2360 XL%=INP(B+4): XH%=INP(B+4)
2370 D%=65535!-256*XH%-XL%
2380 RETURN
2390 A$="A:D"+RIGHT$(STR$(DFN),LEN(STR$(DFN))-1)
2400 OPEN"R",#2,A$,24
2410 FIELD#2,8 AS X$,8 AS AX$,8 AS Y$:N=LOF(2)/24
2420
GET#2,1:XMIN=CVD(AX$):YMIN=CVD(Y$):YMAX=CVD(Y$):GET#2,N:XMAX

```



```

=CVD(AX$)
2430 FOR I=2 TO N
2440 GET#2,I:Y=CVD(Y$)
2470 IF Y>YMAX THEN YMAX=Y
2480 IF Y<YMIN THEN YMIN=Y
2490 NEXT I
2500 WN=N
2510 CLOSE#2
2520 INC=(XMAX-XMIN)/4
2530 KEY OFF: CLS
2540 LOCATE 25,3:PRINT USING "####.##";XMIN :LOCATE
25,19:PRINT USING "####.##";XMIN+INC
2550 LOCATE 25,38:PRINT USING "####.##";XMIN+2*INC:LOCATE
25,57:PRINT USING "####.##";XMIN+3*INC
2560 LOCATE 25,72:PRINT USING "####.##";XMAX
2570 LOCATE 1,1:PRINT 100:LOCATE 7,2:PRINT 75:LOCATE
13,2:PRINT 50
2580 LOCATE 19,2:PRINT 25:LOCATE 22,1
2590 LINE(38,0)-(38,334): LINE(38,332)-(719,332)
2600 FOR I=0 TO 3
2610 XT=((I+1)*170)+38:YT=(I*83)
2620 LINE(XT,332)-(XT,334):LINE(36,YT)-(38,YT)
2630 NEXT I
2640 OPEN"R",#2,A$,24
2650 FIELD#2,8 AS X$,8 AS AX$,8 AS Y$:N=LOF(2)/24
2660 GET#2,1:WX=CVD(AX$):WY=CVD(Y$)
2670 FOR I=2 TO N
2680 GET#2,I:X=CVD(AX$):Y=CVD(Y$)
2690 X1=38+INT((WX-XMIN)*681/(XMAX-XMIN))
2700 X2=38+INT((X-XMIN)*681/(XMAX-XMIN))
2710 Y1=332-INT((WY-YMIN)*332/(YMAX-YMIN))
2720 Y2=332-INT((Y-YMIN)*332/(YMAX-YMIN))
2730 LINE (X1,Y1)-(X2,Y2)
2740 WX=X: WY=Y
2750 NEXT I
2760 CLOSE#2
2770 LOCATE 1,1
2780 RETURN
2790 X=AWL/16437.86859#
2800 AST=INT(ATN(X/SQR(-X*X+1))/.0000044)
2810 RETURN
2820 AWL=16437.86859#*SIN(AST*.0000044)
2830 RETURN
3000 CLS:INPUT"ENTER N, THE NUMBER OF INTENSITY MEASUREMENTS.
",N
3010 PRINT"PRESS F5 TO START.":STOP
3020 ST=TIMER:B=784
3030 FOR I=1 TO N
3040 OUT B+7,&H30
3050 OUT B+4,&HFF: OUT B+4,&HFF
3060 OUT B+7,&HB8
3070 OUT B+6,&H5: OUT B+6,&H0

```

```
3080 IF (INP(B+2) AND &H10)<16 THEN GOTO 3080
3090 OUT B+7,&H0
3100 XL%=INP(B+4): XH%=INP(B+4)
3110 Y(I)=65535!-256*XH%-XL%
3120 NEXT
3130 FT=TIMER:C=792:OUT C,0:OUT C+1,128:FOR I=1 TO
1000:NEXT:OUT C,0:OUT C+1,0
3140 OPEN"I",#2,"DFN":INPUT#2,DFN:CLOSE#2
3150 DF$="A:D"+RIGHT$(STR$(DFN),LEN(STR$(DFN))-1)
3160 OPEN"R",#2,DF$,8
3170 FIELD#2,4 AS X$,4 AS Y$
3180 FOR I=1 TO N
3190 LSET X$=MK$$(I):LSET Y$=MK$$(Y(I)):PUT#2,I
3200 NEXT I
3210 CLOSE#2
3220 OPEN"O",#2,"DFN":PRINT#2,DFN+1:CLOSE#2
3230 CLS:PRINT"DATA FILENAME: ";DF$
3240 PRINT"ELAPSED TIME IN SECONDS:";FT-ST
3250 PRINT"PRESS F5 TO LIST DATA.":STOP
3260 CLS:
3270 FOR I=1 TO N
3280 PRINT I;Y(I)
3290 NEXT
3300 PRINT"PRESS F5 TO CONTINUE.":STOP
3310 RETURN
```

A.2 Program 2 -- Plot Data

This program plots the spectra collected using program 1. The cursor can be positioned to any data point on the plot using key board commands. Any range within the limits of the data can be plotted. The grating position, wavelength, and intensity which correspond to the point are printed at the bottom of the screen. A look-up table can be used with the program to adjust the spectra with respect to internal wavelength references. Hard copies of the plot can be output.

```

10 REM LIST OF VARIABLES AND ARRAYS USED WITHIN THE MAIN
    PROGRAM AND PASSED
20 REM BETWEEN SUBROUTINES. DUMMY ARGUMENTS ARE ONLY USED
    WITHIN THE
30 REM SUBROUTINES AND ARE "NOT" INPUTS OR RETURNS OF THE
    SUBROUTINES.
40 REM LU$ ---- LOOK-UP TABLE FILENUMBER.
50 REM DF$ ---- DATA FILENAME.
60 REM NP ----- NUMBER OF SCREENS.
70 REM NP(I) -- SCREEN LIMITS.
80 REM LR ----- LOWER DATA RECORD NUMBER FOR INPUT AND
    SCREEN PLOT.
90 REM UR ----- UPPER DATA RECORD NUMBER FOR INPUT AND
    SCREEN PLOT.
100 REM FP ----- DIMENSION OF DATA ARRAYS INPUT.
110 REM X#(I) -- INPUT DATA ABSCISSA ARRAY. (e.g. GRATING
    POSITION)
120 REM AX#(I) - INPUT DATA ADJUSTED ABSCISSA ARRAY. (e.g.
    WAVELENGTH)
130 REM Y#(I) -- INPUT DATA ORDINATE ARRAY. (e.g.
    INTENSITY/COUNTS)
140 REM YMAX# -- MAXIMUM VALUE IN Y#(I).
150 REM YMIN# -- MINIMUM VALUE IN Y#(I).
160 REM FLAG --- FLAG=1 INITIATES CURSOR POSITION CALC. FOR
    STORE.
170 REM STORE -- ADJUSTED ABCISSA VALUE WHERE CURSOR SHOULD
    BE POSITIONED.
180 REM PO ----- CURRENT SCREEN CURSOR POSITION INDEX.
190 REM XP(I) -- ABSCISSA SCREEN COORDINATE FOR CURSOR.
200 REM YP(I) -- ORDINATE SCREEN COORDINATE FOR CURSOR.

```

```

210 REM B% ----- CURSOR SHAPE.
220 REM C% ----- CURSOR SHAPE.
230 REM D% ----- CURSOR SHAPE.
240 REM E% ----- CURSOR SHAPE.
250 REM SC ----- CURRENT SCREEN NUMBER. (0<SC<NP)
260 REM DUMMY ARGUMENTS ---
X$,AX$,Y$,RX$,RY$,RZ$,OX$,OAX$,OY$,AF$,I,J,K,N,X#,LO,
270 REM UP,MD,RX#,RXL#,RYL#,RXU#,RYU#,XT,YT,WX#,WY#,X1,Y1,
280 REM CNP,Z,AX#,X1#,AX1#,X2#,AX2#,A$,B$,C$,D$,INC#,LL#,MR,
290 REM UL#,NPP,A%
300 REM
310 REM
320 REM MAIN PROGRAM
330 REM *****
340 REM *****
350 DIM
A%(350),B%(35),C%(35),D%(35),E%(35),X%(683),Y%(683),AX%(683)
,XP(683)
360 DIM YP(683),NP(500)
370 REM LIST FILES ON DISK IN DRIVE A
380 CLS:FILES"A:
390 INPUT"ENTER THE DATA FILENAME. (DON'T FORGET DRIVE
DESIGNATION.) ",DF$
400 INPUT"ENTER THE LOOK-UP TABLE FILENUMBER. ENTER 0 (ZERO)
IF NO LOOK-UP TABLE WILL BE USED. ",LU$
410 REM CALCULATE ADJUSTED ABCISSA VALUES IF LOOK-UP TABLE IS
USED.
420 IF LU$<>"0" THEN GOSUB 950
430 REM SAVE CURSOR SHAPES
440 GOSUB 3160
450 REM CALCULATE THE NUMBER OF SCREENS AND THE SCREEN LIMITS.
460 GOSUB 1270
470 REM INPUT DATA TO BE USED IN PLOTTING SCREEN 1.
480 LR=NP(0)+1:UR=NP(1):FLAG=0:SC=1
490 REM INPUT DATA, PLOT SCREEN, POSITION CURSOR, AND PRINT
CURSOR POSITION
500 GOSUB 1400:GOSUB 1560:GOSUB 1840:GOSUB 1970
510 REM *****
520 REM * READ CHARACTERS FROM THE KEYBOARD TO DETERMINE *
530 REM * THE SUBROUTINE TO EXECUTE. *
540 REM *****
550 A$=INKEY$
560 IF LEN(A$)=0 THEN 550
570 IF ASC(A$)=42 THEN GOSUB 2540 '{PrtSc} OUTPUT HARDCOPY'
580 IF ASC(A$)=42 THEN GOTO 550
590 IF ASC(A$)=46 THEN GOSUB 2050 '{Del} CHOOSE RANGE OF PLOT
FROM GIVEN LIMITS'
600 IF ASC(A$)=46 THEN GOTO 500
610 IF ASC(A$)=48 THEN GOSUB 2340 '{Ins} CHOOSE PARTICULAR
ADJUSTED ABCISSA'
620 IF ASC(A$)=48 THEN GOTO 500
630 IF ASC(A$)=13 THEN GOSUB 2860 '{Enter} SET LIMITS FOR PLOT'

```

```

640 IF ASC(A$)=13 THEN GOTO 500
650 IF ASC(A$)=54 THEN P=1 '{-->} STEP CURSOR TO PT. WITH NEXT
HIGHEST ABSCISSA'
660 IF ASC(A$)=52 THEN P=-1 '{<--} STEP CURSOR TO PT. WITH
NEXT LOWEST ABSCISSA'
670 IF ASC(A$)=43 THEN P=INT(FP/10) '{+} STEP CURSOR FORWARD
1/10 ABSCISSA RANGE'
680 IF ASC(A$)=45 THEN P=-INT(FP/10) '{-} STEP CURSOR BACK 1/10
ABSCISSA RANGE'
690 IF ASC(A$)=56 THEN Z=1: GOTO 760 '{8} PLOT NEXT SCREEN'
700 IF ASC(A$)=50 THEN Z=-1: GOTO 760 '{2} PLOT FORMER SCREEN'
710 IF ASC(A$)=27 GOTO 790 '{Esc} END PROGRAM'
720 IF PO+P>FP THEN P=0
730 IF PO+P<1 THEN P=0
740 GOSUB 1840:PO=PO+P:GOSUB 1840:GOSUB 1970
750 GOTO 550
760 IF Z+SC>NP THEN 550
770 IF Z+SC<1 THEN 550
780 SC=SC+Z:LR=NP(SC-1)+1:UR=NP(SC):GOTO 500
790 CLS: KEY ON
800 REM IF LOOK-UP TABLE WAS USED, PRINT THE NAME OF THE NEW
FILE CREATED
810 IF LU$<>"0" THEN PRINT"THE ADJUSTED FILE ";DF$;" WAS
CREATED."
820 END
830 REM*****
840 REM*****
850 REM
860 REM
870 REM *****
880 REM * SUBROUTINE TO ADJUST ABSCISSA VALUES WITH *
890 REM * RESPECT TO LOOK-UP TABLE ABSCISSA VALUES. *
900 REM * ARGUMENTS INPUT----LU$,DF$ *
910 REM * DUMMY ARGUMENTS----RX$,RZ$,RY$,X$,AX$,Y$,AF$, *
920 REM * OX$,OAX$,OY$,N,I,X#,LO,UP, *
925 REM * MD,RX#,RXL#,RYL#,RXU#,RYU#*
930 REM * RETURN-----CREATES NEW DF$ IN *
935 REM * C:\SCOTT\BACK\DIRECTORY *
940 REM *****
950 OPEN"R",#1,"C:\SCOTT\BACK\LU"+LU$,24
960 FIELD#1,8 AS RX$,8 AS RZ$,8 AS RY$
970 OPEN"R",#2,DF$,24
980 FIELD#2,8 AS X$,8 AS AX$,8 AS Y$
990 AF$="C:\SCOTT\BACK\A"+RIGHT$(DF$,LEN(DF$)-2)
1000 OPEN"R",#3,AF$,24
1010 FIELD#3,8 AS OX$,8 AS OAX$,8 AS OY$
1020 N=LOF(2)/24
1030 FOR I=1 TO N
1040 GET#2,I:X#=CVD(X$):LO=1:UP=LOF(1)/24
1050 GET#1,1:IF X#<=CVD(RX$) THEN 1140
1060 GET#1,UP:IF X#>=CVD(RX$) THEN LO=UP-1:GOTO 1140
1070 MD=LO+INT((UP-LO)/2)

```

```

1080 IF MD=LO THEN 1140
1090 GET#1,MD:RX#=CVD(RX$)
1100 IF X#=RX# THEN LO=MD:GOTO 1140
1110 IF X#>RX# THEN LO=MD
1120 IF X#<RX# THEN UP=MD
1130 GOTO 1070
1140
GET#1,LO:RXL#=CVD(RX$):RYL#=CVD(RY$):GET#1,LO+1:RXU#=CVD(RX$)
):RYU#=CVD(RY$)
1150 LSET OX$=X$:LSET
OAX$=MKD$(RYU#-((RYU#-RYL#)*(RXU#-X#)/(RXU#-RXL#)))
1160 LSET OY$=Y$:PUT#3
1170 NEXT
1180 CLOSE#1:CLOSE#2:CLOSE#3:DF$=AF$
1190 RETURN
1200 REM *****
1210 REM * SUBROUTINE WHICH CALCULATES THE NUMBER *
1220 REM * OF SCREENS AND THE SCREEN LIMITS. *
1230 REM * ARGUMENTS INPUT----DF$ *
1240 REM * DUMMY ARGUMENTS----N,I *
1250 REM * RETURN-----NP,NPP,NP(I) *
1260 REM *****
1270 OPEN"R",#2,DF$,24:N=LOF(2)/24:CLOSE#2
1280 NP=INT(N/341)
1290 IF NP=0 THEN NP=1:GOTO 1310
1300 NPP=INT(341+(N-INT(N/341)*341)/NP):NP=INT(N/NPP):
1310 NP(0)=0:NP(NP)=N
1320 FOR I=1 TO NP-1:NP(I)=I*NPP:NEXT I
1330 RETURN
1340 REM *****
1350 REM * SUBROUTINE WHICH PUTS DATA INTO X#(I),AX#(I), *
1355 REM * AND Y#(I) ARRAYS. *
1360 REM * ARGUMENTS INPUT---DF$,LR,UR *
1370 REM * DUMMY ARGUMENTS---X$,AX$,Y$,I *
1380 REM * RETURN-----FP,X#(I),AX#(I),Y#(I),YMAX#, *
1385 REM * YMIN# *
1390 REM *****
1400 OPEN"R",#2,DF$,24
1410 FIELD#2,8 AS X$,8 AS AX$,8 AS Y$
1420 GET#2,LR:YMAX#=CVD(Y$):YMIN#=YMAX#
1430 FP=UR-LR+1
1440 FOR I=1 TO FP
1450 GET#2,I+LR-1:X#(I)=CVD(X$):AX#(I)=CVD(AX$):Y#(I)=CVD(Y$)
1460 IF Y#(I)>YMAX# THEN YMAX#=Y#(I)
1470 IF Y#(I)<YMIN# THEN YMIN#=Y#(I)
1480 NEXT
1490 CLOSE#2:RETURN
1500 REM *****
1510 REM * SUBROUTINE THAT PLOTS DATA IN AX#(I) AND *
1515 REM * Y#(I) ARRAYS *
1520 REM * ARGUMENTS INPUT----FLAG,STORE,AX#(I),Y#(I), *
1525 REM * FP,YMAX#,YMIN# *

```

```

1530 REM * DUMMY ARGUMENTS----I, YT, XT, WX#, WY#, X1, Y1      *
1540 REM * RETURN-----PO, XP(I), YP(I)                      *
1550 REM *****
1560 KEY OFF:CLS:LOCATE 1,1:PRINT 100:LOCATE 7,2:PRINT
75:LOCATE 13,2:PRINT 50
1570 LOCATE 19,2:PRINT 25:LOCATE 22,1
1580 LINE(38,0)-(38,334): LINE(38,332)-(719,332)
1590 FOR I=0 TO 3:YT=(I*83):LINE(36,YT)-(38,YT):NEXT
1600 FOR I=1 TO 3:XT=(I*227)+38:LINE(XT,332)-(XT,334):NEXT
1610 PO=1
1620 IF FLAG=0 THEN GOTO 1650
1630 IF STORE=AX#(1) THEN PO=1
1640 IF STORE>AX#(1) THEN PO=1
1650 WX#=AX#(1):WY#=Y#(1):XP(1)=38
1660 YP(1)=332-INT((Y#(1)-YMIN#)*332/(YMAX#-YMIN#))
1670 FOR I=2 TO FP
1680 IF FLAG=0 THEN GOTO 1710
1690 IF STORE=AX#(I) THEN PO=I
1700 IF STORE>AX#(I) THEN PO=I
1710 X1=38+INT((WX#-AX#(1))*681/(AX#(FP)-AX#(1)))
1720 XP(I)=38+INT((AX#(I)-AX#(1))*681/(AX#(FP)-AX#(1)))
1730 Y1=332-INT((WY#-YMIN#)*332/(YMAX#-YMIN#))
1740 YP(I)=332-INT((Y#(I)-YMIN#)*332/(YMAX#-YMIN#))
1750 LINE (X1,Y1)-(XP(I),YP(I))
1760 WX#=AX#(I): WY#=Y#(I)
1770 NEXT I
1780 RETURN
1790 REM *****
1800 REM * SUBROUTINE TO INVERT CURSOR AT POSITION PO.      *
1810 REM * ARGUMENTS INPUT--PO,XP(I),YP(I),B%,C%,D%,E%    *
1820 REM * RETURN-----CURSOR POINTS AT PO INVERTED *
1830 REM *****
1840 IF YP(PO)=0 THEN 1860
1850 IF XP(PO)=719 THEN 1900 ELSE 1870
1860 IF XP(PO)=719 THEN 1890 ELSE 1880
1870 PUT(XP(PO)-1,YP(PO)-1),B%,XOR: GOTO 1910
1880 PUT(XP(PO)-1,YP(PO)),C%,XOR: GOTO 1910
1890 PUT(XP(PO)-1,YP(PO)),D%,XOR: GOTO 1910
1900 PUT(XP(PO)-1,YP(PO)-1),E%,XOR: GOTO 1910
1910 RETURN
1920 REM *****
1930 REM * SUBROUTINE TOO PRINT THE CURSOR LOCATION *
1935 REM * AT THE BOTTOM OF A PLOT. *
1940 REM * ARGUMENT INPUT-PO,X#(I),AX#(I),Y#(I),SC *
1950 REM * RETURN----POSITION OF CURSOR PRINTED *
1955 REM * AT THE BOTTOM OF A PLOT. *
1960 REM *****
1970 LOCATE 25,1:PRINT"X=";X#(PO) TAB(25) "AX=";AX#(PO)
TAB(50) "Y=";Y#(PO) TAB(73) "SC=";SC;
1980 RETURN
1990 REM *****
2000 REM * SUBROUTINE THAT ALLOWS YOU TO CHOOSE THE *

```

```

2005 REM * RANGE OF THE NEXT PLOT *
2010 REM * ARGUMENTS INPUT----DF$,NP *
2020 REM * DUMMY ARGUMENTS----X$,AX$,Y$,CNP,Z,X1#, *
2025 REM * AX1#,X2#,AX2# *
2030 REM * RETURN-----LR,UR,FLAG,SC *
2040 REM *****
2050 CLS:LOCATE 1,1
2060 OPEN"R",#2,DF$,24
2070 FIELD#2,8 AS X$,8 AS AX$,8 AS Y$
2080 PRINT "SCREEN" TAB(14) "RANGE" TAB(36) "ADJ. RANGE"
2090 PRINT "-----" TAB(14) "-----" TAB(36) "-----"
2100 CNP=0
2110 FOR Z=1 TO NP
2120 GET#2,NP(Z-1)+1:X1#=CVD(X$):AX1#=CVD(AX$)
2130 GET#2,NP(Z):X2#=CVD(X$):AX2#=CVD(AX$)
2140 CNP=CNP+1
2150 IF CNP>18 THEN PRINT"PRESS F5 TO SEE MORE OF THE
MENU.":STOP:CLS
2160 IF CNP>18 THEN PRINT "SCREEN" TAB(14) "RANGE" TAB(36)
"ADJ. RANGE"
2170 IF CNP>18 THEN PRINT "-----" TAB(14) "-----" TAB(36)
"-----"
2180 IF CNP>18 THEN CNP=0
2190 PRINT Z TAB(13) INT(X1#*100)/100;"-";INT(X2#*100)/100
TAB(35) INT(AX1#*100)/100;"-";INT(AX2#*100)/100
2200 NEXT Z
2210 PRINT"ENTER 0 (ZERO) IF YOU WANT TO ENTER SPECIFIC
LIMITS."
2220 INPUT"ENTER THE SCREEN #. ",Z
2230 IF Z<0 THEN PRINT"OUT OF RANGE. (SCREEN #=0 TO
";NP;)"":GOTO 2220
2240 IF Z>NP THEN PRINT"OUT OF RANGE. (SCREEN #=0 TO
";NP;)"":GOTO 2220
2250 CLOSE#2
2260 IF Z>0 THEN SC=Z:LR=NP(SC-1)+1:UR=NP(SC):FLAG=0:RETURN
2270 GOSUB 2860:RETURN
2280 REM *****
2290 REM * SUBROUTINE TO CHOOSE A PARTICULAR ADJUSTED *
2295 REM * ABSCISSA VALUE. *
2300 REM * ARGUMENTS INPUT----DF$,NP,NP(I) *
2310 REM * DUMMY ARGUMENTS----X$,AX$,Y$,AX#,AX1#,AX2#,I*
2320 REM * RETURN-----SC,LR,UR,FLAG,STORE *
2330 REM *****
2340 OPEN"R",#2,DF$,24
2350 FIELD#2,8 AS X$,8 AS AX$,8 AS Y$
2360 CLS:LOCATE 10,1
2370 GET#2,1:AX1#=CVD(AX$):GET#2,LOF(2)/24:AX2#=CVD(AX$)
2380 PRINT"ABSCISSA RANGE: ";AX1#;" TO ";AX2#
2390 INPUT"ENTER THE ADJUSTED ABSCISSA VALUE YOU WANT
DISPLAYED. ",STORE
2400 IF STORE<AX1# THEN GOTO 2380
2410 IF STORE>AX2# THEN GOTO 2380

```



```

2420 FOR I=1 TO NP
2430 GET#2,NP(I):AX#=CVD(AX$)
2440 IF STORE>AX# THEN GOTO 2460
2450 SC=I:I=NP
2460 NEXT
2470 LR=NP(SC-1)+1:UR=NP(SC):FLAG=1:CLOSE#2:RETURN
2480 REM *****
2490 REM * SUBROUTINE TO OUTPUT HARD COPY OF SCREEN TO *
2495 REM * PRINTER. *
2500 REM * ARGUMENTS INPUT--X#(I),AX#(I),Y#(I),FP,PO,SC*
2510 REM * DUMMY ARGUMENTS--A$,B$,C$,D$,A%,I,J,K,N,INC#*
2520 REM * RETURN-----HARDCOPY OF SCREEN *
2530 REM *****
2540 GOSUB 1840:INC#=(AX#(FP)-AX#(1))/3
2550 A$=STR$(AX#(1)):D$=STR$(AX#(FP))
2560 IF LEN(A$)>LEN(D$) THEN L=LEN(A$) ELSE L=LEN(D$)
2570
B$=LEFT$(STR$(AX#(1)+INC#),L):C$=LEFT$(STR$(AX#(1)+2*INC#),L)
)
2580 LOCATE 25,1:PRINT SPACE$(80);
2590 LOCATE 25,2:PRINT A$;:LOCATE 25,28-INT(LEN(B$)/2):PRINT
B$;
2600 LOCATE 25,54-INT(LEN(C$)/2):PRINT C$;:LOCATE
25,80-LEN(D$):PRINT D$;
2610 OPEN"LPT1:" AS #2: WIDTH #2,255
2620 LPRINT CHR$(27);"A";CHR$(8);
2630 FOR J=0 TO 716 STEP 16
2640 GET(J,347)-(J+15,0),A%
2650 FOR K=1 TO 2
2660 PRINT #2, CHR$(27);"K";CHR$(92);CHR$(1);
2670 FOR I=347 TO 0 STEP -1
2680 IF K=1 THEN N=(A%(I+2) AND &HFF)
2690 IF K=2 THEN N=(A%(I+2) AND &HFF00)/256
2700 IF N<0 THEN N=N+256
2710 PRINT #2, CHR$(N);
2720 NEXT I:PRINT #2, CHR$(13);CHR$(10);
2730 NEXT K
2740 NEXT J
2750 PRINT #2,CHR$(12)
2760 PRINT #2, CHR$(27);"@"
2770 CLOSE #2
2780 LOCATE 25,1:PRINT SPACE$(80);:GOSUB 1840:GOSUB 1970
2790 RETURN
2800 REM*****
2810 REM*SUBROUTINE WHICH ALLOWS YOU TO SET THE LIMITS FOR*
2815 REM*THE NEXT PLOT. *
2820 REM*ARGUMENTS INPUT----DF$ *
2830 REM*DUMMY ARGUMENTS----X$,AX$,Y$,AX1#,AX2#,LL#,X#,LO *
2835 REM * MR,AX#,UL#,UP,MD *
2840 REM * RETURN----LR,UR,FLAG,SC *
2850 REM*****
2860 CLS

```

```

2870 OPEN"R",#2,DF$,24
2880 FIELD#2,8 AS X$,8 AS AX$,8 AS Y$
2890 GET#2,1:AX1#=CVD(AX$):GET#2,LOF(2)/24:AX2#=CVD(AX$)
2900 PRINT"ABSCISSA RANGE: ";AX1#;" TO ";AX2#
2910 INPUT"ENTER THE LOWER ADJUSTED ABSCISSA LIMIT. ",LL#
2920 IF LL#<AX1# THEN 2900
2930 IF LL#>AX2# THEN 2900
2940 X#=LL#:GOSUB 3030:LR=LO:MR=LR+681
2950 IF MR>LOF(2)/24 THEN MR=LOF(2)/24
2960 GET#2,MR:AX#=CVD(AX$)
2970 PRINT"THE MAXIMUM UPPER ADJUSTED ABSCISSA LIMIT IS
";AX#;". "
2980 INPUT"ENTER THE UPPER ADJUSTED ABSCISSA LIMIT. ",UL#
2990 IF UL#<LL# THEN 2970
3000 IF UL#>AX# THEN 2970
3010 X#=UL#:GOSUB 3030:UR=LO
3020 FLAG=0:CLOSE#2:SC=0:RETURN
3030 UP=LOF(2)/24:LO=1
3040 MD=LO+INT((UP-LO)/2)
3050 IF MD=LO THEN 3110
3060 GET#2,MD:AX#=CVD(AX$)
3070 IF X#=AX# THEN LO=MD:GOTO 3110
3080 IF X#>AX# THEN LO=MD
3090 IF X#<AX# THEN UP=MD
3100 GOTO 3040
3110 RETURN
3120 REM *****
3130 REM * SUBROUTINE TO SAVE CURSOR SHAPES. *
3140 REM * RETURN----B%,C%,D%,E% *
3150 REM *****
3160 CLS
3170 LINE (0,0)-(2,2),,BF: GET (0,0)-(2,2),B%:CLS
3180 LINE (0,0)-(2,1),,BF: GET (0,0)-(2,1),C%:CLS
3190 LINE (0,0)-(1,1),,BF: GET (0,0)-(1,1),D%:CLS
3200 LINE (0,0)-(1,2),,BF: GET (0,0)-(1,2),E%:CLS
3210 RETURN

```

APPENDIX B

B.1 Formulae for Calculating Rotational Lines

Formulae used to calculate the wavenumber, ν , of spectral lines in Programs 3 and 4 [12].

$$\nu = \nu_e + \nu_v + \nu_r$$

where e designates electronic contribution,
 v designates vibrational contribution,
 and r designates rotational contribution.

$\nu_0 = \nu_e + \nu_v$, the band origin, is a constant for a particular vibrational transition. Therefore, $\nu = \nu_0 + \nu_r$.

$$\nu_0 = \nu_e + \nu_v = (T_e' - T_e'') + (G' - G'')$$

where single-primed letters correspond to the upper state, double-primed letters correspond to the lower state, and

$$G = \omega_e(v + 1/2) - \omega_e x_e(v + 1/2)^2 + \omega_e y_e(v + 1/2)^3 - \omega_e z_e(v + 1/2)^4.$$

ν_r is variable and depends on the different values of the rotational quantum number in the upper, J' , and lower, J'' , states. The selection rules applied in the present case are those of a symmetric top. If at least one of the two states

has $\Lambda \neq 0$ then the selection rule for J is

$$\Delta J = J' - J'' = 0, \pm 1.$$

If however, $\Lambda = 0$ in both electronic states, the transition with $\Delta J = 0$ is forbidden and only $\Delta J = \pm 1$ appears. Thus, there are three or two sets of lines (branches), respectively, whose wave numbers follow the following formulae:

R branch ($\Delta J=1$):

$$\nu = \nu_0 + 2B_V' + (3B_V' - B_V'')J'' + (B_V' - B_V'')J''^2 = R(J'')$$

Q branch ($\Delta J=0$):

$$\nu = \nu_0 + (B_V' - B_V'')J'' + (B_V' - B_V'')J''^2 = Q(J'')$$

P branch ($\Delta J=-1$):

$$\nu = \nu_0 - (B_V' + B_V'')J'' + (B_V' - B_V'')J''^2 = P(J'')$$

where

$$B_V = B_e - \alpha_e(v+1/2)$$

The intensity distribution of the rotational structure can be expressed as a product of

- 1) a constant, C_{em} , depending on the change of dipole moment and the number of molecules in the upper state,
- 2) the frequency factor, ν^4 ,
- 3) the inverse of the rotational partition function, $1/Q_r$,
- 4) the line strength, S_j ,

and

5) the Boltzmann factor.

Therefore, $I_{em} = (C_{em}\nu^4/Q_r)S_J \exp[-B_v'J'(J'+1)hc/kT]$, is the intensity distribution in the rotational structure of a symmetric top. The line strengths, S_J , are given by the Hönl-London formulae. The term $(C_{em}\nu^4/Q_r)$ may be considered constant since for a given band ν covers a very small range of values.

For $\Delta\Lambda = 0$ the Hönl-London formulae are

$$S_J^R = (J''+1+\Lambda'')(J''+1-\Lambda'')/(J''+1)$$

$$S_J^Q = (2J''+1)\Lambda''^2/[J''(J''+1)]$$

$$S_J^P = (J''+\Lambda'')(J''-\Lambda'')/J''$$

for $\Delta\Lambda = +1$

$$S_J^R = (J''+2+\Lambda'')(J''+1+\Lambda'')/[4(J''+1)]$$

$$S_J^Q = (J''+1+\Lambda'')(J''-\Lambda'')(2J''+1)/[4J''(J''+1)]$$

$$S_J^P = (J''-1-\Lambda'')(J''-\Lambda'')/4J''$$

for $\Delta\Lambda = -1$

$$S_J^R = (J''+2-\Lambda'')(J''+1-\Lambda'')/[4(J''+1)]$$

$$S_J^Q = (J''+1-\Lambda'')(J''+\Lambda'')(2J''+1)/[4J''(J''+1)]$$

$$S_J^P = (J''-1+\Lambda'')(J''+\Lambda'')/4J''.$$

State	T_e	ω_e	$\omega_e X_e$	$\omega_e Y_e$	B_e	α_e
C $^3\Pi_u$	89147.3	2035.1	17.08	-2.15	1.8529	0.0197
B $^3\Pi_g$	59626.3	1734.11	14.47	----	1.6380	0.0184

all values are in cm^{-1} .

B.2 Program 3 -- Rotational Lines

This program calculates and plots rotational line spectra. Vibrational and rotational constants for the electronic state of the diatomic molecule must be input.

```

5 DIM
R(500),Q(500),P(500),IR(500),IQ(500),IP(500),X(1501),Y(1501)
10 INPUT"ENTER THE NUMBER OF THE FILE CONTAINING THE CONSTANTS
FOR THE ELECTRONIC TRANSITION, 2-->1. ",B$ 11
A$="C:\SCOTT\BACK\CONST"+B$
12 INPUT"IS THIS FILE ALREADY STORED? (Y OR N) ",C$
13 IF C$="Y" OR C$="y" THEN GOTO 195
14 OPEN"O",#1,A$
30 PRINT"ENTER THE CONSTANTS FOR 1, THE FIRST ELECTRONIC
STATE."
40 INPUT"T(1)=",T(1):PRINT#1,T(1)
50 INPUT"W(1)=",W(1):PRINT#1,W(1)
60 INPUT"WX(1)=",WX(1):PRINT#1,WX(1)
70 INPUT"WY(1)=",WY(1):PRINT#1,WY(1)
80 INPUT"WZ(1)=",WZ(1):PRINT#1,WZ(1)
90 INPUT"BE(1)=",BE(1):PRINT#1,BE(1)
100 INPUT"AE(1)=",AE(1):PRINT#1,AE(1)
101 INPUT"LAMBDA(1)=",L(1):PRINT#1,L(1)
110 PRINT"ENTER THE CONSTANTS FOR 2, THE SECOND ELECTRONIC
STATE."
120 INPUT"T(2)=",T(2):PRINT#1,T(2)
130 INPUT"W(2)=",W(2):PRINT#1,W(2)
140 INPUT"WX(2)=",WX(2):PRINT#1,WX(2)
150 INPUT"WY(2)=",WY(2):PRINT#1,WY(2)
160 INPUT"WZ(2)=",WZ(2):PRINT#1,WZ(2)
170 INPUT"BE(2)=",BE(2):PRINT#1,BE(2)
180 INPUT"AE(2)=",AE(2):PRINT#1,AE(2)
181 INPUT"LAMBDA(2)=",L(2):PRINT#1,L(2)
190 CLOSE#1
195 OPEN"I",#1,A$
200 CLS: LOCATE 1,1
210 PRINT,1,2
215 INPUT#1,T(1),W(1),WX(1),WY(1),WZ(1),BE(1),AE(1),L(1)
216 INPUT#1,T(2),W(2),WX(2),WY(2),WZ(2),BE(2),AE(2),L(2)
220 PRINT "T",T(1),T(2)
230 PRINT "W",W(1),W(2)
240 PRINT "WX",WX(1),WX(2)
250 PRINT "WY",WY(1),WY(2)
260 PRINT "WZ",WZ(1),WZ(2)
270 PRINT "BE",BE(1),BE(2)

```

```

280 PRINT "AE",AE(1),AE(2)
281 PRINT "LAMBDA",L(1),L(2)
285 CLOSE#1
286 INPUT"ENTER THE NUMBER OF ROTATIONAL LINES YOU WANT CALC.
FOR EACH BRANCH.",COUNT
290 COUNT=COUNT-1
291 DL=L(2)-L(1)
300 INPUT"ENTER THE VIBRATIONAL QUANTUM NUMBER FOR 1, THE
LOWER ELECTRONIC STATE. ",V(1)
310 INPUT"ENTER THE VIBRATIONAL QUANTUM NUMBER FOR 2, THE
UPPER ELECTRONIC STATE. ",V(2)
315 INPUT"ENTER THE TEMPERATURE FOR THE CALCULATION IN KELVIN.
",T
316 K=.69503
320 FOR I=1 TO 2
330
G(I)=W(I)*(V(I)+.5)-WX(I)*(V(I)+.5)^2+WY(I)*(V(I)+.5)^3-WZ(I)
*(V(I)*.5)^4
340 NEXT I
345 VO=T(2)-T(1)+G(2)-G(1)
350 FOR I=1 TO 2
360 BV(I)=BE(I)-AE(I)*(V(I)+.5)
370 NEXT I
380 FOR J=0 TO COUNT
390 R(J)=VO+BV(2)*(J+1)*(J+2)-BV(1)*J*(J+1)
391 IF DL=0 THEN SJR=(J+1+L(1))*(J+1-L(1))/(J+1)
392 IF DL=1 THEN SJR=(J+2+L(1))*(J+1+L(1))/(4*(J+1))
393 IF DL=-1 THEN SJR=(J+2-L(1))*(J+1-L(1))/(4*(J+1))
395 IR(J)=SJR*EXP((-BV(2)*(J+1)*(J+2))/(K*T))
400 Q(J+1)=VO+BV(2)*(J+1)*(J+2)-BV(1)*(J+1)*(J+2)
401 IF DL=0 THEN SJQ=(2*(J+1)+1)*L(1)^2/((J+1)*(J+2))
402 IF DL=1 THEN
  SJQ=(J+2+L(1))*((J+1)-L(1))*(2*(J+1)+1)/(4*(J+1)*(J+2))
403 IF DL=-1 THEN
  SJQ=(J+2-L(1))*(J+1+L(1))*(2*(J+1)+1)/(4*(J+1)*(J+2))
405 IQ(J+1)=SJQ*EXP((-BV(2)*(J+1)*(J+2))/(K*T))
410 P(J+1)=VO+BV(2)*J*(J+1)-BV(1)*(J+1)*(J+2)
411 IF DL=0 THEN SJP=(J+1+L(1))*(J+1-L(1))/(J+1)
412 IF DL=1 THEN SJP=(J-L(1))*(J+1-L(1))/(4*(J+1))
413 IF DL=-1 THEN SJP=(J+L(1))*(J+1+L(1))/(4*(J+1))
415 IP(J+1)=SJP*EXP((-BV(2)*J*(J+1))/(K*T))
420 NEXT J
430 FOR I=1 TO COUNT+1
440 X(I)=1E+08/R(I-1): Y(I)=IR(I-1)
450 NEXT I
460 FOR I=COUNT+2 TO 2*(COUNT+1)
470 X(I)=1E+08/Q(I-(COUNT+2)+1): Y(I)=IQ(I-(COUNT+2)+1)
480 NEXT I
490 FOR I=2*(COUNT+1)+1 TO 3*(COUNT+1)
500 X(I)=1E+08/P(I-(2*(COUNT+1))): Y(I)=IP(I-(2*(COUNT+1)))
510 NEXT I
8040 XMAX=-1000000!:YMAX=-1000000!:XMIN=1000000!:YMIN=1000000!

```



```

8045 N=3*(COUNT+1)
8050 FOR I=1 TO N
8060 X=X(I): Y=Y(I)
8070 IF X>XMAX THEN XMAX=X
8080 IF X<XMIN THEN XMIN=X
8090 IF Y>YMAX THEN YMAX=Y
8100 IF Y<YMIN THEN YMIN=Y
8110 NEXT I
8130 INC=(XMAX-XMIN)/4
8340 KEY OFF: CLS
8350 LOCATE 25,3:PRINT USING "####.##";XMIN :LOCATE
25,19:PRINT USING "####.##";XMIN+INC
8360 LOCATE 25,38:PRINT USING "####.##";XMIN+2*INC:LOCATE
25,57:PRINT USING "####.##";XMIN+3*INC
8370 LOCATE 25,72:PRINT USING "####.##";XMAX
8380 LOCATE 1,1:PRINT 100:LOCATE 7,2:PRINT 75:LOCATE
13,2:PRINT 50
8390 LOCATE 19,2:PRINT 25:LOCATE 22,1
8400 LINE(38,0)-(38,334): LINE(38,332)-(719,332)
8410 FOR I=0 TO 3
8420 XT=((I+1)*170)+38:YT=(I*83)
8430 LINE(XT,332)-(XT,334):LINE(36,YT)-(38,YT)
8440 NEXT I
8449 J=0
8450 FOR I=1 TO N
8451 X=X(I): Y=Y(I)
8470 X2=38+INT((X-XMIN)*681/(XMAX-XMIN))
8490 Y2=332-INT((Y-YMIN)*332/(YMAX-YMIN))
8500 LINE (X2,332)-(X2,Y2)
8501 J=J+1
8502 IF J<N/3 THEN GOTO 8510
8503 A$=INKEY$: IF LEN(A$)=0 THEN 8503
8504 IF ASC(A$)=32 THEN 8505 ELSE 8503
8505 J=0
8510 NEXT I
8511 A$=INKEY$:IF LEN(A$)=0 THEN 8511
8512 IF ASC(A$)=42 THEN GOSUB 9000
8520 LOCATE 1,1: END
9000 DIM A%(350)
9010 OPEN"LPT1:" AS #2: WIDTH #2,255
9020 LPRINT CHR$(27);"A";CHR$(8);
9030 FOR J=0 TO 716 STEP 16
9040 GET(J,347)-(J+15,0),A%
9050   FOR K=1 TO 2
9055     PRINT #2, CHR$(27);"K";CHR$(92);CHR$(1);
9060     FOR I=347 TO 0 STEP -1
9070       IF K=1 THEN N=(A%(I+2) AND &HFF)
9075       IF K=2 THEN N=(A%(I+2) AND &HFF00)/256
9076       IF N<0 THEN N=N+256
9080       PRINT #2, CHR$(N);
9090     NEXT I:PRINT #2, CHR$(13);CHR$(10);
9095     NEXT K

```

```
9100 NEXT J
9110 PRINT #2,CHR$(12)
9120 PRINT #2, CHR$(27);"@"
9130 CLOSE #2
9140 RETURN
```

B.3 Program 4 -- Rotational Envelope

This programs calculates and plots the envelope of a rotational line spectra. Vibrational and rotational constants for the electronic state of the diatomic molecule must be input.

```

10 DIM
R(500),Q(500),P(500),IR(500),IQ(500),IP(500),X(501),Y(501),N
X(2000),NY(2000)
15 CLS
20 INPUT"ENTER THE NUMBER OF THE FILE CONTAINING THE CONSTANTS
FOR THE ELECTRONIC          TRANSITION, 2-->1.  ",B$
30 A$="C:\SCOTT\BACK\CONST"+B$
40 INPUT"IS THIS FILE ALREADY STORED? (Y OR N)  ",C$
50 IF C$="Y" OR C$="y" THEN GOTO 260
60 OPEN"O",#1,A$
70 PRINT"ENTER THE CONSTANTS FOR 1, THE FIRST ELECTRONIC
STATE."
80 INPUT"T(1)=",T(1):PRINT#1,T(1)
90 INPUT"W(1)=",W(1):PRINT#1,W(1)
100 INPUT"WX(1)=",WX(1):PRINT#1,WX(1)
110 INPUT"WY(1)=",WY(1):PRINT#1,WY(1)
120 INPUT"WZ(1)=",WZ(1):PRINT#1,WZ(1)
130 INPUT"BE(1)=",BE(1):PRINT#1,BE(1)
140 INPUT"AE(1)=",AE(1):PRINT#1,AE(1)
150 INPUT"LAMBDA(1)=",L(1):PRINT#1,L(1)
160 PRINT"ENTER THE CONSTANTS FOR 2, THE SECOND ELECTRONIC
STATE."
170 INPUT"T(2)=",T(2):PRINT#1,T(2)
180 INPUT"W(2)=",W(2):PRINT#1,W(2)
190 INPUT"WX(2)=",WX(2):PRINT#1,WX(2)
200 INPUT"WY(2)=",WY(2):PRINT#1,WY(2)
210 INPUT"WZ(2)=",WZ(2):PRINT#1,WZ(2)
220 INPUT"BE(2)=",BE(2):PRINT#1,BE(2)
230 INPUT"AE(2)=",AE(2):PRINT#1,AE(2)
240 INPUT"LAMBDA(2)=",L(2):PRINT#1,L(2)
250 CLOSE#1
260 OPEN"I",#1,A$
270 CLS: LOCATE 1,1
280 PRINT,1,2
290 INPUT#1,T(1),W(1),WX(1),WY(1),WZ(1),BE(1),AE(1),L(1)
300 INPUT#1,T(2),W(2),WX(2),WY(2),WZ(2),BE(2),AE(2),L(2)
310 PRINT "T",T(1),T(2)
320 PRINT "W",W(1),W(2)

```

```

330 PRINT "WX",WX(1),WX(2)
340 PRINT "WY",WY(1),WY(2)
350 PRINT "WZ",WZ(1),WZ(2)
360 PRINT "BE",BE(1),BE(2)
370 PRINT "AE",AE(1),AE(2)
380 PRINT "LAMBDA",L(1),L(2)
390 CLOSE#1
410 COUNT=30
420 DL=L(2)-L(1)
430 INPUT"ENTER THE VIBRATIONAL QUANTUM NUMBER FOR 1, THE
LOWER ELECTRONIC STATE. ",V(1)
440 INPUT"ENTER THE VIBRATIONAL QUANTUM NUMBER FOR 2, THE
UPPER ELECTRONIC STATE. ",V(2)
450 INPUT"ENTER THE ROTATIONAL TEMPERATURE FOR THE CALCULATION
IN KELVIN. ",T
460 INPUT"ENTER THE WINDOW SIZE IN ANGSTROMS. ",WH
461 INPUT"ENTER THE STEP SIZE IN ANGSTROMS. ",SP
462 PRINT"START ";TIME$
470 K=.69503
480 FOR I=1 TO 2
490
G(I)=W(I)*(V(I)+.5)-WX(I)*(V(I)+.5)^2+WY(I)*(V(I)+.5)^3-WZ(I)
)*(V(I)*.5)^4
500 NEXT I
510 VO=T(2)-T(1)+G(2)-G(1)
520 FOR I=1 TO 2
530 BV(I)=BE(I)-AE(I)*(V(I)+.5)
540 NEXT I
550 FOR J=0 TO COUNT
560 R(J)=VO+BV(2)*(J+1)*(J+2)-BV(1)*J*(J+1)
570 IF DL=0 THEN SJR=(J+1+L(1))*(J+1-L(1))/(J+1)
580 IF DL=1 THEN SJR=(J+2+L(1))*(J+1+L(1))/(4*(J+1))
590 IF DL=-1 THEN SJR=(J+2-L(1))*(J+1-L(1))/(4*(J+1))
600 IR(J)=SJR*EXP((-BV(2)*(J+1)*(J+2))/(K*T))
610 Q(J+1)=VO+BV(2)*(J+1)*(J+2)-BV(1)*(J+1)*(J+2)
620 IF DL=0 THEN SJQ=(2*(J+1)+1)*L(1)^2/((J+1)*(J+2))
630 IF DL=1 THEN
SJQ=(J+2+L(1))*((J+1)-L(1))*(2*(J+1)+1)/(4*(J+1)*(J+2))
640 IF DL=-1 THEN
SJQ=(J+2-L(1))*(J+1+L(1))*(2*(J+1)+1)/(4*(J+1)*(J+2))
650 IQ(J+1)=SJQ*EXP((-BV(2)*(J+1)*(J+2))/(K*T))
660 P(J+1)=VO+BV(2)*J*(J+1)-BV(1)*(J+1)*(J+2)
670 IF DL=0 THEN SJP=(J+1+L(1))*(J+1-L(1))/(J+1)
680 IF DL=1 THEN SJP=(J-L(1))*(J+1-L(1))/(4*(J+1))
690 IF DL=-1 THEN SJP=(J+L(1))*(J+1+L(1))/(4*(J+1))
700 IP(J+1)=SJP*EXP((-BV(2)*J*(J+1))/(K*T))
710 NEXT J
720 FOR I=1 TO COUNT+1
730 X(I)=R(I-1): Y(I)=IR(I-1)
740 NEXT I
750 FOR I=COUNT+2 TO 2*(COUNT+1)
760 X(I)=Q(I-(COUNT+2)+1): Y(I)=IQ(I-(COUNT+2)+1)

```

```

770 NEXT I
780 FOR I=2*(COUNT+1)+1 TO 3*(COUNT+1)
790 X(I)=P(I-(2*(COUNT+1))): Y(I)=IP(I-(2*(COUNT+1)))
800 NEXT I
801 PRINT"STEP 1: CALC. X(I),Y(I) ";TIME$
1000 FOR PASS=1 TO 3*(COUNT+1)-1
1010 FOR PLACE=1 TO 3*(COUNT+1)-PASS
1020 IF X(PLACE+1)<X(PLACE) THEN 1030 ELSE 1060
1030 XSTOR=X(PLACE): YSTOR=Y(PLACE)
1040 X(PLACE)=X(PLACE+1): Y(PLACE)=Y(PLACE+1)
1050 X(PLACE+1)=XSTOR: Y(PLACE+1)=YSTOR
1060 NEXT PLACE
1070 NEXT PASS
1071 PRINT"STEP 2: SEQUENCE X(I),Y(I) ";TIME$
1080 I=1:N=3*(COUNT+1):M=14:C=2.99792E+10:R=8.3144E+07
1100
NX(1)=1/((1/X(1))+5E-08):COUNT=INT(((1/NX(1))-(1/X(N))+5E-08
)/(SP*1E-08))
1101 PRINT"COUNT=";COUNT
1110 FOR I=2 TO COUNT
1120 NX(I)=1/((1/NX(I-1))-SP*1E-08)
1125 PRINT NX(I)
1130 NEXT
1131 PRINT"STEP 3: CALC. NX(I) ";TIME$
1140 FOR I=1 TO COUNT
1150 NY(I)=0
1160 FOR J=1 TO N
1170 IF ABS((1/NX(I))-(1/X(J)))>(WH*1E-08/2) THEN 1190
1180 NY(I)=NY(I)+Y(J)
1190 NEXT
2000 NEXT
2001 PRINT"STEP 4: CALC. NY(I) ";TIME$
2009 YMAX=NY(1):YMIN=NY(1)
2010 FOR I=2 TO COUNT
2011 IF NY(I)>YMAX THEN YMAX=NY(I)
2012 IF NY(I)<YMIN THEN YMIN=NY(I)
2013 NEXT
2014 YSP=YMAX-YMIN
9000 OPEN"I",#1,"DFN":INPUT#1,DFN:CLOSE#1
9005 DF$="D"+RIGHT$(STR$(DFN),LEN(STR$(DFN))-1)
9010 OPEN"R",#2,DF$,24
9020 FIELD#2,8 AS X$,8 AS AX$,8 AS Y$
9021 K=1:W1=0:AST=0
9030 FOR K=1 TO COUNT
9040 LSET X$=MKD$(AST):LSET AX$=MKD$(1E+08/NX(K)):LSET
Y$=MKD$((NY(K)-YMIN)*1000000!/YSP):PUT#2,COUNT-K+1
9050 NEXT K
9060 CLOSE#2
9070 OPEN"O",#1,"DFN":PRINT#1,DFN+1:CLOSE#1
9080 PRINT"DATA FILENAME: ";DF$
9085 PRINT"FINISH";TIME$
9090 END

```

APPENDIX C

C.1 Nitrogen Purity and Supplier

U. S. Welders Supply Co.
1800 Fifth Avenue
River Grove, Illinois 60171

Gas Data (Nitrogen, Oxygen Free)

Molecular Nitrogen -----	M.W. 28.013
Cylinder Pressure -----	2490 psig @ 70°F
Contents -----	257 ft ³
Cylinder Valve Outlet -----	CGA No. 580
Certified Oxygen Content -----	<5 ppm
CAS Registry No. -----	7727-37-9

REFERENCES

1. S.P. McGlynn, T. Azumi, and M. Kinoshita, *Molecular Spectroscopy of the Triplet State* (Prentice Hall, Englewood Cliffs, New Jersey, 1969), p. 3.
2. G. N. Lewis and M. Kasha, *J. Am. Chem. Soc.*, **66**, 2100 (1944); *J. Am. Chem. Soc.*, **67**, 994 (1945).
3. K. N. Walzl, C. F. Koerting, and Kuppermann, *J. Chem. Phys.* **87**, 3796 (1987).
4. C. F. Koerting, Ph.D thesis, California Institute of Technology, Pasadena, California (1985).
5. A. Kupperman, J.K. Rice, and S. Trajmar, *J. Phys. Chem.* **72**, 3894 (1968); S. Trajmar, J. K. Rice, and A. Kupperman, *Adv. Chem. Phys.* **18**, 15 (1970).
6. J. L. Tomer, K. W. Holtzclaw, and D. W. Pratt, *J. Chem. Phys.* **88**, 1528 (1988).
7. L. H. Spangler and D. W. Pratt, *J. Chem. Phys.* **84**, 4789 (1986); L. H. Spangler, D. W. Pratt, and F. W. Briss, *J. Chem. Phys.* **85**, 3229 (1986).
8. A. Frad, F. Lahmani, A. Tramer, and C. Tric, *J. Chem. Phys.* **60**, 4419 (1974)
9. M. Karplus and R. N. Porter, *Atoms and Molecules* (Benjamin/Cummings Publishing, Menlo Park, California, 1970), p.534.
10. N. A. Borisevich, A. A. Kotov, and G. B. Tolstorozhev, *Spectroscopy Letters* **6**, 399 (1973).
11. A. Lofthus and P. H. Krupenie, *J. Phys. Chem. Ref. Data* **6**, 113 (1977).
12. Herzberg, *Spectra of Diatomic Molecules* (Van Nostrand Reinhold, New York, 1950), p. 51.
13. W. B. Maier II, *J. Chem. Phys.* **55**, 2699 (1971); W. B. Maier II and R. F. Holland, *J. Chem. Phys* **52**, 2997 (1970); W. B. Maier II, *J. Chem. Phys.* **47**, 859 (1967).

14. K. R. Ryan, *J. Chem. Phys.* **51**, 570 (1969).
15. J. J. Leventhal and L. Friedman, *J. Chem. Phys.* **46**, 997 (1967).
16. A. Kantrowitz and J. Grey, *Rev. Sci. Instr.* **22**, 328 (1951).
17. D. V. Brumbaugh, J. E. Kenney, D. H. Levy, *J. Chem. Phys.* **78**, 3415 (1983).
18. D. H. Levy, *Photoselective Chemistry, Advances in Chemical Physics*, edited by J. Jortner, R. D. Levine, and S. A. Rice (Wiley-Interscience, New York, 1981), Part I, Vol. 47, pp. 323-362.
19. D. Golomb, R. E. Good, and R. F. Brown, *J. Chem. Phys.* **52**, 1545 (1970).
20. S. J. Harris, S. E. Novick and W. Klemperer, *J. Chem. Phys.* **60**, 3208 (1974); S. J. Harris, K. C. Janda, S. E. Novick, and W. Klemperer, *J. Chem. Phys.* **63**, 881 (1975).
21. W. M. Fawzy and M. C. Heaven, *J. Chem. Phys.* **92**, 909 (1990).
22. J. C. Miller, *J. Chem. Phys.* **86**, 3166 (1987).
23. L. B. Loeb, *Electrical Coronas* (University of California Press, Berkeley and Los Angeles, 1965).
24. C. F. Eyring, S. S. Mackedown, and R. A. Millikan, *Phys. Rev.* **31**, 900 (1928).
25. D. M. Lubman, C. T. Rettner, and R. N. Zare, *J. Phys. Chem.* **86**, 1129 (1982)
26. A. T. Droege and P. C. Engelking, *Chem. Phys. Lett.* **96**, 316 (1983).
27. V. Borkenhagen, H. Malthan, and J. P. Toennies, *J. Chem. Phys.* **63**, 3173 (1975).
28. R. E. Smalley, L. Wharton, and D. H. Levy, *J. Chem. Phys.* **63**, 4977 (1975).
29. J. B. Hopkins, D. E. Powers, and R. E. Smalley, *J. Chem. Phys.* **72**, 5039 (1980).
30. P. G. Carrick and P. C. Engelking, *J. Chem. Phys.* **81**, 1661 (1984).

31. R. P. Mariella, Jr., S. K. Neoh, D. R. Herschbach, and W. Klemperer, *J. Chem. Phys.* **67**, 2981 (1977).
32. S. G. Kukolich, D. E. Oates, and J. H. S. Wang, *J. Chem. Phys.* **61**, 4686 (1974).
33. R. W. Kessler and B. Koglin, *Rev. Sci. Instr.* **37**, 682 (1966).
34. D. H. Winicur, A. L. Moursund, W. R. Devereaux, L. R. Martin, and A. Kuppermann, *J. Chem. Phys.* **52**, 3299 (1970).
35. S. I. Chan, M. R. Baker and N. Ramsey, *Phys. Rev. A* **136**, 1224 (1964).
36. S. N. Foner and R. L. Hudson, *J. Chem. Phys.* **37**, 1662 (1962).
37. R. W. Bickes and R. B. Bernstein, *Chem. Phys. Lett.* **4**, 111 (1970).
38. G. M. McClelland, K. L. Saenger, J. J. Valentini, and D. R. Herschbach, *J. Phys. Chem.* **83**, 947 (1979).
39. J. B. Anderson and J. B. Fenn, *Phys Fluids*, **8**, 780 (1964); J. B. Anderson, R. P. Andres, J. B. Fenn, and G. Maise, *Rarefied Gas Dynamics*, 4th Symposium, Vol. II, edited by J. H. de Leeuw (Academic Press, New York, 1966), p 106.
40. P. G. Carrick, S. D. Brossard, and P. C. Engelking, *J. Chem. Phys.* **83**, 1995 (1985).
41. P. C. Engelking, *Rev. Sci. Instr.* **57**, 2274 (1986).
42. C. S. Feigerle and J. C. Miller, *J. Chem. Phys.* **90**, 2900, (1989).
43. D. Pleiter, *Can. J. Phys.* **41**, 1245 (1963).
44. D. E. Shemansky and A.L. Broadfoot, *J. Quant. Spectrosc. Radiat. Transfer* **11**, 1385 (1971).
45. R. G. Benett and F. W. Dalby, *J. Chem. Phys.* **31**, 434 (1959).
46. R. S. Freund, *J. Chem. Phys.* **56**, 4344 (1972); *J. Chem. Phys.* **51**, 1979 (1969); *J. Chem. Phys.* **50**, 3734 (1969).
47. D. Stedman and D. W. Setser, *J. Chem. Phys.* **50**, 2256 (1967).

48. S. Sharpe and P. Johnson, Chem. Phys. Lett. **107**, 35 (1984); J. Chem. Phys. **85**, 4943 (1986).

VITA

The author of this dissertation, Scott Miller Hurst, was born to Frank Pierce Hurst and Frances Miller Hurst on June 11, 1962, in Logan, West Virginia.

His schooling began at Justice Grade School in Logan, West Virginia. He pursued his secondary education at Logan Central Junior High School followed by Logan High School. He graduated from Logan High School in May of 1980.

He was accepted to the Honors Program of West Virginia University in August of 1980. In May of 1985, he successfully completed a Bachelor of Science Degree in Chemistry at West Virginia University. He was awarded a Graduate Assistantship in 1985 by the Department of Chemistry, West Virginia University. He married Pamela Jay Wellman, the daughter of Jayce Wellman and Ellen Wellman, on August 15, 1987.

In August of 1987, he transferred to Loyola University of Chicago. He was awarded a Graduate Assistantship in 1987, by the Graduate School and Department of Chemistry, Loyola University of Chicago. While at Loyola, he was elected the Graduate Representative to the Faculty by the Chemistry Graduate Student Organization. He became a member of the American Chemical and American Physical Societies during his tenure at Loyola.

He completed his Doctorate of Philosophy in Chemistry in 1991.

DISSERTATION APPROVAL SHEET

The dissertation submitted by Scott M. Hurst has been read and approved by the following committee:

Dr. Daniel J. Graham
Assistant Professor, Chemistry
Loyola University of Chicago.

Dr. Charles Brodbeck
Professor, Physics
Loyola University of Chicago.

Dr. Elliott Burrell
Associate Professor, Chemistry
Loyola University of Chicago.

Dr. Leslie Wo-Mei Fung
Professor, Chemistry
Loyola University of Chicago.

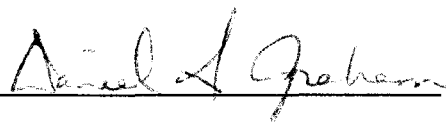
Dr. Robert J. Gordon
Professor, Chemistry
University of Illinois at Chicago.

The final copies have been examined by the director of the dissertation and the signature which appears below verifies the fact that any necessary changes have been incorporated and the dissertation is now given final approval by the committee with reference to content and form.

The dissertation is therefore accepted in partial fulfillment of the requirements for the degree of Doctor of Philosophy.

4-1-91

Date



Director's Signature